

Geologic Map of the Monticello 7.5-minute Quadrangle, Sierra and Socorro Counties, New Mexico

By

Daniel J. Koning, Andrew P. Jochems, Shari A. Kelley, Virginia T.
McLemore, and Colin T. Cikoski

June 2014

New Mexico Bureau of Geology and Mineral Resources
Open-file Digital Geologic Map OF-GM 245

Scale 1:24,000

This work was supported by the U.S. Geological Survey, National Cooperative Geologic Mapping Program (STATEMAP) under USGS Cooperative Agreement G13AC00186 and the New Mexico Bureau of Geology and Mineral Resources.



New Mexico Bureau of Geology and Mineral Resources
801 Leroy Place, Socorro, New Mexico, 87801-4796

The views and conclusions contained in this document are those of the author and should not be interpreted as necessarily representing the official policies, either expressed or implied, of the U.S. Government or the State of New Mexico.

**PRELIMINARY GEOLOGIC MAP OF THE MONTICELLO
QUADRANGLE, SIERRA AND SOCORRO COUNTIES, NEW
MEXICO -- REPORT**

by

Daniel J. Koning, Andrew P. Jochems, Shari A. Kelley, Virginia T.
McLemore, and Colin T. Cikoski

New Mexico Bureau of Geology and Mineral Resources
New Mexico Institute of Mining and Technology
801 Leroy Place
Socorro, NM 87801

June of 2014

EXECUTIVE SUMMARY

The Monticello quadrangle encompasses the southern end of the San Mateo Mountains and the northern arm of the Palomas Basin, which we refer to as the Monticello graben (*sensu* McLemore, 2012a). This area exhibits a variety of sedimentary and volcanic strata. ~960 m of Pennsylvanian strata comprise the oldest rocks. These include fossiliferous marine limestones and shales that lie above a shelf-margin sequence of interbedded pebbly sandstones, conglomerates, and limestones. Unconformably overlying the Pennsylvanian strata is a ~1200 m-thick sequence of upper Eocene volcanic strata of the Red Rock Ranch Formation, which consists of a lower package of dacitic volcanoclastic sediment, interbedded with dacite-andesite flows, and an upper package of trachyandesite flows. Two tongues of relatively fine-grained, lacustrine sediment (i.e., the Placitas Canyon Member) are found in the middle of the Red Rock Ranch Formation. A newly named unit, the tuff of Aragon Draw, occurs as a tongue in the upper part of the Red Rock Ranch Formation. The Rock Springs Formation (upper Eocene to lower Oligocene) overlies the Red Rock Ranch Formation and consists of trachytic-andesitic lavas and volcanoclastic sediment. Intertonguing with the Rock Springs Formation are four formation-rank, felsic tuffs (which we exclude from the Rock Springs Formation) that are called, from lower to upper: Lower Luna Park Tuff, Upper Luna Park Tuff, Hells Mesa Tuff (31.97 ± 0.12 Ma), and Vicks Peak Tuff (28.39 ± 0.19 Ma) [ages from Chapin et al., 2004]. Stratigraphically higher strata that have returned radiometric ages practically identical to the Vicks Peak Tuff (28.4 Ma; McLemore, 2010) are preserved along the western quadrangle border. These younger volcanic strata include 50-220 m of rhyolite (rhyolite of Alamosa Creek) and ~150 m of several ash flows collectively referred to as the Tuff of Shipman Canyon. Rhyolite intrusions cross-cut the Vicks Peak Tuff and older volcanic strata. Unconformably overlying the volcanic rocks, and preserved in the Monticello graben in the western quadrangle, is 1600-1700

m of largely Miocene-Pliocene basin-fill strata of the Santa Fe Group. The Santa Fe Group, which is composed mainly of sandy gravel and pebbly sands, is laterally contiguous with the Palomas Formation to the south, but on this quadrangle we have not identified a mappable contact that would demarcate the base of a Plio-Pleistocene age Palomas Formation. Cementation of the basin-fill increases down-section and laterally towards the basin margins. Five prominent Pleistocene terraces are correlated along Alamosa Creek, the highest of which correlates to the Cuchillo surface to the south. Modern valleys are filled by Holocene sediment.

The primary geologic structure on the Monticello quadrangle is a half-graben tilted east towards the west-down Deep Canyon fault. Santa Fe Group sediment filling the Monticello graben have been tilted towards this fault and generally strike northwest. However, strata within 3 km (2 mi) south of the northern quadrangle border strike northwest and dip to the southwest, indicating that throw decreases northward along the Deep Canyon fault from the vicinity of the northern quadrangle boundary.

Interesting fault relations occur in the southeastern quadrangle, in the vicinity of Seferino and Fifty-fifty Hill. The north-striking, west-down Willow Draw fault extends between these two hills from the south. The upper surface of the Santa Fe Group is not notably offset as it is to the south (e.g., McCraw and Williams, 2012; Cikoski and Koning, 2013), indicating that throw along the Willow Draw fault is decreasing northwards. The southern Deep Canyon fault appears to tie into the Willow Springs fault via two east-west faults that lie on either side of Seferino Hill.

Several north- to northeast-striking faults lie on the footwall of the Deep Canyon fault that have throws as much as 300 m. Displacement of rhyolitic stocks and dikes is minimal along most of these faults. Also, in the northeast quadrangle (in Street Canyon)

underlying Rock Spring Formation strata dip more steeply than the Vicks Peak Tuff. These relations indicate that notable tilting and faulting occurred between the inception of Rock Springs deposition and emplacement of the Vicks Peak Tuff.

GEOGRAPHIC AND TECTONIC SETTING

The Monticello quadrangle lies between the northern Sierra Cuchillo and southernmost San Mateo Mountains at a location 34-48 km northwest of the town of Truth or Consequences, in south-central New Mexico (Fig. 1 – **All figures are included at the end of the report**). The area is drained by the southeast-flowing Alamosa Creek, which extends upstream into the adjoining Winston basin to the northwest. The Palomas basin extends into north into this area as a narrow, arm-like feature. The relatively smooth, undissected floor of the Palomas basin (the Cuchillo surface of McCraw and Love, 2012) is quite dissected in the map area due to incision of Alamosa Creek over the past million years (Fig. 1).

The Monticello quadrangle includes two distinctive physiographic elements (Fig. 2). To the east lies hilly terrain of the southernmost San Mateo Mountains. This area is underlain by bedrock and increases in elevation northwards, from 5500 ft to 7,000-7,600 feet. This elevation gradient is accompanied by a transition in vegetation, from creosote-dominated Chihuahuan scrubland to a sparse juniper-pinon woodland. To the west lies southwest-trending canyons that flow into the southeasterly flowing Alamosa Creek. These canyons are separated by low (<300 ft), rounded ridges. The southeast corner of the quadrangle includes east-flowing tributaries to Alamosa Creek. The western quadrangle is primarily a Chihuahuan scrubland, but the higher ridges (i.e., >6,000 ft) are characterized by grasses with only sparse creosote.

Precipitation averages 35 cm (13.9 inches) in the town of Winston, located 19 km (12 mi) southwest of Monticello at an approximately similar elevation as most of the quadrangle (U.S. Climate data, 2014, using normals for 1961-1990). The average high temperature is 68.6°F and the average low temperature is 34.8°F at Winston.

Tectonically, the western Monticello quadrangle lies in the Monticello graben of McLemore (2012a). This graben is a northern extension of the Palomas basin between the northern Sierra Cuchillo and southern San Mateo Mountains (Fig. 3). It lies between the Winston graben on the west and the northern Engle Basin on the east.

PREVIOUS WORK

Prior to the mid 1960s, geologic studies of the map area were regional or focused on ore deposits. Harley (1934) described the geology and mine workings by Aragon Hill. Weber's (1963) regional study included the volcanic rocks in the northernmost quadrangle.

Since the mid 1960s, the complex volcanic relations of the eastern quadrangle, and the role they play in the volcanic evolution of the area in the Eocene-Oligocene, received the attention of numerous master's theses and dissertations. One of the more notable studies was a Ph.D. dissertation by Farkas (1969), who covered a large area of the southern San Mateo Mountain and established a workable regional stratigraphic framework of the volcanic rocks which we've applied in our study. Foruria (1984) included the northeastern and east-central parts of the quadrangle in his geologic and precious metal study of the southern San Mateo Mountains, but elected to use a different stratigraphic nomenclature than that of Farkas (1969). Hermann (1986) conducted a detailed and impressive volcanic study northwest of the Monticello

quadrangle, extending slightly into the north-central part of the quadrangle. He concluded that the southern margin of the Nogal caldera, proposed by Deal and Rhodes, 1976), was 1.6 km (1 mi) north of the northern boundary of the Monticello quadrangle and coincided with the arcuate, southern part of the Rock Springs fault.

Two master's theses focused on smaller areas, compared to Farkas (1969), in the Monticello quadrangle. Davis investigated the geology and mineral resources of Aragon Hill, in the northeastern quadrangle. Smith (1992) mapped and described volcanic rocks north of Red Rock Ranch.

Work in adjoining areas also focused on volcanic rocks. Maldonado (1974, 1980, and 2012) studied the northern Sierra Cuchillo. Volcanic rocks north of Maldonado's study area, near the Monticello box, were mapped by McLemore (2010, 2012b). In addition to Hermann (1986) and Foruria (1984), other volcanic studies of the southern and central San Mateo Mountains during the 1960s through 1980s include Furlow (1965), Deal and Rhodes (1976), Atwood (1982), and Ferguson (1986). Cox (1985) investigated the geology and gold-silver deposits found in the San Jose mining district, whose southern end lies ~3.5 km north of the northeastern corner of the Monticello quadrangle.

The rate of new work on volcanic rocks in the southern and central San Mateo Mountains decreased since the 1980s. The most notable advances were by Lynch (2003) and Ferguson et al. (2007). A useful synopsis of Oligocene calderas in the San Mateo Mountains is provided by Ferguson et al. (2012). Preliminary geologic mapping and stratigraphic correlations in the eastern quadrangle by McLemore (2012c) laid the foundation for this mapping effort.

STRATIGRAPHY

Numerous stratigraphic units were differentiated during the course of the mapping. Our stratigraphic nomenclature generally follows the scheme proposed by Farkas (1969), but we choose to not include thick tuffs in his Rock Springs Formation because they are likely regional in extent and could be considered as formation-rank units. Figure 4 illustrates how our stratigraphy compares with previous workers. Detailed descriptions of them are presented in Appendix 1. Here, we summarize these units, from oldest to youngest, and present photos for many of them. Previous master student studies conducted petrologic work on many of the Red Rock Ranch units, and reference to them are made where applicable.

Paleozoic strata

Using the older nomenclature of the Caballo Mountains and Mud Springs Hills (Cather et al., 2013), we have differentiated three formations in the carbonate-dominated Magdalena Group, which are Pennsylvanian in age. Compared to exposures in the Caballo Mountains, Fra Cristobal Mountains, and Mud Springs Hills, the formations are two to three times thicker in the Monticello quadrangle. The oldest Pennsylvanian unit, the Red House Formation, is 550-560 m thick and consists of interbedded maroon to pinkish white sandstone and conglomerate, dark gray shale (typically poorly exposed), and light gray- to yellowish tan-weathering limestone (Fig. 5). The sandstone and conglomerate beds are laterally discontinuous. Limestone beds are commonly composed of thin- to thick-bedded, fossiliferous packstone containing brachiopods (including Order *Spiriferida*), crinoid columnals, and fusulinids, with the latter found in the upper 30 m (98 ft) of section.

The overlying Nakaye Formation is comprised of ~330 m of limestone and poorly exposed grayish yellow shale. Chert is more abundant than in the Red House Formation (Fig. 5). The limestone is tannish to dark maroon-gray, thin- to thick-bedded, and forms ledges that weather into blocks (Fig. 5). Limestone commonly consists of wavy bedded, fossiliferous, and cherty packstone and wackestone; grainstone and micrite are subordinate. Fossils include brachiopods, bryozoans (*Fenestella*), and echinoderm fragments. Sponges replaced by chert are found in the upper part, though beds near the top of the section are typically fossil-poor.

The youngest carbonate-dominated unit, the Bar B Formation, is relatively thin compared to the other Paleozoic units (~75 m thick) and consists of dark gray to dark brownish gray, thin- to medium-bedded limestone and conglomerate. Limestone beds consist of massive, fossiliferous, chert-poor wackestone and packstone. Fossils include bryozoans (*Fenestella*), echinoderm fragments (especially crinoid columnals), fusulinids, and vertical burrows (*Skolithos?*). Marine conglomerate -- containing granules and pebbles of limestone, dolostone, and chert -- occurs in the upper 10 m (33 ft) of the section. Covered intervals below the conglomerate are underlain by poorly exposed gray shale.

Upper Eocene-lower Oligocene volcanic rocks

The volcanic rocks preserved in the eastern part of the quadrangle, and the mineral deposits they hosted, are what attracted earlier geologists to this area. Unfortunately, these earlier workers often created different stratigraphic schemes for the volcanic rocks, which creates difficulties for later investigators (Fig. 4). We favor the stratigraphic scheme proposed by Farkas (1969) and found it to be very workable in the field. Farkas's two formations, the older Red Rock Ranch and the younger Rock Springs

Formations, are treated separately below and their internal stratigraphic relations are depicted in Figure 6.

Red Rock Ranch Formation

The Red Rock Ranch Formation consists of a lower package of dacitic-andesitic volcanoclastic detritus, interbedded with dacite and andesite flows, and an upper package dominated by flows of trachyandesites, basaltic trachyandesite, and andesites. Two tongues of lacustrine sediment, called the Placitas Canyon Member, occur near the middle of the unit. As noted by Farkas (1969), the lower package, called the Whiskey Hill Member), becomes younger to the southeast; upper Whiskey Hill strata in the southeastern quadrangle intertongue to the northwest with flows of trachyandesite and basaltic trachyandesite (Fig. 6). Following Farkas (1969), we define the top of the Red Rock Ranch Formation at the base of the Lower Luna Park Tuff.

Compared to the overlying Rock Springs Formation, there are relatively few tuffs interbedded in the Red Rock Ranch Formation. A 25-40 m thick, felsic ash-fall tuff is mapped in the uppermost Red Rock Ranch Formation and is called the tuff of Aragon Draw (the "lithic-flow breccia unit of Smith, 1992). This tuff may correlate to the 40 m-thick tuff of Jose Maria Canyon to the south, which was called the Jose Maria Canyon andesite by Farkas (1969). As in the overlying Rock Springs Formation, we elected not to include thick tuffs in the Red Rock Ranch Formation because they likely are regional, formation-rank features. Much thinner tuffs in the Whiskey Hill Member are retained in the Red Rock Ranch Formation.

Whiskey Hill Member

The lower package of the Red Rock Ranch Formation consists of gray volcanoclastic sediment interbedded with dacite and lesser andesite flows. Cross-section construction

indicates a total thickness of about 320-330 m; a minimum thickness of 270 m (900 ft) is obtained using bedding attitudes west of Red Rock Ranch. We have broken the Whiskey Hill Member into several subunits (Appendix 1), particularly west of Red Rock Ranch. By far the largest subunit is **Trrws**, which is volcanoclastic pebble-cobble gravel and sandstone interbedded with dacite flows (Fig. 7). The dacites are porphyritic and have the following phenocrysts: 30-40% plagioclase and sanidine phenocrysts, trace to 15% biotite, trace to 8% hornblende, and trace to 7% pyroxene. Mappable bodies of dacite containing biotite and hornblende phenocrysts (unit **Trrwb**) are relatively common. These lavas are well-distributed throughout the section and form the oldest and youngest mapped flows in the Whiskey Hill Member. Forest Road 139 passes through one distinctive dacite body in the vicinity of the Red Rock shooting range. This dacite is light gray, becoming whiter and more altered to the west, and includes the following phenocrysts, which are euhedral: 5% biotite (0.5-2.0 mm long), 2% hornblende (1-4 mm long), and 12% plagioclase and sanidine (1-6 mm long and commonly altered). Another stratigraphically low unit, **Trrwl**, underlies the hill labeled 5923, located 0.8 km northwest of the shooting range. Hornblende-bearing dacite have been differentiated into the following subunits: 1) porphyritic dacite with 4-30% phenocrysts of plagioclase (up to 3 mm long) and hornblende (mostly 2-10 mm long), and pyroxene (<1 mm) (unit **Trrwh**); equigranular, hornblende-phyric dacite (unit **Trrwhe**); porphyritic dacite lava with 10% needle-like hornblende phenocrysts (unit **Trrwhn**). Other subunits include: 1) plagioclase-phyric andesites (containing plagioclase phenocrysts with lesser pyroxene +/- hornblende phenocrysts (unit **Trrwa**); 2) crystal-rich dacite lava with phenocrysts that include gray feldspar, hornblende, and pyroxene (unit **Trrwx**); 3) Pyroxene-bearing, porphyritic dacite with 15% phenocrysts of plagioclase, potassium feldspar, hornblende, and pyroxene (unit **Trrwp**); 4) pink to white, dacitic tuff (unit **Trrwt**); 5) a dacite flow with phenocrysts of potassium feldspar (unit **Trrwk**); and an upper biotite-bearing dacite having 3% xenoliths and phenocrysts

of plagioclase, pyroxene, hornblende, and trace biotite (unit **Trrwbu**). On a low hill, located 0.3 km southwest of where Forest Road 139 intersects the eastern quadrangle boundary, lies an aphanitic, flow-laminated rhyolite (unit **Trrwr**) interbedded within Whiskey Hill sandy conglomerate. Hermann (1986) exhibits two thin sections made from volcanoclastic sediment to the north of the quadrangle that likely correlates with unit **Trrws**.

Placitas Canyon Member (Trrp1 and Trrp2)

A particularly noteworthy member of the Red Rock Ranch Formation is the Placitas Canyon Member of Farkas (1969), who described it as composed of fissile or laminated lacustrine shale and minor tuffs. At a location 0.5 km (0.3 mi) west of Red Rock Ranch, Farkas (1969) discovered fossil plants consisting of imprints and casts of needles, cone scales, and leaves. These were further studied by Axelrod (1975), Axelrod and Bailey (1976), Meyer (1986), and Meyer (2012). These workers have used the identification of these flora to interpret paleoenvironmental conditions at the time the Placitas Canyon member was deposited. Axelrod and Bailey (1976) interpreted that the flora represents the boundary between broadleaved and coniferous forest. However, Meyer (2012) interpreted a coniferous forest environment and relatively cool temperatures (mean annual temperatures of 5-10°C; Meyer, 1986). Paleoelevation estimates, obtained using the types of flora identified, range from 1280 m (Axelrod and Bailey, 1976) to 3050-3800 m (Meyer, 1986).

The Placitas Canyon Member was originally restricted to relatively thin (<6 m) of shaly sediment underlying the Uvas Canyon trachyandesite (Farkas, 1969). Our mapping, however, has discovered another shaly tongue, with abundant interbeds of limestone, overlying the Uvas Canyon trachyandesite. Consequently, we have differentiated a

lower Placitas Canyon Member (**Trrp1**) and an upper Placitas Canyon Member (**Trrp2**). These are described separately below.

In the east (near Red Rock Ranch), the lower tongue of the Placitas Canyon member (**Trrp1**) is about 15 m thick and consists of light gray to very dark gray, thinly laminated with occasional ripple laminae, fissile and carbonaceous, silty shale. Locally interbedded within the shale are very thin to thin, tabular to lenticular beds of very pale brown to pale brown sandstone and silty sandstone. The sandstone is very fine- to medium-grained, subangular, well to moderately sorted, and composed of a tuffaceous volcanic litharenite.

The lower tongue thickens significantly to the west (to 75 m), where it exhibits a fining-upward trend and rests unconformably (in a buttress relation) with underlying hornblende-phyric lavas. As a whole, this interval becomes finer-grained northward (up-section), transitioning from interbedded sandstone and siltstone-shale to strata dominated by horizontal-laminated, light to dark gray shale (Fig. 8). Its lower 15-20 m (50-65 ft) consists of light greenish gray, very fine- to medium-grained sand interbedded with siltstone-shale. These are massive or in thin to thick, tabular beds. There are 5% interbeds of coarse-very coarse sandstone and pebbly sandstone (pebbles are <6 mm long) in thin to medium beds. Overlying sediment (~20 m thick) consists of pale yellow to light olive gray, very fine- to medium-grained sandstone, in very thin to thin, tabular beds, interbedded with minor light gray to dark gray shale. Sandstone in the lower 35-40 m is subangular, well sorted, and composed of feldspar and quartz grains with minor (~3%) biotite and other mafics; volcanic lithic grains are not obvious, except for feldspar-phyric volcanic pebbles. Asymmetric ripplemarks and toolmarks are relatively common and indicate a northerly paleoflow direction (Fig. 8). These paleoflow data, along with the presence of a 35-40 m-thick, lower interval with

abundant arkosic sandstone, strongly suggests that a drainage entered the lake via a northeastward-sloping canyon cut into hornblende dacite at a location 3.5 km northwest of Red Rock Ranch. The arkosic nature of the sediment also suggests that this northeastward flowing canyon tapped a large area of arkosic (probably Proterozoic) terrain to the southwest of the Deep Canyon fault.

Correlating the lower Placitas tongue to the "shale member" (unit Ts) of Hermann (1986) is reasonable both lie in the same stratigraphic position (i.e., beneath the Uvas-Garcia Falls andesitic interval and above the Whiskey Hill member). Herman noted that his "shale interval" thins dramatically to the northeast: from 50 m (150 ft) to 3 m (10 ft) in 1.6 km (1 mi). Thus, the lower Placitas tongue appears to have been elongated northwestward, parallel to the present-day Deep Canyon fault, and the thickest accumulations of lake sediment were to the west, closest to the fault. Moreover, the northeast side of the lake contained the highest ratios of shale:sandstone. Another important observation is that the Uvas basaltic trachyandesite is locally interbedded with Placitas sediment in the Red Rock Ranch area. Given these observations, the idea of Farkas (1969) that the lake was formed by lava dams is reasonable. The damming lava appears to have been the Uvas basaltic trachyandesite, which must have flowed to the southeast --consistent with southerly paleocurrents measured southeast of Red Rock Ranch (Fig 9). Northeast-draining canyons, including the one noted above, provided discharge to the lake. Another possible source of discharge could have been springs near what is now the Deep Canyon fault. The fact that the lake sediments thicken to the west probably indicates longer sediment accumulation times before the Uvas-Garcia Falls lavas overlapped towards the west and (episodically) filled in most of the lake.

The upper tongue of the Placitas Canyon member (**Trrp2**) also contains shale interbedded with sandstone, but it also contains relatively abundant limestone beds

(Fig. 10). Sandstone interbeds become more common to the north. The main body lies stratigraphically between the top of the Uvas basaltic trachyandesite and the top of the Garcia Falls trachyandesite. However, 1-5 m-thick interbeds of this unit are present in the lower part of the overlying Luna Peak trachyandesite. The shale is light to dark gray, finely laminated and friable, and contains up to 25% organic-rich, very dark grayish brown shale. To the south is 0.5-1%, gray, very fine- to fine-grained, lithic-rich sandstone beds containing fine to very coarse grains of angular feldspar. Also found locally to the south are 0-5%, biotite-bearing, altered ash interbeds (up to 4 cm thick). Limestone is micritic, light gray to gray, and in very thin to thick, tabular beds. To the north, the unit consists of a 10-15 cm-thick limestone overlain and underlain by fine- to coarse-grained, volcanoclastic sandstone. The upper tongue of the Placitas Canyon member lies in roughly the same area as the lower tongue, and we envision a similar northwest-elongated lake blocked by lava flows to the northeast. In this case, the damming lava flows consisted of the Luna Peak trachyandesite, given that interbeds of the upper tongue are found in the western extent of this lava. The highest shale:sandstone ratios are about 2.5 km (1.5 mi) northwest of Red Rock Ranch, suggesting this was near the deepest part of the lake. The unit is 1-50 m thick, thinning to the north.

Uvas basaltic trachyandesite and Garcia Falls trachyandesite (Trru and Trrg)

The lower part of the aforementioned, upper stratigraphic package of the Red Rock Ranch Formation is occupied by the Uvas Canyon basaltic trachyandesite and the Garcia Falls trachyandesite. Farkas (1969) named the former the Uvas Canyon pyroxene andesite, but whole rock chemical analyses indicate that its composition corresponds with that of a trachyandesite (Fig. 11). Similarly, the Garcia Falls andesite of Hermann (1986) is actually a trachyandesite (Fig. 11). The two units appear to intertongue with one another 3.5 km northwest of Red Rock Ranch. At this intertonguing zone, the

Garcia Falls trachyandesite stands 120 m (400 ft) above the present day surface of the more erodible Uvas Canyon member, so it is possible that the Garcia Falls trachyandesite may have prograded over the Uvas Canyon basaltic trachyandesite.

The Uvas Canyon basaltic andesite is a gray to dark gray, porphyritic, relatively coarse-grained basaltic trachyandesite whose weathered surfaces are typically varnished (Fig. 12). Thickness is 300-480 m. It is generally underlain and overlain by thin sediments of the Placitas Canyon member (described above). Phenocrysts include: 30-70% plagioclase, 3-10% pyroxene, trace to 5% megacrysts of plagioclase and pyroxene (10-18 mm long), and trace olivine(?). Chlorite locally is an alteration product and phenocrysts may be altered to goethite or limonite. The lava weathers to form spheroidal, crumbly outcrops. It is relatively erodible and forms gentle slopes or underlies valley bottoms. This unit has been dated by K/Ar techniques at 36.7 ± 1.1 Ma (reported in Meyer, 1986, based on U.S. Geological Survey memorandum from J.C. Von Essen, 2 May 1983, potassium-argon report no. 153, Menlo Park).

The Garcia Falls trachyandesite is greenish gray to gray (weathering to brown), porphyritic, and vesicular (Fig. 13). It is at least 400 m thick. Similar to the Uvas Canyon basaltic trachyandesite, it is overlain and underlain by sediment correlated to the Placitas Canyon Member (note that the underlying sediment is observed 0.7 km (0.4 mi) north of the northern quadrangle boundary, as shown in Hermann, 1986). Phenocrysts in the lava include 15-80% plagioclase that are locally aligned, 5-10% pyroxene, and trace to 1% hornblende. Commonly propylitically altered to a chlorite-epidote±albite assemblage, especially near the Deep Canyon Fault. Detailed petrographic descriptions are given in Hermann (1986) and Smith (1992), although

some descriptions from the latter worker may not actually be from the Garcia Falls trachyandesite (as mapped by us and Hermann, 1986).

Rhyolite southeast of Stanley Springs (Trrrs)

A previously unrecognized stratigraphic unit is a 100-110 m thick rhyolite that caps the hill labeled 6779 southeast of Stanley Springs. This rhyolite is a light bluish to light greenish gray, porphyritic, and mostly fine-grained. Phenocrysts include: 10-15% hornblende (0.1-4.0 mm long), 8-10% potassium feldspar + lesser plagioclase (0.2-5.0 mm), and 1-3% quartz (0.5-2.0 mm). The lava is well foliated (wavy to irregular) and may occupy the same stratigraphic position as the fine-grained andesite east of Luna Peak (unit **Trrael**).

Andesite west of Luna Peak (Trrael)

Called the upper andesite member of the Red Rock Formation by Hermann (1986), this is a 100-120 m thick, fine-grained andesite located on the west slopes of Luna Peak, where it lies stratigraphically between the Garcia Falls trachyandesite (bottom) and Luna Peak andesite (top). The lava is gray, weathering to light gray to brownish gray, and porphyritic (Fig. 14). Phenocryst assemblage includes: 25-40% plagioclase (0.2-10 mm) and 1-10% pyroxene (1-6 mm). Plagioclase crystals are locally aligned and locally some are 10-18 mm long. The lower part of the unit forms relatively smooth slopes but the upper 10 m is a cliff-former. Most of the upper ~30 m is a tongue of Garcia Falls trachyandesite.

Luna Peak trachyandesite (Trrl)

The large plagioclase phenocrysts of the Luna Peak trachyandesite makes its recognition relatively easy (Fig. 15). It is a gray to light gray, plagioclase-megacrystic trachyandesite flow, where $\geq 10\%$ of the plagioclase phenocrysts are ≥ 10 mm. Although

Farkas (1969) and Hermann (1986) called the unit "Luna Peak andesite," whole rock chemical analyses indicate it is actually a trachyandesite (Fig. 11). The lava commonly weathers to produce corestone topography (Fig. 16). Fresh colors are light to gray, but it weathers to brown to light brown colors. Phenocrysts include: 40-70% plagioclase that are commonly aligned (0.5-28 mm long) and 0.5-7% pyroxene (0.5-9 mm long, locally altered to a reddish brown mineral). Groundmass is ≤ 0.2 mm and composed of plagioclase with minor mafic grains. There are 3-35% vesicles 0.5-20 mm long (some to 7 cm long), some of which are filled with calcite or an amorphous black substance. Calcite- or quartz-filled geodes are present to the south. This lava is 120 m thick in the north-central part of the quadrangle, but thins to the south-southeast until it pinches out near Jose Maria well. This thickness trend suggests that the eruptive center for this trachyandesite was north of the quadrangle boundary. Detailed petrographic descriptions are given in Hermann (1986) and Smith (1992).

Red Rock Arroyo andesite and overlying sediment (Trrr and Trrsm)

Overlying the Luna Peak trachyandesite is a gray (typically weathering to a light brown or reddish brown), plagioclase-phyric lava with minor pyroxene phenocrysts. (Fig. 17) The lavas typically form ledges and are vesicular. The unit sharply overlies the underlying Luna Peak trachyandesites (**Trrl**), with the contact being undulatory and exhibiting local buttersses as much as 1 m tall (Fig. 18). An angular unconformity is interpreted for this contact in lower Uvas Canyon (Smith, 1992, p. 32), and Foruria (1984) also interprets this contact as an unconformity. Phenocrysts include: 7-25% plagioclase (0.2-11 mm long) and 0.5-5% pyroxene (0.1-2.0 mm). Hornblende is locally seen (trace to 3%, 1-15 mm), especially north of Red Rock Ranch. Vesicles are 0.5-10 mm long, but locally are as long as 60 cm. Amygdules filled with calcite or quartz are locally seen. This unit is thickest near Forest Road 139 (~110 m) and thins to the north and south. Tongues of andesitic lava occur in volcanoclastic sediment of the Whiskey

Hill Member southeast of Red Rock Ranch. Lithologically, these most closely resemble the Red Rock Arroyo andesite and are assigned to that member. This correlation, together with the geographic and stratigraphic position of these lower lavas (i.e., below the Uvas basaltic trachyandesite to the north), implies that the eruptive center of the Red Rock Arroyo andesite may have been east of the centers associated with the Luna Peak trachyandesite and the Garcia-Uvas member lavas. Petrographic descriptions of the Red Rock Arroyo andesite member is provided by Smith (1992).

The Red Rock Arroyo andesite is overlain by 1-10 m of sediment. To the south, this sediment is composed of very fine- to fine-grained sand and silty sand, but to the north it is coarser and includes volcanoclastic sandy pebbles to pebbly sand (Fig. 19). This sediment is overlain by the tuff of Aragon Draw, which is described below.

Andesite of Questa Spring and overlying volcanoclastic sediment (Trraq and Trrsu)

Overlying the tuff of Aragon Draw in upper Uvas Canyon is a distinctive, brownish to greenish gray, highly porphyritic andesite that is 30-90 m thick. Phenocrysts include 30-50% plagioclase with lesser amounts of pyroxene and magnetite. The plagioclase crystals are conspicuously large and are generally 5 to 8 mm long. Overlying this andesite is at least 5 m of reddish gray to light greenish maroon siltstone, sandstone, and minor pebbly sandstone in laminated to very thin, tabular beds.

Upper trachyte (Trrtu)

The stratigraphically highest unit of the Red Rock Ranch Formation near the northern quadrangle border is 20-45 m of a bluish-gray, fine-grained lava inferred to be a trachyte. It contains <1% phenocrysts of sanidine (1-2 mm long) in an aphanitic to crystalline matrix. Pinching out to the east, it appears to have filled rugged

paleotopography that developed on top of the Questa Spring andesite and it underlies lower Luna Park Tuff.

Tuffaceous, fine-grained sediment (Trrst)

In the southeastern quadrangle, south of Forest Road 139, the stratigraphically highest unit of the Red Rock Ranch Formation corresponds to a tuffaceous (locally pumiceous), mostly massive sediment that is at least 15 m thick (Fig. 20). It overlies the tuff of Aragon Draw and thus lies at a similar stratigraphic interval as the andesite of Questa Spring and the upper trachyte to the north-northwest (units **Trraq** and **Trrtu**). Being light-colored (white to tan to pink), this tuffaceous unit consists of clay, subordinate sand, and 1-15% scattered pebbles composed of andesite-dacite pebbles. To the south, 0.7 km northeast of Jose Maria well, 3-4% fresh biotite crystals are observed in the matrix. There, the unit partly fills a paleovalley cut into the tuff of Aragon Draw and it fines up-section from a massive to horizontal-planar bedded, very fine- to very coarse-grained sandstone (Fig. 20) to a red, tuffaceous clay. It is interpreted as a mudflow possibly derived from a volcanic edifice associated with the tuff of Aragon Draw.

Seferino Conglomerate member

Possibly the youngest member of the Red Rock Formation is the Seferino Hill conglomerate, which underlies Seferino and Fifty-fifty Hills in the southeastern part of the quadrangle. It consists of a brownish red, silica-indurated, massive conglomerate containing clasts up to 1.5 m (4.9 ft) long (Fig. 21). These clasts are composed of reworked Jose Maria tuff and hornblende andesites from the underlying Whiskey Hill member. At Fifty-fifty Hill, the matrix contains many voids partially filled by globular chalcidony. The conglomerate ranges from approximately 35-65 m (114-213 ft) thick.

Rock Springs Formation

In contrast to previous workers (e.g., Farkas, 1969; Hermann, 1986), we have excluded from the Rock Springs Formation thick, distinctive, regional tuffs. These tuffs have been mapped far beyond what has previously been considered the Rock Springs Formation (e.g., the Hells Mesa Tuff), or have the potential to be regional ignimbrites, so we believe they are best considered as formation-rank units. Consequently, the Rock Springs Formation, as used here, consists of interbedded volcaniclastic sediment, andesite flows, and trachyte flows that lie above the Lower Luna Park Tuff and below the Vicks Peak Tuff. These strata intertongue with the thick ignimbrites that include the Upper Luna Park Tuff and the Hells Mesa Tuff. Like in the Red Rock Ranch Formation, we summarize the units of the Rock Springs Formation in ascending order.

Interbedded sedimentary rocks and andesite flows (Trssv1 and Trssv2)

The lower of these two units (**Trssv1**) is ~15 m thick and lies between the Lower and Upper Luna Park Tuffs. It consists of a reddish brown, volcaniclastic, pebble conglomerate with a sandy to silty matrix. Overlying this conglomerate are brown, foliated, porphyritic andesites whose phenocrysts include plagioclase, feldspar (<5 mm long), and pyroxene (~1 mm long).

The upper of these two units (**Trssv2**) is 3-15 m thick and consists of red, silty to conglomeratic, volcaniclastic sedimentary rocks interbedded with andesites (Fig. 22). It locally lies between the Upper Luna Park Tuff and the Hells Mesa Tuff. Two lithologic types are found in this unit: 1) vesicular andesites containing 15-20% plagioclase phenocrysts (1-2 mm long) and <1% xenocrystic quartz (3-4 mm long) in a fine-grained crystalline matrix; 2) relatively aphanitic lavas with a fine-grained crystalline matrix.

Trachyte lava interbedded with sedimentary rocks (Trst and Trssv3)

A 150-180 m (500-600 ft)-thick sequence of trachyte lavas and a middle tongue of volcanoclastic sediment is located east of Red Rock Arroyo (Fig. 22). The trachyte contains less than 1% phenocrysts of sanidine and pyroxene in an aphanitic to trachytic matrix. Individual flows are less than 30 m thick. Farkas (1969) provides detailed descriptions of lava flows in this stratigraphic interval, but whether they actually are the trachytes found here is somewhat uncertain (note that he calls them the "upper andesite flows"). The sediment is about 30 m thick and consists of a clast-supported conglomerate or breccia. The gravel includes angular to subrounded clasts of light gray, trachytic lava with hornblende and sanidine phenocrysts. The trachyte underlying the middle volcanoclastic sediment tongue interfingers eastward with volcanoclastic sediment.

Tuffs below the Vicks Peak Tuff

Three tuffs are differentiated as tongues within the Rock Springs Formation, and one tuff is mapped in the upper Red Rock Ranch Formation. These are described in ascending order.

Tuff of Aragon Draw (Ttad and Ttadw) and the tuff of Jose Maria Canyon (Ttjmc)

Throughout the eastern study area is a relatively coarse-grained, upward-coarsening tuff whose basal 1-12 m is commonly welded (Fig. 23). It occurs as a 25-40 m-thick tongue in the upper Red Rock Ranch Formation. The lower, welded part increases in thickness to the south, is reddish, and contains 10-20% fiamme 5-20 mm long and 1-4 mm tall. Phenocrysts include trace to 12% (mostly <8%) mafic grains (hornblende and biotite), both 0.2-2 mm long, and 5-20% sanidine-dominated potassium feldspar (0.5-4.0 mm long). The overlying, non-welded tuff is a reddish, massive, breccia-like, hard unit consisting of scattered pebble- to cobble-size clasts (minor boulder-size) in a silt to fine sand matrix. The clasts contain three main lithologic types (listed from most to least

common): 1) fine-grained and laminated tuff, typically flattened (up to a few 10s of cm long and a <5 cm tall) parallel to the lower contact and commonly folded; 2) 1-8% white igneous granules to pebbles (containing feldspar and minor hornblende, with very minor biotite and quartz) -- granules of this type is also found in the welded, basal part of the unit; and 3) 1-5% plagioclase-phyric, light gray-gray-reddish gray andesite. Locally, the tuff clasts enclose the gray, plagioclase-phyric clasts. Gravel-size increases up-section, where the tuff clasts (#1) are as large as 45x45 cm. The matrix contains up to 30% scattered coarse to very coarse feldspar grains (probably from disintegration of the white igneous clasts; locally present in the matrix is trace biotite and/or hornblende <2 mm long, where the biotite is locally deformed. Remorphic textures are observed, manifested by the folded or swirly tuff clasts, and are especially prominent in the north-central part of the quadrangle. We infer that the eruptive center associated with this tuff lay a short distance to the east or southeast of the quadrangle, based on the southeasterly thickening of the welded, basalt part of the unit and the presence of the largest clasts near the eastern quadrangle border. This tuff appears to correlate with the lithic-flow breccia unit (upper Spears Formation) of Smith (1992).

Lying south of Jose Maria well, the tuff of Jose Maria Canyon occupies a similar stratigraphic position as the tuff of Aragon Draw and may be a facies of the latter. However, the tuff of Jose Maria Canyon is much finer-grained. It is a light gray (weathering gray to tannish orange), aphanitic tuff that contains trace amounts of medium-grained sanidine and rare lithic fragments up to 1.2 cm long. Sparse fiamme are present that are 1-4 cm wide. This unit was called the "Jose Maria andesite" by Farkas (1969), who describes it in some detail. The tuff is about 40 m thick.

Lower Luna Park Tuff (Tlpl)

Overlying the top of the Red Rock Ranch Formation, the Lower Luna Park Tuff extends across the eastern study area, ranging in thickness from 10 to 100 m. Near its base, this unit has 15-25% sanidine as well as subordinate biotite, plagioclase, magnetite, and a trace of quartz (Fig. 24). The upper part of this unit has 2-15% lithic fragments. The top of this unit near Luna Park Campground is gray, welded, and contains 3-5% biotite, sanidine, and plagioclase phenocrysts with a trace of quartz; the unit here has <1% lithic fragments (~5mm long). The top of the lower Luna Park Tuff on the east side of Red Rock Arroyo has 10-15% lithic fragments. In the southeastern quadrangle, this unit is relatively thin (6-15 m), reddish gray to brown, and contains 10-15% fiamme (up to 18 cm long) and 1-25% volcanic lithic fragments (mostly aphanitic, some with local biotite or hornblende phenocrysts). The phenocryst assemblage in the southeast includes: 5-10% sanidine (up to 5 mm long), 1-3% biotite, and 0.5% hornblende. A basal 2-3 m-thick vitrophyre is locally present. The pumice in the less welded parts of the unit is crystal-poor and vapor-phase altered. Numerous samples were collected from this unit for $^{40}\text{Ar}/^{39}\text{Ar}$ geochronologic analyses, but the results are pending. Smith (1992) and Foruria (1984) group this tuff, along with the Upper Luna Park Tuff, with Foruria's "latite ash-flow tuff unit" and provide detailed descriptions. We speculate that this tuff might correlate with the Bell Top tuff 3 (35.69±0.12 Ma; Chapin et al., 2004) or with tuffs from the Organ Mountains caldera (35.5-36.2 Ma; Chapin et al., 2004).

Upper Luna Park Tuff (Tlpu)

Near the northern quadrangle border, the Upper and Lower Luna Park tuffs are separated by ~15 m of volcanoclastic sediment and andesite flows (**Trssv1**), but this intervening unit is lacking to the southeast. The Upper Luna Park Tuff is tan to white, approximately 75 m thick, and contains 5-15% phenocrysts of sanidine, plagioclase, and biotite (Fig. 25). Welding is variable but generally most pronounced at the base and less

welded near the top. The welded intervals are gray and can have rheomorphic fluidal textures. The top of Luna Park Tuff in the north-central part of the quadrangle has 5-10% lithic fragments (up to 0.5 m long), but most lithics are <15 cm in diameter. In the southeastern quadrangle, the lower part of this unit is distinctly reddish (2.5-7.5YR 6-7/2) and contains 15-30% sanidine (0.2-2.0 mm), trace biotite, trace quartz, and trace hornblende. Smith (1992) and Foruria (1984) group this tuff, along with the Lower Luna Park Tuff, with Foruria's "latite ash-flow tuff unit" and provide detailed descriptions. As in the Lower Luna Park Tuff, results are pending for samples collected for $^{40}\text{Ar}/^{39}\text{Ar}$ geochronologic analyses. We speculate this unit may correlate with the 34.98 ± 0.19 Ma Datil Well Tuff or 34.96 ± 0.04 Ma Bell Top tuff 4 (Chapin et al., 2004).

Hells Mesa Tuff (Thm)

This distinctive, laterally extensive tuff is 15-60 m thick. It is a white to pink to peach-colored, lithic-poor (<5%), moderately welded tuff with 5-20% phenocrysts of quartz, biotite, sanidine, titanite, and sparse hornblende (Fig. 22). Detailed descriptions of this tuff are found in Foruria (1984), Hermann (1986), Smith (1992), and Farkas (1969); the latter calls it the "upper latite tuff." An $^{40}\text{Ar}/^{39}\text{Ar}$ age is 31.97 ± 0.12 Ma has been obtained from this unit (Chapin et al., 2004).

Vicks Peak Tuff and overlying volcanic rocks

Except for the extreme northwestern corner of the quadrangle, upper volcanic strata are related to the Vicks Peak Tuff or rhyolites that extruded immediately after the emplacement of this tuff.

Vicks Peak Tuff (Top)

The laterally extensive, crystal-poor Vicks Peak Tuff was sourced from the nearby Nogal caldera (Furlow, 1965; Farkas, 1969; Deal and Rhodes, 1976; Ferguson et al.,

2012). It is a pink to white, welded tuff with less than 1% sanidine and is commonly foliated (Fig. 26). A greenish black vitrophyre is common near the base. In places, a 1-3 m-thick, ledge-forming interval of gray to pink, crystal-poor, flow-banded tuff with trace amounts of sanidine, pyroxene, and quartz is present below the vitrophyre. The tuff filled in irregular topography developed immediately prior to its eruption, including paleovalleys >120 m (>400 ft) deep (Fig. 26). Detailed descriptions of this tuff are also found in Farkas (1969), Foruria (1984), Hermann (1986), and Smith (1992). The top of the tuff is not preserved, and the maximum thickness on the quadrangle is 105 m.

Rhyolite of Alamosa Creek (Trac)

The Rhyolite of Alamosa Creek forms the bedrock hills along the western margin of the quadrangle, although its existence in the Ramos Hills (southwestern quadrangle corner) is questionable because permission to field check it there was denied. The rock is a light to gray (weathering to a reddish brown to brown), fine-grained, flow-banded rhyolite that is massive to vesicular to granular (Fig. 27). It has trace to 2% sanidine phenocrysts (0.5-2.0 mm long). It contains several flows whose margins (including tops and bases) exhibit thick (tens of meters) breccia zones. The base of this unit was not observed on the quadrangle, but the rhyolite is 50-220 m thick in the Montoya Butte quadrangle to the northwest (McLemore, 2010). The rhyolite yielded a $^{40}\text{Ar}/^{39}\text{Ar}$ age of 28.4 ± 0.04 Ma (McLemore, 2010). This rhyolite may extend into the northern Ramos Hills, but near the quadrangle boundary the bedrock has been mapped as a rhyolitic tuff by Heyl et al. (1983), which they call the "coarse Moonstone porphyritic rhyolite tuff (unit Tcrt)". We were not able to access the Ramos Hills to map the contact between the two units.

Tuff of Shipman Canyon (Tsc)

Overlying the Rhyolite of Alamosa Creek in the northwestern corner of the quadrangle, the tuff of Shipman Canyon is a cliff-former composed of interbedded tuffs. The tuffs

are generally purplish gray (weathering brownish tan), massive to thick-bedded, and porphyritic to aphanitic. Phenocrysts include: 6-8% quartz (up to 3 mm), 2% sanidine (up to 2 mm), and trace to 1% biotite (up to 1 mm). The tuff, which is non- to densely welded and relatively unaltered, also contains 2-3% glass shards up to 2.5 mm. Pumice fragments display flattening (length:width) ratios between 3:1 and 9:1. Some interbeds consist of light purplish gray air-fall tuff containing lapilli to fine bombs of aphanitic rhyolite and tuff. Spherulitic to vesicular tuff and rhyolite may also be present. A $^{40}\text{Ar}/^{39}\text{Ar}$ age of 28.4 Ma (Lynch, 2003; McLemore, 2010) is virtually indistinguishable from the ages of the Vicks Peak Tuff and Rhyolite of Alamosa Creek -- so the contacts between the units can be considered as conformable.

Upper Eocene-lower Oligocene intrusive rocks

Three types of intrusive rocks have been identified in the quadrangle. The oldest likely are dacite intrusions that form dikes near the eastern quadrangle boundary, south of Forest Road 139. These dacites are light gray (fresh), but weather to produce a strong varnish), and composed of: 1) plagioclase (0.2-2.0 mm, euhedral to subhedral), 7% hornblende; (0.5-4.0 mm, euhedral), 2-4% biotite (0.2-1.0 mm, eu to subhedral), and <5% quartz. Another type of intrusive rock are intermediate, gray dikes found in 0.8-2.1 km within the northern quadrangle boundary (Fig. 28). These intermediate intrusives are either: 1) fine-grained, with an equigranular matrix and no obvious phenocrysts, or 2) have <1% plagioclase and pyroxene phenocrysts (<2mm long) in an aphanitic matrix. The most abundant intrusive rock, occupying dikes and (less commonly) plugs, are rhyolites with potassium feldspar and lesser quartz phenocrysts (Fig. 28). In the Aragon Hill area, rhyolitic intrusions are altered to iron oxides, clay, and traces of alunite, pyrite, and native gold.

Santa Fe Group basin-fill

In contrast to the volcanic rocks, the Santa Fe Group on this quadrangle has not received significant attention from earlier workers. The basin-fill is 1800-1900 m thick, is generally tilted to the east-northeast, and consists of sandy gravel and pebbly sand along with minor sand beds. On this quadrangle, there are two general stratigraphic levels in the Santa Fe Group that do not appear to correlate directly with how the Santa Fe Group is differentiated in the southern Palomas Basin. The lower level (**Tsflc**) is coarser-grained, grayer, and more cemented than the upper level. The upper level (**QTsf**) generally has less than 20% moderate to strong cementation over a given 10 m stratigraphic interval. In addition, it contains relatively common orange pebbly sand beds (these tend to be gray in unit **Tsflc**). Within the upper stratigraphic level is a gray lithosome associated with the Garcia Falls drainage, which interfingers laterally with unit **QTsf**. This lithosome is divided into an upper, finer (i.e., sandier) part and a lower, coarser part (**Tsfgu** and **Tsfgl**, respectively).

There is no direct age constraints for the Santa Fe Group on the quadrangle. In the Montoya Butte quadrangle to the northwest, basalt flows that lie at or very near the base of the Santa Fe Group have returned $^{40}\text{Ar}/^{39}\text{Ar}$ ages of 18.7 Ma (McLemore et al., 2012b). A basalt flow outcropping adjacent to 27.8 Ma rhyolite (Heyl et al., 1983) in poorly exposed Santa Fe sediment near Priest Tank, located 5.1 km (3.2 mi) south-southeast of the southwestern corner of the quadrangle, returned an $^{40}\text{Ar}/^{39}\text{Ar}$ age of 19.06 ± 0.05 Ma. These stratigraphic relations strongly suggest that the base of the Santa Fe Group on this quadrangle is 19-20 Ma. The aforementioned, 18.7 Ma basalt flows locally overlie a well-cemented, poorly sorted conglomeratic sandstone that may possibly correlate to unit **Tsflc**. If so, then the boundary between **QTsf** and **Tsflc** is 18-19 Ma. **QTsf** is contiguous to what has been mapped as Palomas Formation to the southeast (Heyl et al., 1983; Cikoski and Koning, 2013), which is 4.5-0.78 Ma in age

(Morgan and Lucas, 2012, and paleontologic work cited therein; Repenning and May, 1986; Mack et al., 1993, 1998; Leeder et al., 1996; Seager and Mack, 2003). Thus, the upper Santa Fe Group on this quadrangle (**QTsf**) includes Pliocene strata, and may very well extend into the late Miocene. The top of the unit may possibly be Pleistocene in age. Over the past few decades, workers have restricted the Palomas Formation to Pliocene-Pleistocene strata. Because **QTsf** probably extends into the late Miocene, to be consistent with the Palomas concept we elected not to use the term "Palomas Formation" in this quadrangle.

Lower, coarse-grained Santa Fe Group (Tsflc)

The lower-middle Santa Fe Group is composed of ~1500 m of sandy conglomerate, with minor pebbly sandstone, that is mostly in very thin to medium, tabular to lenticular beds (Fig. 29). Cross-stratification is relatively minor. Gravel is poorly to moderately sorted and subrounded to subangular. The gravel is composed of predominately of light gray, crystal-poor rhyolite and Vicks Peak Tuff, with minor tuff with distinct fiamme, crystal-rich rhyolite, and dark gray, plagioclase- +/- px-phryic andesite, and 0-5% vesicular, dark gray basalt. The sand is mostly a medium- to very coarse-grained, subrounded, moderately to poorly sorted, volcanic litharenite. Weak to strong cementation is pervasive, with >15% moderate to strong cementation over a given 10 m-thick stratigraphic interval. The contact between **Tsflc** and the overlying **Santa Fe Group** is conformable and gradational over several 10s of meters of stratigraphic distance. The lower ~30 m (100 ft) of the unit is steeply tilted and dominated by clasts reworked from unit **Trac**.

Santa Fe Group, upper part (QTsf)

The upper Santa Fe Group differs from the lower, coarser-grained part in that it is less cemented and contains more orange pebbly sand beds (Fig. 30). Beds range from very

thin to thick, tabular to lenticular, with minor cross-stratification. As in unit **Tsflc**, the gravel are poorly to moderately sorted and subrounded to subangular. Clasts are composed of crystal-poor rhyolite and Vicks Peak Tuff, with minor porphyritic rhyolite, welded tuff with distinct fiamme, and 10-20% plagioclase- +/- pyroxene-phyric andesite. As one approaches Garcia Canyon, the proportion of andesite clasts increases. The orange color in many of the pebbly sand beds comes from clay films or chips, which occupy 1-3% of the sand fraction, and locally as much as 10-15%,

Garcia Falls lithosome

Santa Fe Group sediment deposited by the Garcia Falls drainage is sufficiently distinct to differentiate on the geologic map and can be broken into a lower and upper unit. The lower unit consists of sandy conglomerate in medium to thick, tabular to broadly lenticular beds. It is at least 25 m thick. The poorly to moderately sorted clasts contain subequal proportions of plagioclase-phyric andesite (generally correlative to the Garcia Falls trachyandesite), crystal-poor Vicks Peak Tuff, and aphanitic rhyolite. The matrix is grayish brown to light gray, silty fine- to coarse-grained sand.

The upper unit contains less gravel than the lower unit and is approximately 75-80 m thick (Fig. 31). Sand or pebbly sand beds comprise 85% of the unit. Gravelly strata are in thin to thick, tabular beds. Sandy strata are massive to broadly planar cross-stratified. Gravels are poorly to moderately sorted and dominated by intermediate volcanic rock types, including 30-40% clasts of the Garcia Falls trachyandesite. The matrix consists of light brownish gray to light gray, well sorted, silt to fine -grained sand.

Quaternary terraces and high-level piedmont deposits

Relatively thin, unconsolidated and non-cemented, high-level piedmont deposits that disconformably overlie the Santa Fe Group are probably common on the broad ridges between drainages developed in the Santa Fe Group, but lack of exposure makes their identification questionable. However, there are two places in the quadrangle where exposures do allow definitive interpretations that these piedmont deposits exist. One is along the Burma Road on the south side of the head of Garcia Falls Canyon (**Qpag**). Good exposures here reveal sandy pebbles-cobbles in medium to thick, tabular beds, overlying the light gray Garcia Falls lithosome (Fig. 31). Clasts are moderately sorted, subangular, and consist of subequal proportions of Vicks Peak Tuff and Garcia Falls andesite. At a location 0.5 km south of Garcia Falls, this piedmont deposit is in a buttress relation with the underlying Santa Fe Group (**Tsfgu**) and 70 m (230 ft) thick. On the north side of the canyon, 0.5 km west of Garcia Falls, the deposit is ~35 m (120 ft) thick. This piedmont deposit gradually thins outward (west, southwest, and south) away from the head of Garcia Falls Canyon. It is very likely Pliocene in age and correlative to the Palomas Formation to the southeast.

The other high-level piedmont deposit, identified with certainty because of adequate exposure, is located south of Seferino Hill. There, it is a pebble-cobble gravel in medium to thick, tabular beds. Clasts are poorly to moderately sorted, subangular to subrounded, and comprised of 50-60% pebbles, 35-45% cobbles, and sparse boulders ($\leq 5\%$). Gravels mostly correlate to the Seferino Hill Conglomerate (unit **Trrs**). This deposit is rarely more than 3 m thick.

Pleistocene terrace gravel differ from the underlying Santa Fe Group in that they contain higher proportions of cobbles and boulders (a well-graded distribution of pebbles through boulders is not uncommon), whereas the Santa Fe Group is dominated

by pebbles, and there are ~10-15% tan andesites(?) with 3-10 mm long plagioclase phenocrysts. Other clasts include: 40-75% light gray to gray to pink, fine-grained rhyolite or Vicks Peak tuff, 10-40% light gray to tan, porphyritic (commonly feldspar-phyric) rhyolite or dacite, a1-10% tuffs with distinct fiamme, 5-30% dark gray, plagioclase- to pyroxene-phyric andesite, and trace to 1% basalt. The sand is light brown to reddish brown and mostly medium to very coarse-grained.

Deposits associated with five terrace levels were mapped along Alamosa Creek (Fig. 32), which are summarized from oldest (highest) to youngest (lowest). The surface (tread) of the highest of these terraces, **Qta5**, projects to the Cuchillo surface. The strath of **Qta4** lies 65-85 m above modern stream grade and it is 4-8 m thick. The **Qta4** terrace contains a thicker fill, 7-15 m thick, and its strath lies 45-54 m above modern stream grade. Sediment is also relatively thick in the **Qta3** terrace (12-18 m) and its strath lies 30-38 m above modern stream grade. **Qta2** is relatively thick downstream (Fig. 33) but thins in an upstream direction. Its strath lies 18-30 m above modern stream grade, and locally it can be subdivided into three subunits whose treads differ in height by 1-6 m. **Qta1** is the lowest and most laterally extensive terrace. Its sediment is generally thin (2-6 m) and coarser than higher terrace deposits (Fig. 33). Its tread lies 8-15 m above modern stream grade. Like **Qta2**, it is locally subdivided into three subunits whose treads differ in height by 1-3 m. Whereas the older terraces seem mostly to be fill terraces, except the upstream end of **Qta2**, **Qta1** can be considered a strath terrace throughout the quadrangle. Table 1 correlates these terraces with those mapped downstream by McCraw and Williams (2012). Following McCraw and Williams, we infer that the terraces formed in response to glacial-interglacial cycles but we infer that the lowest terrace (**Qta1**) formed during the transition between oxygen isotopes 5 and 6. Table 1 also presents are inferred ages for the terraces, but more work needs to be done to establish the ages of the terraces (perhaps using OSL).

TABLE 1. Terrace correlations with McCraw and Williams and our inferred ages*

Terrace map unit	Height above the floodplain (m)	Correlation with McCraw and Williams (2012)	Inferred age (ka)
Qta1	8-15	Qt6	40-140
Qta2	18-30	Qt5	200-270
Qta3	30-38	Qt4	300-350
Qta4	65-85	Qt2	620-650
Qta5	400	Cuchillo surface	780-800

* Note that our inferred ages differ from those of McCraw and Williams (2012)

GEOMORPHOLOGY OF THE WESTERN QUADRANGLE

Two prominent geomorphic surfaces are present in the western quadrangle (Figs 2, 34). The higher is called the Burma surface (McCraw and Love, 2012) and occupies the broad, concordant ridges southwest of Garcia Falls. Much of it appears to be underlain by the sandy gravel of unit **Qpag**. The lower surface, called the Cuchillo surface (Lozinsky, 1986; Lozinsky and Hawley, 1986; Maxwell and Oatman, 1990; McCraw and Love, 2012). The Cuchillo surface coincides with the tread of our highest terrace, **Qta5**. Near Monticello, about ~100 m (300 ft) separates the two surfaces. Stage III to IV calcic horizons are commonly present on the Cuchillo surface (e.g., McCraw, 2012, and McCraw and Love, 2012). However, calcic horizons on the Burma surface are weaker (e.g., no stage IV soils were observed), probably due to erosion and higher surface instability. The age of the Cuchillo surface is well constrained at 0.78-0.8 Ma (Mack et al., 1993, 1998; Mack and Leeder, 1999; Mack et al., 2006). The Burma surface was speculated to be Pliocene and possibly Miocene (McCraw and Love, 2012). Other geomorphic surfaces exist in the Palomas Basin, such as the Willow Spring Draw Fan, but the height difference between them and the Cuchillo surface are much less than 100 m (300 ft).

McCraw and Love (2012) proposed the Cuchillo surface overlies older deposits upstream along Canada Alamosa (i.e., Pleistocene downstream and pre-Pleistocene near Monticello). We interpret that the 4-8 m of sandy gravel underlying the Cuchillo surface (i.e., the **Qta5** deposit) is still Pleistocene in age but thickens downstream. In lower Canada Alamosa, the upper 80-100 ft of the Palomas Formation is coarser than underlying sediment (Daniel Koning, unpublished data). It is possible that this coarser interval correlates with the **Qta5** deposit. However, it is true that the **Qta5** deposit, which is readily recognizable due to the presence of coarse-porphyrific, leucocratic volcanic or intrusive rocks, overlies Miocene sediment in the vicinity of Monticello (**QTsf** and **Tsflc**).

Given that the aforementioned stratigraphic relations of the Cuchillo and Burma surfaces, we interpret that erosion was occurring on this quadrangle concomitant with at least part of Palomas Formation aggradation to the southeast (Fig. 34). Perhaps aggradation of **Qpag** and the lower Palomas Formation was time-equivalent, but that was followed by incision of Alamosa Creek on this quadrangle. The resulting detritus was transported downstream and incorporated into Palomas aggradation. The driver of this erosion may have been climatic, perhaps coinciding with increased discharges at the start of the Pleistocene at 2.6 Ma. The increased discharge, coupled with lower tectonic subsidence rates (Koning, 2012), may have also spurred basin spill-over in the Winston basin to the northwest. This spill-over would have greatly enhanced the drainage area of Alamosa Creek and provided it with increased discharge -- further enhancing its erosive capability. In summary, we interpret that Alamosa Creek likely integrated in the early Pleistocene, as a result of low tectonic subsidence rates in the Winston graben and increased discharges due to a change into stronger glacial-interglacial climates, and this integration led to erosion of the Santa Fe Group near Monticello while the upper Palomas Formation was aggrading to the southeast.

Another interesting aspect of the geomorphology in the western quadrangle is the extensive presence of recent alluvium (historical and modern) in the bottoms of major drainages (e.g., Alamosa Creek, Placitas Canyon, Lemes Canyon, Canada Quirino) and extensive hillslope erosion. Instead of incised arroyos that are so common in many areas of the southwest, the streams here are wide and readily migrate laterally. Recent gullying of hillslopes is also evident, as illustrated in Fig. 35 and as observed on the southwest slope of Alamosa Creek southeast of Placitas. Evidently, the eroding hill slopes are providing so much detritus to the stream bottoms that the valley bottoms are rapidly aggrading.

Much slower aggradation of the valley bottoms occurred earlier in the Holocene (prior to ca. 800 years ago), as reflected in the cumulic soils and finer textures seen in the older Holocene deposits (**Qay**). At a study site 6.5 km (4 mi) km northwest of the northwest corner of the Monticello quadrangle, Monger et al. (2014) interpret that between 3180 and 160 yr B.P., **Qay** experienced aggradation during drier periods, and stability or even incision during wetter periods and enhanced grass cover. Furthermore, they are able to constrain the timing of major incision of Canada Alamosa to 700-600 years ago, based on C-14 dates in uppermost Qay deposits and in buried soils on the valley floor (Monger et al., 2014). The prominent **Qaha** deposit along Canada Alamosa, which is presently farmed by local residents (Fig. 32) appears to have largely formed between 600-100 years ago -- overlapping with the Little Ice Age.

STRUCTURE

The most noteworthy structural feature on the quadrangle is the Monticello graben of McLemore (2012a). Our mapping demonstrates that it is a half-graben tilted eastward towards the Deep Canyon fault. The Deep Canyon fault, a name used by both Farkas (1969) and Hermann (1986), extends virtually the entire length of the quadrangle (13

km), generally separating Santa Fe Group on the west from older bedrock on the east. At Placitas Canyon, the uppermost Santa Fe Group overlapped 0.6 km eastward onto the fault footwall. On the immediate southeast side of Placitas Canyon, where it crosses the fault, there appears to be a degraded fault scarp, ~10 m tall, developed on the surface of unit **QTsf**. We did not measure any slickenlines along the fault, but exposures of it near Garcia Falls indicate it dips 50-70° W, consistent with a west-down normal fault.

At Seferino Hill, the Deep Canyon fault appears to link with the Willow Draw fault via two east-west faults that bound the north and south sides of Seferino Hill. The southern of these east-west faults is offset, in a right-stepping manner, by the Willow Draw fault. This offset suggests that the Deep Canyon fault is older than the Willow Draw fault. The Willow Draw fault continues southward at least 17 km, where it forms prominent fault scarps on the surface of the Palomas Formation that are as much as 6 m tall (McLemore et al., 2012a, Stop 4; Cikoski and Koning, 2013) and has offset the upper terraces along Alamosa Creek, indicating it has moved in the middle Pleistocene (McCraw and Williams, 2012). On this quadrangle, however, the upper Santa Fe Group surface is not notably offset, indicating decreasing throw rates to the north along the Willow Draw fault.

There is no evidence of a fault bounding the western side of the Monticello graben, at least on this quadrangle. Rather, the basal Santa Fe Group clearly overlies, or is in a buttress relation, with underlying bedrock (i.e., the Rhyolite of Alamosa Creek, **Trac**) (Fig. 36). The lower Santa Fe Group, unit **Tsflc** preserved west of Alamosa Creek, is tilted 10-26° E. In contrast, upper Santa Fe Group strata (unit **QTsf**), preserved east of Alamosa Creek, is tilted less than 7° E. This younging-upward decrease in tilt provides evidence that the Monticello graben was filling up with sediment during extension-related tilting and faulting along the Deep Canyon fault. On the cross-section,

extending the 10-15° dips to the east results in the Santa Fe Group being as thick as 5900-6200 ft (1800-1900 m). This thickness is not unreasonable, given that an oil exploratory well 12 km south-southeast of the southeastern quadrangle boundary (the Gartland 1 Garner) TD'd in the Santa Fe Group at a depth of 5900 ft (1800 m).

As illustrated in the cross-section, the upper Santa Fe Group (**QTsf**) is tilted much less than older strata (**Tsflc**), 0-6° vs. 10-25°. Near the cross-section and also at Lemes Canyon, dips decrease by half (from 13 degrees to 5-6 degrees near the cross-section, and from 20-26 to 7 degrees in Lemes Canyon) in the lowest 120-230 m (400-750 ft) of **Tsflc**. Assuming relatively constant sedimentation rates, it appears that extensional tectonism was strongest during deposition of unit **Tsflc**, which postdates 20 Ma and probably extends through the Early and Middle Miocene. High rates of late Early and Middle Miocene tectonism are consistent with tectonic interpretations by Cather et al. (1994).

Stratal dips in the Santa Fe Group are generally northwest, parallel the Deep Canyon fault, and dips are to the southeast. However, within 3 km of the northern boundary of the quadrangle, strikes are northeast to northwest but dips are to the south. This indicates that throw on the Deep Canyon fault very likely increases southward of the northern quadrangle border.

In bedrock east of the Deep Canyon fault, faults generally trend due-north to 060°. We generally did not observe exposures of fault planes in this area, but we agree with past workers that the faults are likely high-angle, normal faults (Farkas, 1969; Davis, 1986; The faults are not exposed, and we make the assumption that they are normal faults. We make note of the three longest, highest-displacement faults in this bedrock terrain. One of these long faults is a north-striking (bending to the northeast in its middle part),

east-down fault that extends from the northern quadrangle boundary to upper Uvas Canyon to the Burma Road. It has a maximum throw of ~240 m (800 ft), increasing to the north. The second of the three longest faults is a northeast-striking, northwest-down fault that extends from the lower Burma Road (where it strikes almost due east) to the northeast corner of the quadrangle (where it strikes ~020°). Near its center, it has a throw of about 300 m (1000 ft). The third of the longest faults is a west-down fault located 0.5-1.0 km west of the eastern quadrangle boundary, extending into lower Aragon Draw. According to cross-section A-A', it has a throw of 400 m (1300 ft).

In the northeastern quadrangle, faults on the footwall of the Deep Canyon fault have affected the Vicks Peak Tuff, so younger movement on them post-dates 28.4 Ma. However, to the west many of the rhyolitic dikes extend across the faults without being notably offset. Evidence of faulting during Rock Springs time is preserved on the east side of Red Rock Canyon. Here, a northwest-striking fault, located immediately north of La Questa de Trujillo, offsets Hells Mesa Tuff and older Rock Springs strata, but is buried by younger trachytic lavas and volcanoclastic sediment (i.e., units **Trst** and **Trssv3**). Also, in Street Canyon, tilting of strata occurred prior to emplacement of the Vicks Peak Tuff, presumably in conjunction with faulting. Davis (1986) note that faults in the Aragon Hill area predated the rhyolite intrusions (**Tir**). In addition, Hermann (1986) notes evidence of syn-eruptive (during Rock Springs volcanism) displacement on the Rock Springs fault, located 1.6 km (1 mile) north of the central northern quadrangle border. Like the #1 and #2 faults mentioned in the previous paragraph, the Rock Springs fault bends from a northeast to a northerly strike. Given their similar geometry, it is likely that these faults were likely active during the same time period (i.e., 35-28.5 Ma, the age range of the Rock Springs Formation). The rhyolites have yet to be dated, but are likely related to rhyolitic volcanism immediately postdating the Vicks Peak Tuff eruption (28.0-28.4 Ma). Considering the low amounts of fault displacement of the

rhyolite dikes, it appears that most fault movement of the eastern faults occurred between 35 and 28.5 Ma, with some activity continuing past 28 Ma that affected the Vicks Peak Tuff.

Smith (1992) interprets that the rhyolite stocks and dikes trend 285° and another set of faults and dikes trends 030-065,° and that this trend does not correspond well with the east-west extension preposed to have existed in the Rio Grande rift in the early Oligocene (Foruria, 1984). This led Smith (1992) and Davis (1988) to infer that this trend could be related to tensional stresses related to the Nogal Caldera. Davis (1988, p. 28) actually states that east-trending faults near Aragon Hill may correspond to a caldera ring-fracture zone. Based on interpretations of faults and the southern caldera margin by Hermann (1986), we do not believe the northeast-trending faults are related to the Nogal Caldera, nor do we think there are major ring-fracture faults on this quadrangle. However, it's possible that the west-northwest-trending dikes and faults did initiate from stresses associated with caldera formation. We note, however, that the west- to northwest-trending faults commonly terminate at northerly trending structures and that they locally offset the Vicks Peak Tuff.

GEOLOGIC HISTORY

Pennsylvanian strata exposed in the Monticello quadrangle are Morrowan to Missourian in age and were generally deposited in deep marine shelf environments, excluding local tidal-fluvial siliciclastic beds found near the bottom of the Red House Formation and shale-limestone intervals of the Bar B Formation. The ancestral Rocky Mountain orogeny coincides with the deposition of Pennsylvanian strata, beginning during the latest Morrowan to Atokan (Kues and Giles, 2004). Among the early events of this orogeny were uplift and erosion of the Pedernal uplift to the east and subsequent transgression throughout the state (Ye et al., 1996). Coarse-grained facies in the Red House were likely sourced from the Pedernal uplift and perhaps more proximal

highlands. Transgression reached a maximum during the Desmoinesian age (Kues and Giles, 2004), with sedimentation into a slowly subsiding basin resulting in the formation of the Nakaye Formation. The shale-rich Bar B Formation represents deposition on a shallower marine shelf during the Desmoinesian-Missourian, with turbidity current events resulting in limestone conglomerate beds near the top of the formation. Soreghan (1994) interpreted glacio-eustatic cyclicity in Bar B strata, though the exact stratigraphic context of these cycles is unclear (Lucas et al., 2012). Lucas et al. (2012) note that thickness differences and facies changes between Pennsylvanian sections in the Mud Springs and Fra Cristobal-Caballo Mountains may be explained by Pennsylvanian tectonism, including differential subsidence along the Caballo uplift during Bar B deposition. Perhaps multiple episodes of local deformation throughout deposition of Pennsylvanian strata account for the substantially (~2-3x) thicker section in the Monticello quadrangle.

Prior to post-38 Ma volcanism, the quadrangle was uplifted during the Laramide orogeny. This uplift allowed erosion that stripped away the Mesozoic and Permian strata observed elsewhere in the region. This erosion resulted in hilly topography and valleys, which were filled in by post-38 Ma lavas and volcanoclastic sediment. West of Red Rock Ranch, comparison of attitudes between the Whiskey Hill Member and Pennsylvanian strata indicates the latter dip much more steeply, as illustrated in cross section A-A'. We speculate that there may have been monoclinial folding and possibly reverse faulting along the Deep Canyon fault during Laramide time, which resulted in a steepening of strata to the east of this structure prior to emplacement of the Whiskey Hill Member.

A period of intense volcanism began in the late Eocene, probably around 38 Ma, given the volcanic stratigraphy and age control in the northern Sierra Cuchillos (i.e., the

$^{40}\text{Ar}/^{39}\text{Ar}$ age of 37.5 Ma from the andesite-latitude of Montoya Butte and its correlation to the thick andesite sequence to the south (Maldonado, 2012)). Early deposition was a mix of volcanoclastic sediment and dacite (minor andesite) flows, represented by the Whiskey Hill Member of the Red Rock Ranch Formation. Later, andesitic lavas flowed into the study area from the north (Fig. 8). These lavas are represented by the Uvas Canyon basaltic trachyandesite, Garcia Falls trachyandesite, Luna Peak trachyandesite, and the Red Rock Arroyo andesite. The lower of these lavas, the Uvas Canyon basaltic trachyandesite, has been dated by K/Ar techniques at 36.7 ± 1.1 Ma (reported in Meyer, 1986, based on U.S. Geological Survey memorandum from J.C. Von Essen, 2 May 1983, potassium-argon report no. 153, Menlo Park).

The andesitic lavas of the middle Red Rock Ranch Formation, particularly the Uvas Canyon-Garcia Falls members and the Luna Peak trachyandesite, blocked drainages flowing northeast, resulting in a northwest-elongated lake and deposition of lacustrine sediment of the Placitas Canyon Member (Fig. 8). Two tongues of the Placitas Canyon Member are mappable, which were deposited at the start and end of Uvas Canyon basaltic andesite emplacement. Springs flowing up from the Deep Canyon fault may also have fed this lake. With time, a given lava likely spilled into the lake and prograded over the Placitas Canyon Member. Higher evaporation rates, or higher concentrations of dissolved calcium carbonate in the lake water, resulted in episodic precipitation of limestone beds in the upper tongue of the Placitas Canyon Member.

The tuff of Aragon Draw was deposited shortly after emplacement of the Red Rock Arroyo andesites. Given the boulders found in the top of the tuff, a nearby source is inferred, probably a short distance east of the quadrangle. Remorphic textures in the tuff indicates a relatively steep paleoslope.

An unknown period of time passed between emplacement of the tuff of Aragon Draw and the Lower Luna Park Tuff. During this time, 60-150 m (200-500 ft) of andesite and trachyte flows accumulated in the north-central part of the quadrangle, with a period of erosion and valley carving occurring between the andesite and trachyte flows.

Paleovalleys were also carved in the tuff of Aragon Draw in the southeastern quadrangle, which were filled by andesitic lavas and a tuffaceous, relatively massive sediment (together being as much as 40 m (130 ft) thick. The andesite was then carved by another paleovalley, which was backfilled by the tuff of Jose Maria Canyon.

Signaling the end of Red Rock Ranch deposition, the Lower Luna Park Tuff is the lowest of three regional tuffs that intertongue with the Rock Springs Formation. Based on speculative correlations of the Luna Park Tuffs ($^{40}\text{Ar}/^{39}\text{Ar}$ ages are pending), the Rock Springs Formation may span from 35.5 Ma to 28.4 Ma (the age of the Vicks Peak Rhyolite), whereas the underlying Red Rock Ranch Formation is 38-35.5 Ma. The Rock Springs Formation is composed of interbedded volcanic flows (i.e., trachytes and andesites) and volcanoclastic sediment that was deposited in the time between tuff emplacement. This interbedded package of tuffs and Rock Springs Formation is less than 300 m (1000 ft) thick, compared to 760-1100 m (2500-3600 ft) for the Red Rock Ranch Formation. Given available age control for the two stratigraphic packages, it appears that stratal accumulation rates decreased drastically after ca. 35 Ma.

The Vicks Peak Tuff erupted from the Nogal caldera at 28.4 Ma, forming a >100 m-thick blanket of ash over an erosional landscape with paleovalleys. Tectonism and tilting of strata had occurred prior to the Vicks Peak Tuff eruption, as shown by an angular unconformity in Street Canyon. Crystal-poor rhyolites, that likely tapped the same magma chamber as the Vicks Peak Tuff, were extruded immediately after the tuff.

These rhyolites were then covered by more felsic tuffs related to the Shipman Canyon tuff complex.

Deposition in the Monticello graben began shortly after 20 Ma. Westward onlap may have occurred if tilt rates were initially high; if so, basal Santa Fe Group deposits may possibly be older adjacent to the Deep Canyon fault than the basal deposits preserved on the distal hanging wall side, near the western quadrangle border. Tilt rates appear to have been relatively rapid during the late Early and Middle Miocene, as manifested by the 10-20° change in dip in the lower Santa Fe Group unit (**Tsflc**), compared to the 0-6° change in the upper Santa Fe Group (**QTsf**).

After aggradation of the Santa Fe Group ceased, several interesting geomorphic events took place (Fig. 34). First, erosion near the northern Deep Canyon fault occurred that was followed by sedimentation -- as exemplified by high-level piedmont deposits near Garcia Falls. The Burma surface formed on top of these piedmont deposits and probably extends onto the maximum aggradational surface of the older Santa Fe Group (**QTsf**). An extensive period of erosion then occurred, resulting in ~100 m (300 ft) difference between the Burma surface and the tread of the highest terrace (**Qta5**), the latter projecting to the Cuchillo surface to the south.

Nowhere else in the northern Palomas basin do we find two geomorphic surfaces separated by such a large magnitude of height, so we infer that something unique happened here to result in this phenomena. The most likely event, in our interpretation, is the integration of Alamosa Creek with the Winston graben to the northwest. Koning (2012) implies this integration took place in the early Pliocene. But given the inferred Pliocene age of the Burma surface and the well-constrained age of the Cuchillo surface (0.78-0.8 Ma; Mack et al., 1993, 1998; Mack and Leeder, 1999; Mack et al., 2006), it is

more likely that the integration took place in the early Pleistocene -- perhaps as early as 2.6 Ma. Remarkably, erosion occurred on the Monticello quadrangle concomitant with Palomas Formation aggradation to the south-southeast (Fig. 35).

Erosion continued on the Monticello quadrangle through the middle and late Pleistocene, resulting in four terrace levels (**Qta4** through **Qta1**) inset into the northern projection of the Cuchillo surface (**Qta5**). Significant hillslope gullying and erosion (Fig. 35) is occurring today in the western quadrangle, filling the valley floors faster than sediment can be moved downstream by drainages. Consequently, historical and modern alluvium cover large areas of valley floors, although the heads of low order drainages typically are underlain by older Holocene alluvium that is gullied.

SAN MATEO MOUNTAINS MINING DISTRICT

by Virginia T. McLemore

Introduction

The San Mateo Mountains mining district covers portions of the Monticello, Sierra Fijardo, and Priest Tank 7.5 minute topographic quadrangles in the southern San Mateo Mountains and also is known as Goldsboro, Goldsborough, and Monticello district. The names of the district are from Harley (1934) and File and Northrop (1966). Volcanic-epithermal vein, volcanogenic uranium, placer gold, and placer tin deposits are found in the district. Names of types of mineral deposits are from Cox and Singer (1986), North and McLemore (1986, 1988), and McLemore (1996, 2001). Many of the mines and prospects in this report are described in the New Mexico Mines Database (McLemore et al., 2002, 2005a, b) and are identified by a unique mine identification number (Mine id), beginning with NM (for example NMSI1765).

The U.S. Bureau of Mines examined the northern and central San Mateo Mountains as part of evaluating the mineral resource potential of the Withington and Apache Kid Wilderness Study Areas (Neubert, 1983). In 1995, the U.S. Bureau of Mines released a report with chemical analyses of samples collected from the San Mateo Mountains district during an evaluation of the U.S. Bureau of Land Management's Caballo Resource Area (Korzeb et al., 1995). The U.S. Geological Survey (USGS) with this author examined the area again in the late 1990s, and a CD-ROM of data was published (Green and O'Neill, 1998), but the collective data was never interpreted because of time constraints. The author examined the mines and prospects in 2013-2014 as part of the Statemap program. The San Mateo Mountains district was briefly described by McLemore (2012d) and the geology was summarized by McLemore (2012b).

The mines found in the San Mateo Mountains district are listed in Appendix 3 and chemical analyses of mineralized samples collected from the district are in Appendix 4. Appendix 3 includes chemical analyses of unmineralized igneous rocks collected from the district.

Mining and exploration history

Total production from the San Mateo Mountains district is unknown, but estimated to be less than \$10,000. Most of the gold production from the district probably came from the Aragon Hill mines (NMSI1765, NMSI1761, NMSI1763, NMSI1764, NMSI1762, NMSI1767, NMSI0268; Appendix 3). Only sporadic exploration and prospecting for gold has occurred in the district over the last 20 years, but at least two companies have examined the district in recent years in response to the increase in the price of gold.

Gold is found along a silicified fault-zone at Fifty-fifty Hill (Questa Blanca Canyon; NMSI0270) in sections 5 and 6, T11S, R5W prior to 1930. Apache Energy and Minerals

Co. acquired the property in 1979 and conducted exploration drilling at Fifty-fifty Hill in 1980. Fifteen rotary holes were drilled totaling 6,165 ft.

Placer gold deposits are found near Aragon Hill (NMSI0267) and placer tin (NMSI0272) deposits are found in Monticello Canyon. Gold placer production has been small and there has been no tin produced. Several active placer claims are near Aragon Hill, where prospectors sporadically process the gravels for a few ounces of gold.

Uranium was discovered at the Terry deposit (NMSI0273) in 1948 by E.H. Terry, who leased the property to Hanosh Mining Co. and then to McDaniel Investment Co. In 1955 and 1960, McDaniel Investment Co. produced 127 short tons of ore containing 359 lbs of U₃O₈ (0.14%) and 27 lbs V₂O₅ from the Terry mine. After 1960, mining ceased because the mill could not recover uranium from the ore from the Terry mine. The property was evaluated by Apache Energy and Minerals Co. in 1979-1980, but no additional development occurred.

Brief description of Mineral Deposits

Volcanic-epithermal vein deposits

At Aragon Hill in the San Mateo Mountains district, quartz-fluorite veins and mineralized shear zones with gold cut an altered Tertiary rhyolite intrusion and andesite. The veins and mineralized shear zones are 3-10 ft wide, trend predominantly north-south, and consist of quartz, iron oxides, kaolinite, pyrite, native gold, and traces of barite, malachite, azurite, and bornite (Harley, 1934; Farkas, 1969; Lovering and Heyl, 1989; Davis, 1988). Cassiterite is reported at Aragon Hill by Korzeb et al. (1995, #745), but the chemical analyses (Appendix 4) indicated all samples contained <20 ppm Sn. The rhyolite is highly silicified and altered to kaolinite, sericite, and iron oxides, whereas the andesite is less altered to chlorite and quartz. Acid leaching and silica replacement of the rhyolite are indicated by vuggy and fine-crystalline textures (acid

sulfae alteration). Samples contained 210 to 660 ppb Au (Appendix 3). Assays of samples reported by Davis (1988) range from <1.6 to 260 ppm Au and 3 to 347 ppm Ag. Alunite is found in the altered areas at Aragon Hill. The acid-sulfate alteration is similar to that found in Norris geyser basin, Yellowstone National Park (Kharaka et al., 2000) and Steeplerock district, Grant County, New Mexico (McLemore, 1993), which is related to geothermal activity. A similar origin is envisioned for the alteration and mineralization at Aragon Hill (Henley and Ellis, 1983).

Prospect pits on the Douglas claims (NMSO0017, NMSI0269, NMSO0568, NMSO0574, NMSO0569, NMSO0570, NMSO0571, NMSO0572, NMSO0573, NMSO0567) in section 35, T9S, R6W expose bleached and silicified rhyolite dikes and quartz veins. The rhyolite is highly silicified and altered to kaolinite, sericite, and iron oxides, whereas the andesite is less altered to chlorite and quartz. Acid leaching and silica replacement of the rhyolite are indicated by vuggy and fine-crystalline textures. Pyrite contents are locally as much as 5%. Smith (1992) reports assays of 0.2-1.3 ppm Au and 0.17-1.26 ppm Ag (Smith, 1992). Our samples contained <2-15 ppb (Appendix 4).

The Terry or Pitchblende Strike deposit (NMSI0273) is a radioactive, fluorite-bearing volcanic-epithermal vein along the contact between Magdalena Group limestones and a Tertiary andesite sill. Both the limestone and andesite are silicified and local jasperoid zones are common within the limestone along the intrusive contact. Other minerals found include fluorite, uranophane, tyuyamunite, carnotite, and uraniferous opal from the deposit (Bassett, 1954; Berry et al. 1982; Broomfield and Pierson, 1982; McLemore, 1983). The andesite has been altered to chlorite, kaolinite, and sericite (Bassett, 1954). Six drill holes encountered fluorite, but no chemical analyses are available. Jasperoid samples from the Terry deposit and adjacent areas contain as much as 10% F, 700 ppm V, 700 ppm Y, 300 ppm Pb, 1,000 ppm Cu, 50 ppm W, 3,000 ppm Ba, and traces of silver

and gold (Lovering and Heyl, 1989). A sample of the vein collected by the author in 1980 assayed 0.05% U₃O₈ (McLemore, 1983). Three samples collected and assayed by Korzeb et al. (1995, #741–743, Appendix 4) ranged from 128 to 1,430 ppm U.

Fifty-fifty Hill (Questa Blanca Canyon) in sections 5 and 6, T11S, R5W is a silicified rhyolite plug. A northwest-trending fault west of Fifty-fifty Hill (NMSI0270) is mineralized and developed by a shaft and several prospect pits. Assays of drill cuttings by Apache Energy and Minerals Co. were sporadic, but 13 holes encountered mineralized zones that assayed as much as 0.75 oz/short ton (24 ppm) Au and 1.5 oz/short ton (48 ppm) Ag (Table 2; Apache Energy and Minerals Co., unpublished report dated March 1981, on file at the Anaconda Geological Document Collection, American Heritage Center, University of Wyoming, #43207.01). Calcite veins with trace amounts of pyrite and some quartz are found along the Questa Blanca Canyon north of the Fifty-fifty shaft. A short adit was developed along additional calcite veins on Sererino Hill (NMSI1769).

Placer gold deposits

Placer gold deposits are found in the arroyos draining Aragon Hill (NMSI0267) and have been mined on small scale, mostly by individuals. The gold is found within stream gravels. The deposits are small and irregular; depth to bedrock is less than 10 ft. There is no official reported production, but several individuals have worked the arroyos for approximately 20 years and obtained enough gold to use in making jewelry. Fourteen stream-sediment samples were collected from several arroyos in the San Mateo Mountains district to evaluate the mineral resource potential. Gold ranges from <2 to 9 ppb (Table 3), indicating limited gold potential in the area.

Placer tin deposits

Placer tin deposits are found in the arroyos draining the Sierra Cuchillos near Monticello (NMSI0272). There is no information on the size and grade of these deposits.

Mineral Resource Potential

There are no active mines or exploration permits in the San Mateo Mountains district. However, in recent years, several companies and individuals have staked claims in the district in response to the recent increase in gold and silver prices. There is mineral resource potential for gold and silver in these districts, but the potential needs to be re-evaluated because of the change in economics of precious metals. The fluorite, uranium, and tin deposits are small, low grade and uneconomic. The rare earth elements (REE) are low in both the mineralized and unmineralized samples (Figs. 37 and 38) indicating no REE potential.

TABLE 2. Average grade of entire sampled vertical holes drilled at Fifty-fifty Hill (Questa Blanca project) by Apache Energy and Minerals Co. in 1980 (Apache Energy and Minerals Co., unpublished report dated March 1981, on file at the Anaconda Geological Document Collection, American Heritage Center, University of Wyoming, #43207.01).

HOLE NO.	TOTAL DEPTH (ft)	Au (oz/short ton)	Ag (oz/short ton)	APPARENT THICKNESS (ft)	COMMENTS
0-0	145	0.03	0.39	145	9 ft of 0.02% eU ₃ O ₈
38S-29W	425	0.05	0.42	310	primary sulfides at 355-425 ft
90S-216E	340	0.05	0.34	320	primary sulfides at 300-340 ft
123S-480N	740	0.02	0.02	40	abandoned because of water at 740 ft
291N-351W	400	0.03	0.38	330	—
360N-231W	505	0.08	0.60	330	primary sulfides at 460-505 ft
441S-228E	125	0.03	0.32	125	no sulfides
486N-411W	?	0.01	0.18	300	—
501S-42E	525	0.08	0.33	385	primary sulfides at 515-525 ft
600N-771W	570	0.16	0.39	370	water at 440 ft
864N- 1131W	290	0.01	0.04	200	water at 255
961S-228E	455	0.06	0.33	320	no sulfides
1361S-458E	405	0.04	0.25	405	trace sulfides
1739S-548E	365	0.04	0.20	365	water at 80 ft
2339S-998E	205	0.05	0.02	195	—

TABLE 3. Stream sediment samples from selected arroyos in the San Mateo Mountains district. The samples were sieved to <2 mm in the field and analyzed by Activation Laboratories by INNA and ICP. Analyses are in ppm (parts per million) except for gold, which is in ppb (parts per billion). Latitude and longitude are in NAD27.

Sample no.	Latitude	Longitude	Ag	As	Au ppb	Mo	Sb	U	Y	Zn	La	Ce
VTM 01-96	33.4891532	- 107.4125956	<5	2.3	3	6	0.5	3.9	32	68	46	89
VTM 02-96	33.4894446	- 107.4135057	<5	2.4	<2	1	0.6	2.3	30	95	48	94
VTM 03-96	33.4874907	- 107.4132875	<5	1.9	<2	<1	0.7	3.4	28	67	45	95
VTM 04-96	33.4841226	- 107.4151208	<5	3	5	2	0.7	3.8	37	180	58	120
VTM 05-96	33.4830974	- 107.4148464	<5	3	<2	2	0.4	4.1	36	110	63	120
VTM 06-96	33.4822821	- 107.4143728	<5	3.2	<2	6	0.9	3.7	32	130	51	100
VTM 07-96	33.4795249	- 107.4148292	<5	1.7	<2	6	0.8	3.5	35	120	52	110
VTM 08-96	33.472352	- 107.4127036	<5	1.9	<2	<1	0.5	3.1	31	<50	47	91
VTM 09-96	33.4631772	- 107.4163429	<5	2.2	<2	<1	0.8	5.3	40	97	66	120
VTM 10-96	33.4584021	- 107.4110464	<5	1.9	9	<1	0.7	4.8	35	62	58	110
VTM 11-96	33.4754185	- 107.3874148	<5	7	4	3	2.3	5.2	46	90	60	130
VTM 12-96	33.4754185	- 107.3874148	<5	3.7	<2	4	1.5	3.8	46	89	67	140
VTM 13-96	33.4725074	- 107.3887286	<5	2.8	3	5	1.3	4.3	48	<50	63	130
VTM 14-96	33.4687162	- 107.3893623	<5	2.6	4	5	1.2	4	47	100	58	120

REFERENCES

- Atwood, G. W., 1982, *Geology of the San Juan Peak area, San Mateo Mountains, Socorro County, New Mexico; with special reference to the geochemistry, mineralogy, and petrogenesis of an occurrence of riebeckite-bearing rhyolite* [unpublished M.S. thesis]: Albuquerque, University of New Mexico, 168 p.
- Bassett, W. A., 1954, Mineralogical and geological investigation of the Terry uranium prospect near Monticello, New Mexico: *New Mexico Bureau of Mines and Mineral Resources, Open-file Report 19*, 15 p.
- Berry, V. P., Nagy, P. A., Spreng, W. C., Barnes, C. W., and Smouse, D., 1982, Uranium resource evaluation Tularosa quadrangle, New Mexico: *U.S. Department of Energy, Report GJO-014(82)*, 22 p.
- Birkeland, P. W., Machette, M. N., and Haller, K. M., 1991, Soils as a tool for applied Quaternary geology: *Utah Geological and Mineral Survey, Miscellaneous Publication 91-3*, 63 p.
- Birkeland, P. W., 1999, *Soils and geomorphology*: New York, Oxford University Press, 430 p.
- Broomfield, C. S. and Pierson, C. T., 1982, Uranium in the San Mateo Mountains, New Mexico: *in: Geological Survey Research, Fiscal Year 1981: U.S. Geological Survey, Professional Paper 1375*, p. 34.
- Cather, S. M., Chamberlin, R. M., Chapin, C. E., and McIntosh, W. C., 1994, Stratigraphic consequences of episodic extension in the Lemitar Mountains, central Rio Grande rift: *in: Keller, G.R., and Cather, S.M., eds., Basins of the Rio Grande Rift: Structure, Stratigraphy, and Tectonic Setting: Geological Society of America Special Paper 291*, p. 157-170.
- Chapin, C. E., McIntosh, W. C., and Chamberlin, R. M., 2004, The late Eocene-Oligocene peak of Cenozoic volcanism in southwestern New Mexico: *in: Mack, G.H., and Giles, K.A., eds., The Geology of New Mexico—A geologic history, New Mexico Geological Society Special Publication 11*, p. 271-293.

- Cikoski, C. T., and Koning, D. J., 2013, Geologic map of the Huerfano Hill quadrangle, Sierra County, New Mexico: *New Mexico Bureau of Geology and Mineral Resources, Open-file Geologic Map 243*, scale 1:24,000.
- Compton, R. R., 1985, *Geology in the field*: New York, John Wiley & Sons, Inc., 398 p.
- Cox, E. W., 1985, *Geology and gold-silver deposits in the San Jose mining district, southern San Mateo Mountains, Socorro County, New Mexico* [unpublished M.S. thesis]: Socorro, New Mexico Institute of Mining and Technology, 115 p.
- Cox, D. P., and Singer, D. A., 1986, Mineral deposit models, *U.S. Geological Survey, Bulletin 1693*, 379 p.
- Davis, D. R., 1988, *Geology of the Aragon Hill area, Sierra and Socorro Counties, New Mexico* [unpublished M.S. thesis]: Odessa, University of Texas of the Permian basin, 61 p.
- Deal, E. G., and Rhodes, R. C., 1976, Volcano-tectonic structures in the San Mateo Mountains, Socorro County, New Mexico: *in: Elston, W.E., and Northrop, S.A., eds., Cenozoic volcanism in southwestern New Mexico: New Mexico Geological Society, Special Publication No. 5*, p. 51-56.
- Farkas, S. E., 1969, *Geology of the southern San Mateo Mountains, Socorro and Sierra Counties, New Mexico* [Ph.D. dissertation]: Albuquerque, University of New Mexico, 181 p.
- Ferguson, C. A., 1986, Geology of the east-central San Mateo Mountains, Socorro County, New Mexico: *New Mexico Bureau of Mines and Mineral Resources, Open-file Report 252*, 124 p.
- Ferguson, C. A., Osburn, G. R., and McCraw, D. J., 2007, Preliminary geologic map of the Welty Hill quadrangle, Socorro County, New Mexico: *New Mexico Bureau of Geology and Mineral Resources, Open-file Geologic Map 148*, scale 1:24,000.
- Ferguson, C. A., Osburn, G. R., and McIntosh, W. C., 2102, Oligocene calderas in the San Mateo Mountains, Mogollon-Datil volcanic field, New Mexico [minipaper]: *New Mexico Geological Society Guidebook, 63rd Field Conference*, p. 74-77.
- Foruria, J., 1984, *Geology, alteration, and precious metal reconnaissance of the Nogal Canyon area, San Mateo Mountains, New Mexico* [unpublished M.S. thesis]: Fort Collins, Colorado State University, 178 p.

- File, L., and Northrop, S. A., 1966, County, township, and range locations of New Mexico's Mining Districts: *New Mexico Bureau of Mines and Mineral Resources Circular 84*, 66 p.
- Furlow, J. W., 1965, *Geology of the San Mateo Peak area, Socorro County, New Mexico* [M.S. thesis]: Albuquerque, University of New Mexico, 83 p.
- Gile, L. H., Peterson, F. F., and Grossman, R. B., 1966, Morphological and genetic sequences of carbonate accumulation in desert soils: *Soil Science*, v. 101, p. 347-360.
- Green, G. N. and O'Neill, J. M., 1998, Digital earth science database, Caballo resource area, Sierra and Otero counties, south-central New Mexico: *U.S. Geological Survey, Open-file Report OF-98-780*, CD-ROM.
- Harley, G. T., 1934, The geology and ore deposits of Sierra County, New Mexico: *New Mexico Bureau of Mines and Mineral Resources Bulletin 10*, 220 p.
- Henley, R. W., and Ellis, A. J., 1983, Geothermal systems, ancient and modern: a geochemical review: *Earth Science Reviews*, v. 19, p. 1-50.
- Hermann, M. L., 1986, *Geology of the southwestern San Mateo Mountains, Socorro County, New Mexico* [unpublished M.S. thesis]: Socorro, New Mexico Institute of Mining and Technology, 192 p.
- Heyl, A.V., Maxwell, C.H., and Davis, L.L., 1983, Geology and Mineral Deposits of the Priest Tank quadrangle, Sierra County, New Mexico: *U.S. Geological Survey, Miscellaneous Field Studies Map MF-1665*, scale 1:24,000.
- Ingram, R.L., 1954, Terminology for the thickness of stratification and parting units in sedimentary rocks: *Geological Society of America Bulletin*, v. 65, p. 937-938, table 2.
- Jahns, R. H., 1955, Geology of the Sierra Cuchillo, New Mexico: New Mexico Geological Society Guidebook of south-central New Mexico: *New Mexico Geological Society, 6th Field Conference*, p. 96-104.
- Kharaka, Y. K., Sorey, M. L., and Thordsen, J. J., 2000, Large-scale hydrothermal fluid discharges in the Norris-Mammoth corridor, Yellowstone National Park, USA: *Journal of Geochemical Exploration*, v. 69-70, p. 201-205.
- Koning, D. J., 2012, The Santa Fe Group in the northern Winston graben, southwest New Mexico, and how changing Rio Grande rift tectonism may have influenced its

deposition and erosion: *New Mexico Geological Society Guidebook, 63rd Field Conference*, p. 457-474.

- Korzeb, S. L., Kness, R. F., Geroyan, R. I., and Ward, D. A., 1995, Mineral resource assessment of the Caballo Resource Area, Sierra and Otero Counties, New Mexico: *U.S. Bureau of Mines, Open-file Report MLA 5-95*, 177 p.
- Kues, B. S. and Giles, K. A. , 2004, The late Paleozoic ancestral Rocky Mountains system in New Mexico: *in: Mack, G. H. and Giles, K. A., eds., The geology of New Mexico: A geologic history: New Mexico Geological Society, Special Publication 11*, p. 95-136.
- Leeder, M. R., Mack, G. H., and Salyards, S. L., 1996, Axial-transverse fluvial interactions in a half-graben -- Plio-Pleistocene Palomas Basin, southern Rio Grande rift, New Mexico, USA: *Basin Research*, v. 12, p. 225-241.
- Lovering, T. G. and Heyl, A. V., 1989, Mineral belts in western Sierra County, New Mexico, suggested by mining districts, geology, and geochemical anomalies: *U.S. Geological Survey, Bulletin 1876*, 58 p., <http://pubs.er.usgs.gov/usgspubs/b/b1876> (accessed September 5, 2010).
- Lozinsky, R. P., and Hawley, J. W., 1986, The Palomas Formation of south-central New Mexico – a formal definition: *New Mexico Geology*, v. 8, no. 4, p. 73-78 and 82.
- Lucas, S. G., Krainer, K., and Spielmann, J. A., 2012, Pennsylvanian stratigraphy in the Fra Cristobal and Caballo Mountains, Sierra County, New Mexico: *in: Lucas, S. G., McLemore, V. T., Lueth, V. W., Spielmann, J. A., and Krainer, K. (eds.), Geology of the Warm Springs Region: New Mexico Geological Society, 63rd Annual Field Conference Guidebook*, p. 327-344.
- Lynch, S. D., 2003, *Geologic mapping and ⁴⁰Ar/³⁹Ar geochronology in the northern Nogal Canyon caldera, within and adjacent to the southwest corner of the Blue Mountain quadrangle, San Mateo Mountains, New Mexico* [unpublished M.S. thesis]: Socorro, New Mexico Institute of Mining and Technology, 102 p.
- Mack, G. H., and Leeder, M. R., 1999, Climatic and tectonic controls on alluvial fan and axial-fluvial sedimentation in the Plio-Pleistocene Palomas half-graben, southern Rio Grande rift: *Journal of Sedimentary Research*, v. 69, p. 635-652.
- Mack, G. H., Salyards, S. L., and James, W. C., 1993, Magnetostratigraphy of the Plio-Pleistocene Camp Rice and Palomas Formations in the Rio Grande rift of southern New Mexico: *American Journal of Science*, v., 293, p. 49-77.

- Mack, G. H., Salyards, S. L., McIntosh, W. C., and Leeder, M. R., 1998, Reversal magnetostratigraphy and radioisotopic geochronology of the Plio-Pleistocene Camp Rice and Palomas Formations, southern Rio Grande rift: *in*: Mack, G. H., Austin, G. S., and Barker, J. M. (eds.), *Guidebook of the Las Cruces Country II: New Mexico Geological Society, Guidebook 49*, p. 229-336.
- Mack, G. H., Seger, W. R., Leeder, M. R., Perez-Arlucea, M., and Salyards, S. L., 2006, Pliocene and Quaternary history of the Rio Grande, the axial river of the southern Rio Grande rift, New Mexico, USA: *Earth-Science Reviews*, v. 79, p. 141-162.
- Maldonado, F., 1974, *Geologic map of the northern part of the Sierra Cuchillo, Socorro and Sierra Counties, New Mexico* [unpublished M.S. thesis]: Albuquerque, University of New Mexico, 59 p.
- Maldonado, F., 1980, Geologic map of the northern part of the Sierra Cuchillo, Socorro and Sierra Counties, New Mexico: *U.S. Geological Survey, Open-File Report 80-230*, scale of 1:24,000 <<<http://pubs.er.usgs.gov/usgspubs/ofr/ofr80230>>> (accessed June 17, 2014)
- Maldonado, F., 2012, Summary of the geology of the northern part of the Sierra Cuchillo, Socorro, and Sierra Counties, southwestern New Mexico: *in*: Lucas, S. G., McLemore, V. T., Lueth, V. W., Spielmann, J. A., and Krainer, K. (eds.), *Geology of the Warm Springs Region: New Mexico Geological Society, 63rd Annual Field Conference Guidebook*, p. 211-218.
- Maxwell, C. H., and Oakman, M. R., 1990, Geologic map of the Cuchillo quadrangle, Sierra County, New Mexico: *U.S. Geological Survey, Geologic Quadrangle Map GQ-1686*, scale 1:24,000.
- McCraw, D. J., 2012, Cuchillo surface overview and soils: *in*: Lucas, S. G., McLemore, V. T., Lueth, V. W., Spielmann, J. A., and Krainer, K. (eds.), *Geology of the Warm Springs Region: New Mexico Geological Society, 63rd Annual Field Conference Guidebook*, p. 158-161.
- McCraw, D. J., and Love, D. W., 2012, An overview and delineation of the Cuchillo geomorphic surface, Engle and Palomas Basins, New Mexico [non-peer reviewed mini-paper: *in*: Lucas, S. G., McLemore, V. T., Lueth, V. W., Spielmann, J. A., and Krainer, K. (eds.), *Geology of the Warm Springs Region: New Mexico Geological Society, 63rd Annual Field Conference Guidebook*, p. 491-498.
- McCraw, D. J., and Williams, S. F., 2012, Terrace stratigraphy and soil chronosequence of Cañada Alamosa, Sierra and Socorro Counties, New Mexico: *in*: Lucas, S. G.,

McLemore, V. T., Lueth, V. W., Spielmann, J. A., and Krainer, K. (eds.), *Geology of the Warm Springs Region: New Mexico Geological Society, 63rd Annual Field Conference Guidebook*, p. 475-489.

McLemore, V. T., 1983, Uranium and thorium occurrences in New Mexico: distribution, geology, production, and resources; with selected bibliography: *New Mexico Bureau of Mines and Mineral Resources, Open-file Report OF-183*, 950 p., also; U.S. Department of Energy Report GJBX-11 (83).

McLemore, V. T., 1993, *Geology and geochemistry of the mineralization and alteration in the Steeple Rock district, Grant County, New Mexico and Greenlee County, Arizona*. Ph.D. dissertation, University of Texas at El Paso; also *New Mexico Bureau of Mines and Mineral Resources, Open-File Report 397*, 526 p., http://geoinfo.nmt.edu/publications/openfile/downloads/OFR300-399/376-399/397/ofr_397.pdf (accessed March 29, 2012).

McLemore, V. T., 1996, Volcanic-epithermal precious-metal deposits in New Mexico: *in: Cyner, A. R. and Fahey, P. L., eds., Geology and ore deposits of the American Cordillera: Geological Society of Nevada Symposium Proceedings, Reno/Sparks, Nevada, April 1995*, p. 951-969.

McLemore, V. T., 2001, Silver and gold resources in New Mexico: *New Mexico Bureau of Mines and Mineral Resources, Resource Map 21*, 60 p.

McLemore, V. T., 2010, Geology, mineral resources, and geoarchaeology of the Montoya Butte Quadrangle, including the Ojo Caliente No. 2 mining district, Socorro County, New Mexico: *New Mexico Bureau of Geology and Mineral Resources, Open-file Report, OF-535*, 200 p.

McLemore, V. T., 2012a, The Monticello graben, Socorro and Sierra Counties, New Mexico [non-peer reviewed minipaper: *in: Lucas, S. G., McLemore, V. T., Lueth, V. W., Spielmann, J. A., and Krainer, K. (eds.), Geology of the Warm Springs Region: New Mexico Geological Society, 63rd Annual Field Conference Guidebook*, p. 92-94.

McLemore, V. T., 2012b, Preliminary geologic map of the Montoya Butte quadrangle, Socorro County, New Mexico: *New Mexico Bureau of Geology and Mineral Resources, Open-file geologic map OF-GM-69*, 1:24,000.

- McLemore, V. T., 2012c, Geology of the southern San Mateo Mountains, Socorro and Sierra Counties, New Mexico: *New Mexico Geological Society Guidebook, 63rd Field Conference*, p. 261-272.
- McLemore, V. T., 2012d, Mining districts in the San Mateo Mountains, Socorro and Sierra Counties, New Mexico: *New Mexico Geological Society, Guidebook 63*, p. 85-87.
- McLemore, V. T., Donahue, K., Krueger, C. B., Rowe, A., Ulbricht, L., Jackson, M. J., Breese, M. R., Jones, G., and Wilks, M., 2002, Database of the uranium mines, prospects, occurrences, and mills in New Mexico: *New Mexico Bureau of Geology and Mineral Resources, Open file Report OF-461*, CD-ROM, <http://geoinfo.nmt.edu/publications/openfile/details.cfm?Volume=46>, accessed 1/2/14.
- McLemore, V. T., Hoffman, G., Smith, M., Mansell, M., and Wilks, M., 2005a, Mining districts of New Mexico: *New Mexico Bureau of Geology and Mineral Resources, Open-file Report 494*, CD-ROM.
- McLemore, V. T., Krueger, C. B., Johnson, P., Raugust, J. S., Jones, G. E., Hoffman, G. K. and Wilks, M., 2005b, New Mexico Mines Database: *Society of Mining, Exploration, and Metallurgy, Mining Engineering*, February, p. 42-47.
- McLemore, V. T., Love, D. W., McCraw, D. J., Lucas, S. G., Laumbach, K., Spielmann, J. A., and McLemore, J. V., 2012a, Southern San Mateo Mountains, Second-Day road log from Truth or Consequences to Nogal Canyon, Millken Park, Luna Park Campground, Garcia Falls, and Monticello: *in: Lucas, S. G., McLemore, V. T., Lueth, V. W., Spielmann, J. A., and Krainer, K. (eds.), Geology of the Warm Springs Region: New Mexico Geological Society, 63rd Annual Field Conference Guidebook*, p. 49-70.
- McLemore, V. T., Heizler, M., Love, D. W., Cikoski, C. T., and Koning, D. J., 2012b, $^{40}\text{Ar}/^{39}\text{Ar}$ ages of selected basalts in the Sierra Cuchillo and Mud Springs Mountains, Sierra and Socorro Counties, New Mexico: *New Mexico Geological Society Guidebook, 63rd Field Conference*, p. 285-292.
- Meyer, H. W., 2012, Fossil plants from the late Eocene Red Rock Ranch flora, southwestern New Mexico [non-peer reviewed mini-paper]: *in: Lucas, S. G., McLemore, V. T., Lueth, V. W., Spielmann, J. A., and Krainer, K. (eds.), Geology of the Warm Springs Region: New Mexico Geological Society, 63rd Annual Field Conference Guidebook*, p. 88-92.

- Morgan, G. S., and Lucas, S. G., 2012, Cenozoic vertebrates from Sierra County, southwestern New Mexico: *in*: Lucas, S. G., McLemore, V. T., Lueth, V. W., Spielmann, J. A., and Krainer, K. (eds.), *Geology of the Warm Springs Region: New Mexico Geological Society, 63rd Annual Field Conference Guidebook*, p. 525-539.
- Munsell Color, 1994 edition, *Munsell soil color charts*: New Windsor, N.Y., Kollmorgen Corp., Macbeth Division.
- Nakamura, N., 1974, Determination of REE, Ba, Fe, Mg, Na and K I carbonaceous and ordinary chondrites: *Geochimica et Cosmochimica Acta*, v. 38, p. 757-775.
- Neubert, J. T. 1983, Mineral investigation of the Apache Kid and Withington Wilderness Areas, Socorro County, New Mexico: *U.S Bureau of Mines, MLA 2-83*, 34 p.
- North, R. M., 1983, History and geology of the precious metal occurrences in Socorro County, New Mexico: *New Mexico Geological Society, 34th Fall Field Conference Guidebook*, p. 261-268.
- North, R. M., and McLemore, V. T., 1986, Silver and gold occurrences in New Mexico: *New Mexico Bureau of Mines and Mineral Resources, Resource Map 15*, 32 p.
- North, R. M., and McLemore, V. T., 1988, A classification of the precious metal deposits of New Mexico: *in*: *Bulk mineable precious metal deposits of the western United States Symposium Volume: Geological Society of Nevada, Reno, Symposium held April 6-8, 1987*, p. 625-660.
- Repenning, C. A., and May, S. R., 1986, New evidence for the age of the lower part of the Palomas Formation, Truth or Consequences, New Mexico: *in*: Clemens, R. E., King, W. E., Mack, G. H., and Zidek, J. (eds.), *Guidebook of the Truth or Consequences region: New Mexico Geological Society, Guidebook 37*, p. 257-260.
- Seager, W. R., and Mack, G. H., 2003, *Geology of the Caballo Mountains, New Mexico: New Mexico Bureau of Geology and Mineral Resources, Memoir 49*, 136 p.
- Smith, W. R., 1992, *Geology of the southwestern margin of the Nogal Canyon cauldron, San Mateo Mountains, Sierra and Socorro Counties, New Mexico* [unpublished M.S. thesis]: Odessa, University of Texas of the Permian basin, 96 p.
- Soil Survey Staff, 1992, *Keys to Soil Taxonomy*: U.S. Department of Agriculture, SMSS Technical Monograph no. 19, 5th edition, 541 p.

Soreghan, G.S., 1994, Stratigraphic responses to geologic process: Late Pennsylvanian eustasy and tectonics in the Pedregosa and Orogrande basins, ancestral Rocky Mountains: *Geological Society of America Bulletin*, v. 106, p. 1195-1211.

Udden, J. A., 1914, The mechanical composition of clastic sediments: *Geological Society of America Bulletin*, v. 25, p. 655-744.

US Climate Data, 2014, *Climate Winston - New Mexico*:
<<<http://www.usclimatedata.com/climate/winston/new-mexico/united-states/usnm0356>>>. Last accessed June 25, 2014

Weber, R. H., 1963, Cenozoic volcanic rocks of Socorro County: *New Mexico Geological Society, 14th Field Conference Guidebook*, p. 132-142.

Wentworth, C. K., 1922, A scale of grade and class terms for clastic sediments: *Journal of Geology*, v. 30, p. 377-392.

Ye, H., Royden, L., Burchfield, C. and Schuperbach, M., 1996, Late Paleozoic deformation of interior North America: The greater ancestral Rocky Mountain deformation: *American Association of Petroleum Geologists Bulletin*, v. 80, p. 1397-1432.

FIGURES AND FIGURE CAPTIONS

Figure 1. Geographic setting of the Monticello quadrangle. The boundaries of the quadrangle are shown in red.

Figure 2. Topography and geographic names in the Monticello quadrangle, whose boundaries are demarcated in red. Also shown are the approximate extents of the Burma and Cuchillo geomorphic surfaces (green and white, respectively).

Figure 3. Tectonic setting of the Monticello quadrangle. The boundaries of the quadrangle are shown in red.

Figure 4. Various stratigraphic nomenclatures used for volcanic rocks in the eastern Monticello quadrangle. Our scheme is listed on the right. We do not show Hermann's subdivisions of the Rock Springs Formation because of their stratigraphic detail and also because of uncertainty to how they correlate with the stratigraphy to the east and south. Thick tuffs are shown in orange and labeled in red.

Figure 5. Photographs illustrating Paleozoic strata. A) Solitary coral in the Red House Formation. Other fossils found in the Red House Formation include: brachiopods, crinoid columnals, and fusulinids. B) Stratiform jasper replacement of limestone in the Red House Formation; 15 cm-long ruler for scale. C) Common chert lenses in the Nakaye Formation. D) Cliffy exposures of the Nakaye Formation, as exposed in Placitas Canyon.

Figure 6. Schematic diagram illustrating stratigraphic relations of volcanic strata. Note that thicknesses are not to scale.

Figure 7. Photographs illustrating the volcanoclastic part of the Whiskey Hill member of the Red Rock Ranch Formation. A-C) Sandy pebble-boulder conglomerate exposed north of the Red Rock shooting range. The gravel is composed of angular to subrounded dacite and plagioclase-phyric andesite clasts up to 44.5 cm (17.5 in) across. D) Sandy pebble-cobble conglomerate north of Seferino Hill. It is composed of matrix-supported, angular to subangular volcanoclastic gravel. Most clasts in the deposit are pebbles to small cobbles of plagioclase-phyric andesite or biotite-phyric dacite. Pen is 14 cm long. E) Buttress relation of younger sandy pebble-cobble conglomerate (right) against an older, light gray, biotite-hornblende-dacite. The conglomerate to the right lacks bedding and is likely a debris flow. It is composed of subrounded, poorly sorted, very fine to very coarse pebbles with 10-20% cobbles and lesser boulders. At buttress is 25-30 cm-wide, maroon colluvium composed largely of clay with 5% altered volcanic(?) clasts (pen is on left side of the colluvium). Another nearby colluvial wedge, between Paleozoic bedrock and volcanoclastic sediment, is 130 cm wide and also largely clay with sparse, weathered volcanic clasts. Such clay-rich colluvium suggests a moist climate.

Figure 8. Photographs of the lower tongue of the Placitas Canyon member (Red Rock Ranch Formation). There were taken 3 km (2 mi) NNW of the Red Rock shooting range, where the unit is ~75 m thick. A) Strata in middle part of unit are mostly very thin to thin, tabular beds of very fine- to medium-grained sandstone with minor shale and siltstone interbeds. The sandstone is composed of feldspar and quartz, with very little volcanic grains. This composition indicates a quartz-feldspathic source area for the drainage, possibly in uplifted Proterozoic terrain. B) The sandstone-rich middle part grades upward into a shale-dominated upper part. Here, uppermost shale are overlain sharply (but conformably) by plag-

phyric Uvas basaltic trachyandesites. Fossils found in the lower and middle part of the unit (where it is sandstone-dominated) include a bi-valve (clam?) (C) and leaf impressions (D). E, F) Paleocurrent indicators include asymmetrical ripplemarks and bi-directional tool marks (pencil in the latter is orientated parallel to the tool marks). The ripplemarks indicate northerly paleoflow and are perpendicular to the toolmarks.

Figure 9. Paleogeographic map depicting inferred extent of andesitic lavas of the Red Rock Ranch Formation, as well as interpreted location of the lake associated with Placitas Canyon Member deposition. Arrows denote the inferred direction of lava flow movement. Red Rock Ranch and modern longitudes and latitudes are shown for reference.

Figure 10. Photos of the upper tongue of the Placitas Canyon member. A) Thinly bedded, gray limestone overlying organic-rich shale. B) Limestone (top) overlying porphyritic Luna Peak trachyandesite. At right end of ruler, the limestone fills a 10 cm-deep depression on the lava's upper surface. At the extreme right of the photo, the lava fills a 20-25 cm-deep depression.

Figure 11. Les Bas plot showing the chemistry of samples depicted in Appendix 2. The name of the corresponding map unit is shown in red. Note that sample MONT-13-05 does not have a corresponding map unit.

Figure 12. A) Outcrops of the Uvas basaltic andesite tend to be dark-colored, as illustrated here (north of Red Rock Ranch). B) Large phenocrysts of pyroxene are relatively abundant (>2%) in the Uvas basaltic trachyandesite.

Figure 13. Photographs of the Garcia Falls member of the Red Rock Formation. Note the plagioclase and pyroxene phenocrysts.

Figure 14. Depictions of the light-colored, upper andesite west of Luna Peak.

Figure 15. The Luna Peak trachyandesite is recognized by its large proportion of plagioclase megacrysts; specifically. $\geq 10\%$ of the plagioclase phenocrysts are ≥ 10 mm long.

Figure 16. View of the prominent hill west of lower Uvas Canyon, labeled 6506. Here, 20-25 m (70-80 ft) of Red Rock Arroyo Member andesites overlie 130 m (420) ft of Luna Peak trachyandesite. Note the former forms relatively smooth slopes whereas the latter exhibits corestone topography.

Figure 17. Photographs of the Red Rock Arroyo andesite member (Red Rock Ranch Formation) taken 1.9-2.5 km (1.2-1.5 mi) southeast of Red Rock Ranch. A, B) The lavas are typically vesicular and porphyritic, with 7-25% plagioclase and 0.5-5% pyroxene. C) The andesite is typically resistant to erosion and forms ledges. D) View to the southeast, showing the tuff of Aragon Draw (arrows) overlying the Red Rock Arroyo andesite.

Figure 18. Base between the Red Rock Arroyo andesites and the underlying Luna Peak trachyandesites, exposed east of Red Rock Ranch. The base is sharp (A) and undulatory, with up to 1 m of vertical relief (B). It has been interpreted as an unconformity by Foruria (1984) and Smith (1992).

Figure 19. A) Stratigraphic position of the thin sediment layer (Trsm), shown by the arrow, lying between the underlying Red Rock Arroyo andesites (Trrr) and the overlying tuff of Aragon Draw (Ttd).

The arroyo corresponds to upper Jose Maria Canyon. B) Close-up photograph of volcanoclastic gravel exposed on the east side of Jose Maria Canyon. The sediment is weakly consolidated, massive, and monolithic. Clasts are composed of light gray, vesicular, plagioclase-phyric andesite. Although coarse here, to the south the sediment is a very fine- to fine-grained sand and silty sand. Ruler for scale (inches on left side, centimeters on right side).

Figure 20. Photographs of the tuffaceous sediment that lies between the tuff of Aragon Draw and the Lower Luna Park Tuff. A) It is generally tan, fine-grained on the slopes of the hill labeled 6256 (near the eastern quadrangle border); here, it is interpreted as a mudflow and composed mostly clay with subordinate sand and 1-15% scattered andesite-dacite pebbles. B) Near Jose Maria well, the unit fines-upward from a very fine- to very coarse-grained sandstone to a reddish clay, the former being illustrated here.

Figure 21. Cross-bedded sandstone and poorly sorted conglomerate of the Seferino Hill conglomerate. Base of pen (14 cm long) marks prominent erosional surface. Conglomerate consists of matrix-supported pebbles to small cobbles of Jose Maria Canyon tuff and Whiskey Hill Member hornblende andesite deposited in debris flows.

Figure 22. Volcanoclastic sediment and lava flows of the Rock Springs Formation. A) Lava and sediment between the Upper Luna Park Tuff and the Hells Mesa Tuff, as exposed on the east side of Red Rock Arroyo (unit Trssv2). B) Lava flows and breccia found lying between the Hells Mesa Tuff and Vicks Peak Tuff east of Jolla Tank.

Figure 23. The tuff of Aragon Draw extends across the study area. Its best exposures occur immediately east of upper Jose Maria Canyon. A) Here, there is a 3-12 m (10-40 ft)-thick lower welded zone that thickens to the south (**Ttadw**), which overlies a thin sediment layer (**Trasm**). B) The welded, basal zone contains 3% biotite, 0.5-1% hornblende, and 5-10% feldspar that includes sanidine. Note the light gray fiamme. The middle and upper part of the unit is a coarse ash-fall tuff-lapilli that coarsens upward. C) Typical clast assemblages in the southeast part of the quad include: 1) a white, feldspar-rich (minor hornblende(?), intrusive clast (annotated as "I"); 2) gray, plagioclase-phyric andesite (annotated as "A"); 3) The most common clast is a laminated, fine-grained tuff (annotated as "T"). 15 cm-long ruler for scale. D) Down-section, the white, feldspar-rich clast decreases in size. It corresponds to the white specks seen in this photograph. E) The lithic-rich top of the tuff of Aragon Draw in Red Rock Arroyo. F) Basal part of the tuff in upper Uvas Canyon. In this area, the basal welded zone is ~1 m thick or missing. Photographs of the tuff of Aragon Draw in the north-central part of the quadrangle. G) Remorphic textures are observed in the north-central part of the quadrangle (Uvas Canyon). H) Folded tuff clast on the east side of upper Jose Maria Canyon. I) Flattened xenolith with a reaction rim. (the white, feldspar-rich, intrusive clast of photo C).

Figure 24. Photographs of the Lower Luna Park Tuff, which extends across the study area. A) In the north-central part of the quadrangle, it overlies a fine-grained, sanidine-bearing trachyte. B) Close-up shot of the tuff, where it is exposed on the north side of the hill labeled 6256 (near the eastern quadrangle border). Here, it contains 15% flattened, very dark-colored fiamme 0.1-1.8 cm long and 1-25% volcanic lithic fragments. Phenocrysts include 5-15% sanidine and 1-3% biotite and hornblende. The top of the unit contains 10% volcanic detritus comprised of pebbles and coarse to very coarse sand grains. C) Lower Luna Park Tuff (**Tlpl**) intruded by rhyolite (**Tir**).

Figure 25. The Upper Luna Park Tuff is a prominent unit that extends across the study area. In the north-central part of the quadrangle, it is separated from the Lower Luna Park Tuff by ~15 m of volcanoclastic pebble conglomerates and porphyritic andesites (Trrsv1). By the hill labeled 6256 (near the eastern quadrangle border), this intervening sediment is missing. A) View of the lower, sanidine-rich Upper Luna Park Tuff on the hill labeled 6256. B) Close-up view of this tuff on this hill. Ruler is 15 cm long.

Figure 26. A) Pinkish brown, fine-grained Vicks Peak Tuff that is fractured. B) Locally, the Vicks Peak Tuff filled a paleovalleys >120 m deep (>400 ft), as exposed in upper Street Canyon in the northeast corner of the quadrangle.

Figure 27. Photographs illustrating the rhyolite of Alamosa Creek, as exposed in Lemes Canyon. A) Dense rhyolite flow. B) Rhyolitic flow breccia. The flows are largely aphanitic, with trace to 2% phenocrysts of sanidine.

Figure 28. A) Intermediate dike on the west slope of upper Red Rock Arroyo. This porphyritic rock contains 7% pyroxene and 1-3% plagioclase phenocrysts. B). Close-up of a rhyolitic intrusion 1.1 km (0.7 mi) southeast of Garcia Falls. Note the abundant phenocrysts of quartz. C) Photos of the margin of a rhyolite dike, located 1.1 km (0.7 mi) southeast of Garcia Falls. D) Photo of a tongue of rhyolite penetrating the Garcia Falls trachyandesite, located 1.4 km southeast of Garcia Falls.

Figure 29. The lower-middle, grayer, more cemented and tilted part of the Santa Fe Group. Photos taken from Lemes Canyon. A) Note the pervasive strong to moderate cementation and the thin to medium, distinct bedding. B) The lower ~30 m (100 ft) of the unit is steeply tilted and dominated by clasts reworked from unit **Trac**.

Figure 30. Photographs illustrating the upper, lesser cemented part of the Santa Fe Group. Photos taken from lower Cedro Canyon, in the west-central part of the quadrangle. A) The unit contains interbedded gray and orange intervals, both are conglomeratic. B) Note the thin to medium, tabular to lenticular beds and the sparse moderately to well cemented beds. This unit contains <15% moderate to well cemented beds and has relatively common orange pebbly sandstone beds.

Figure 31. Photographs of the high-level piedmont alluvium near Garcia Canyon (**Qpag**) overlying the light gray, relatively gravel-poor Garcia lithosome (**Tsfgu**). A) A paleovalley butte, demarcated by the arrows, is clearly seen on the northeast end of the deposit on the southeastern slope of Garcia Canyon. View is to the west. B) Example of the **Qpag** deposit around the corner of the photograph of A; view is to the northeast. Note the brown color of **Qpag** versus the gray color of the Garcia Falls lithosome. In addition to the difference in color, the units are distinguished by the percentage of coarse clasts: up to 85% of beds in the Garcia Falls lithosome consist of sand/sandstone mostly lacking larger clasts, whereas the younger piedmont deposits are dominated by pebble-cobble gravel. The less resistant Santa Fe Group beds form steep slopes.

Figure 32. Views of the terraces found along Alamosa Creek in the west-central part of the quadrangle. A) Looking northeast at the eastern slope of the Canyon. Note that **Qta1** consists of three strath terraces inset slightly against one another (the strath drops ~ 1m at the butresses between the **Qta1** terraces). Note how an alluvial fan (**Qfaa1**) prograded out onto the **Qta1c** tread. The tread of **Qta2** stands 36 m (120 ft) above the tread of **Qta1b**. **Qta2** stands 25 m (80 ft) above **Qta1**. These terraces have developed on the Santa Fe Group. Nogal Peak lies in the background.

Figure 33. Photographs illustrating the textural and consolidation differences between Pleistocene terrace deposits and older Santa Fe Group. A) The 40 ft)-thick **Qta2b** deposit is browner and less consolidated than underlying redder Santa Fe Group deposits (**QTsf**). Arrows and rock hammer denote the base of **Qta2b**. Photograph taken along the Burma Road 0.45 km (0.3 mi) northeast of the plaza in Monticello. B, C) **Qta1** contains abundant cobbles and boulders, as illustrated in these photographs taken northwest of Monticello [B -- 0.9 km (0.5 mi) NW of the plaza; C -- 1.3 km (0.8 mi) NW of the plaza]. D) Photograph of the **Qta1** base immediately south of the Monticello cemetery.

Figure 34. Schematic diagram illustrating the Burma and Cuchillo surfaces at two locations along Alamosa Creek. The northwest block represents the map area and the southeast block represents Palomas Formation deposits and inset terraces located in lower Alamosa Creek (near the crossing of Interstate 25). On the right is a summary of the inferred geomorphic and sedimentologic history that relates these surfaces to the Palomas Formation downstream.

Figure 35. Example of rills developed on an east-facing hillslope. View is westward towards the western slope of upper Calvario Draw.

Fig 36. Examples of the basal Santa Fe Group contact near the western quadrangle border, where unit **Tsflc** overlies the Rhyolite of Alamosa Creek (**Trac**). Note the slight discordance of bedding in unit **Tsflc** with the rhyolite. This may be due to tectonic tilting between emplacement of **Trac** and deposition of **Tsflc**, or it may reflect a relatively steep paleoslope on the rhyolite surface. A) North slope of Lemes Canyon. B) Unnamed canyon at the west end of Cross-section A-A'; view is to the south.

Figure 37. Chondrite normalized REE plot for mineralized rocks in the San Mateo Mountains district. Chondrite values from Nakamura (1974).

Figure 38. Chondrite normalized REE plot for igneous rocks in the San Mateo Mountains district. Chondrite values from Nakamura (1974).

Figure 01

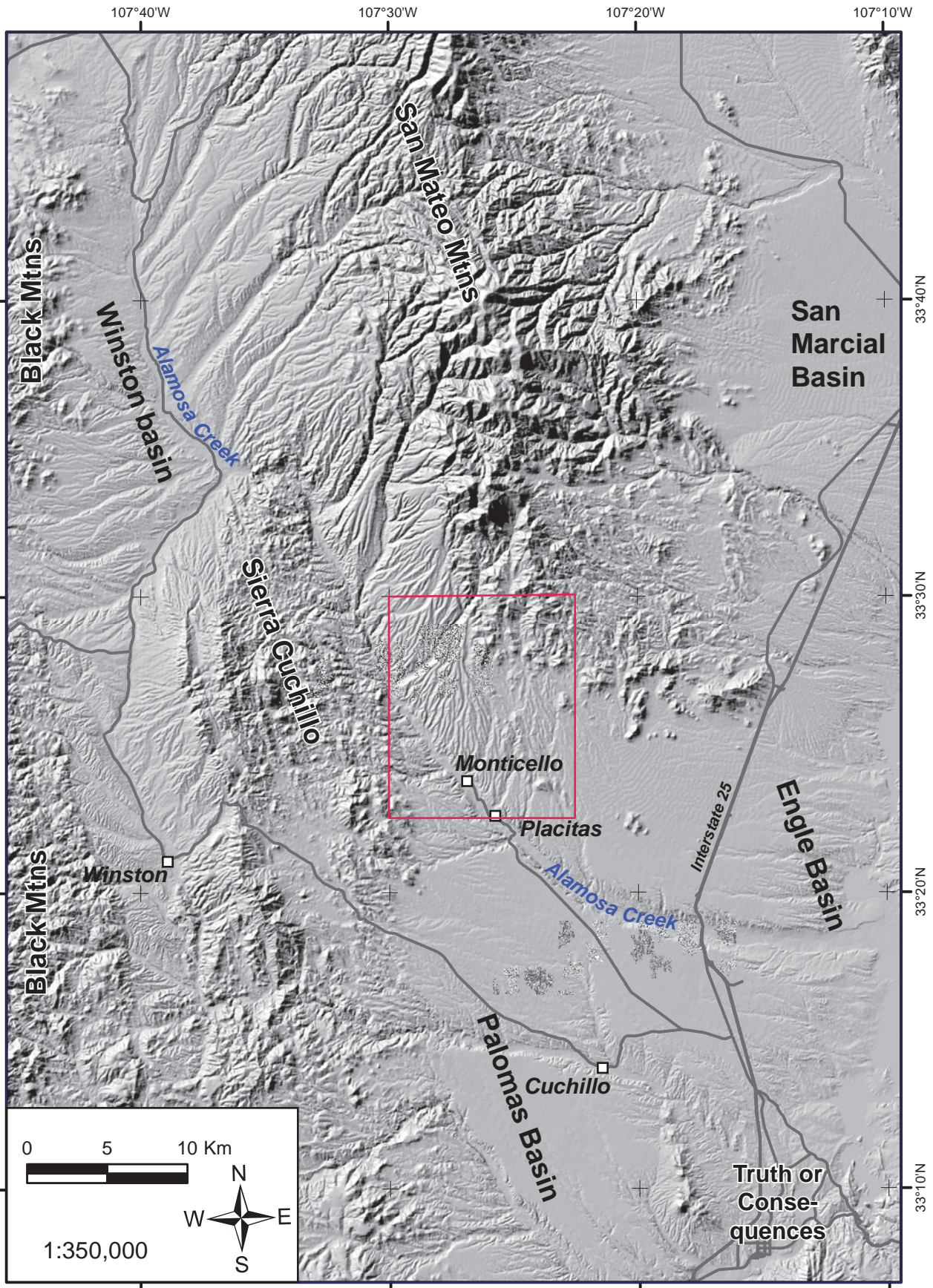


Figure 02

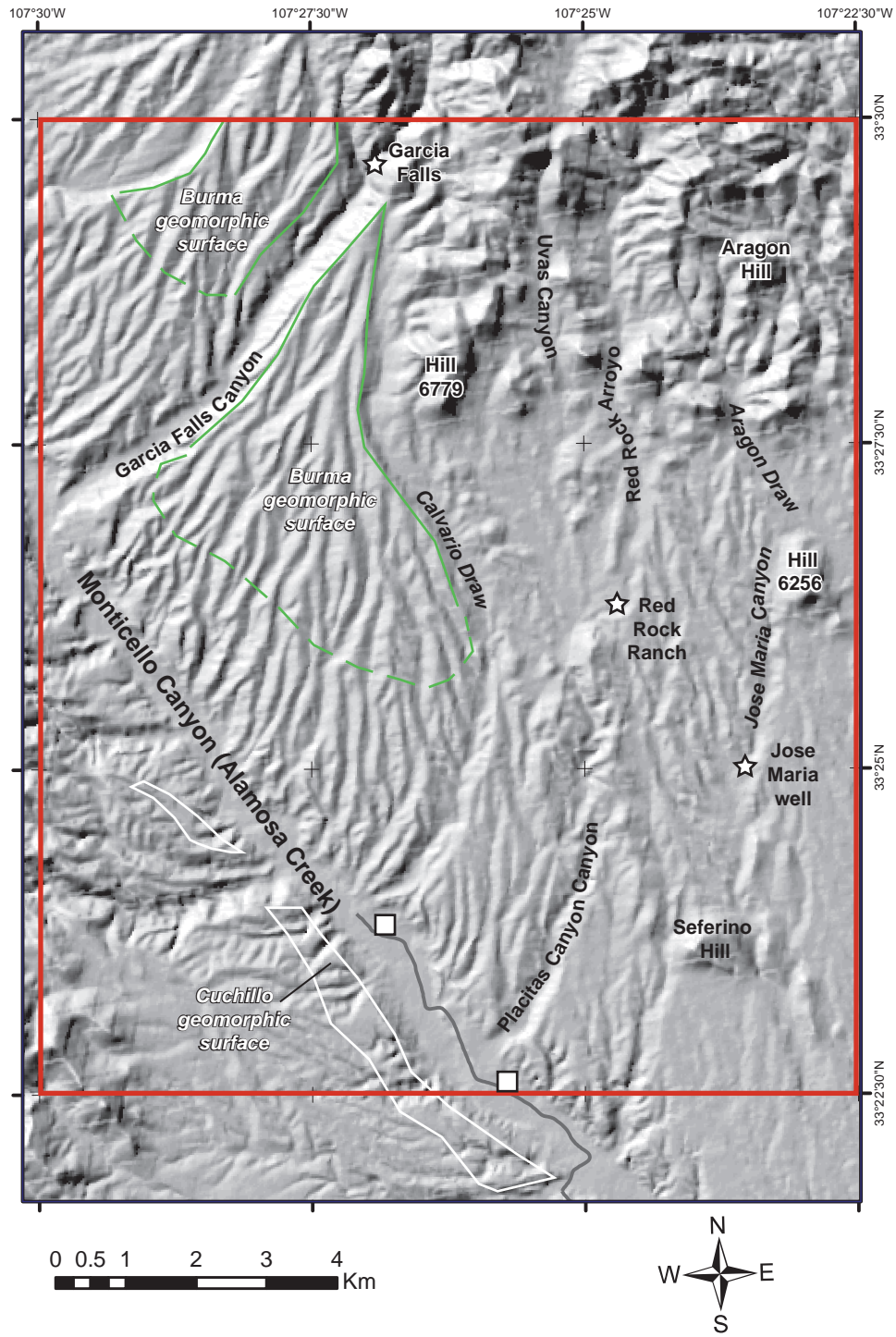


Figure 03

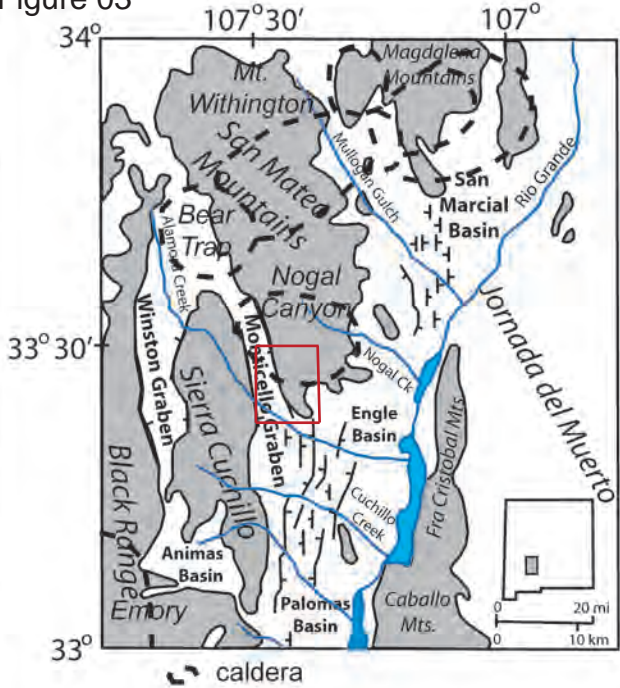


Figure 04

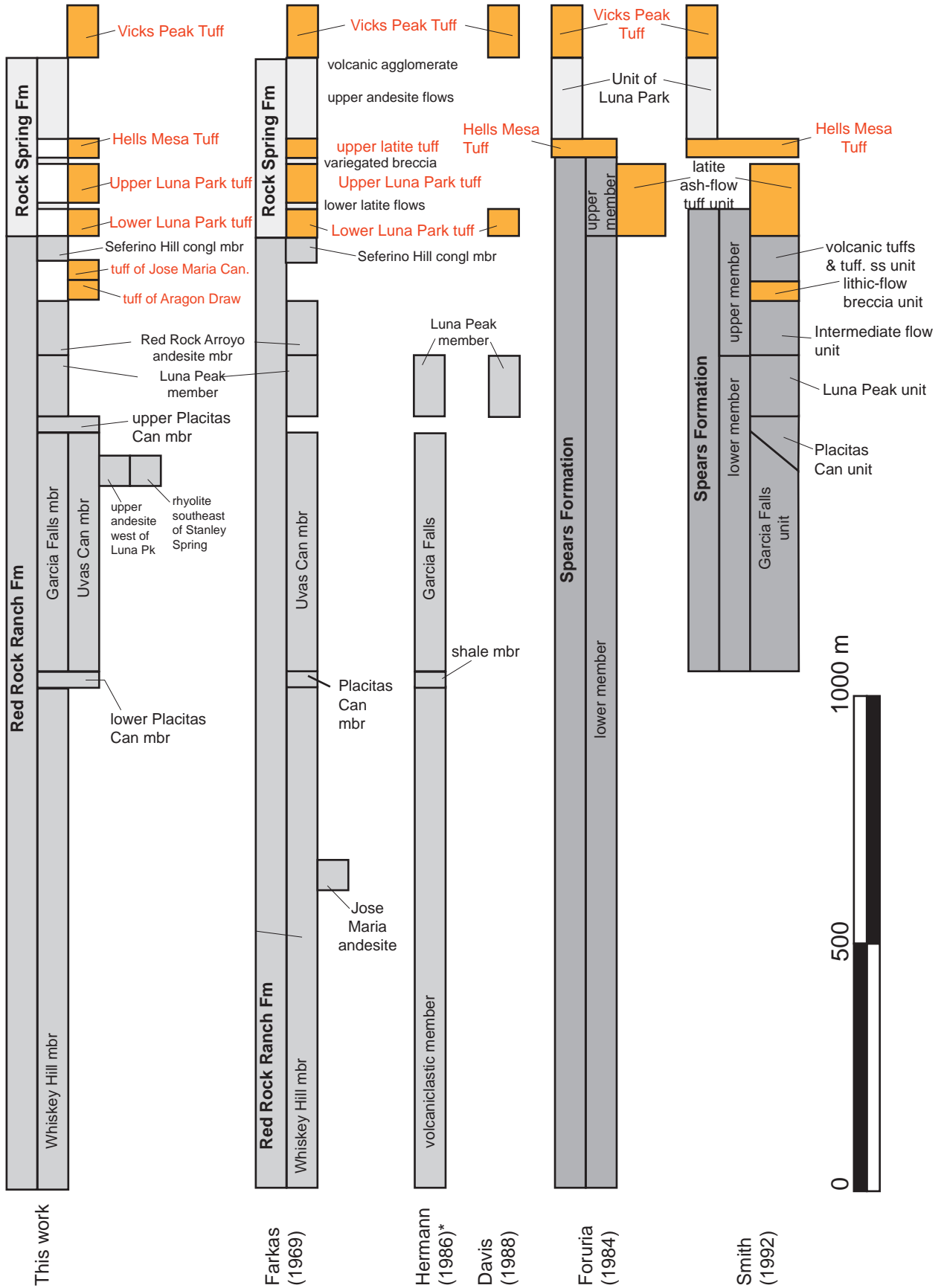


Figure 05

A



B



Figure 06

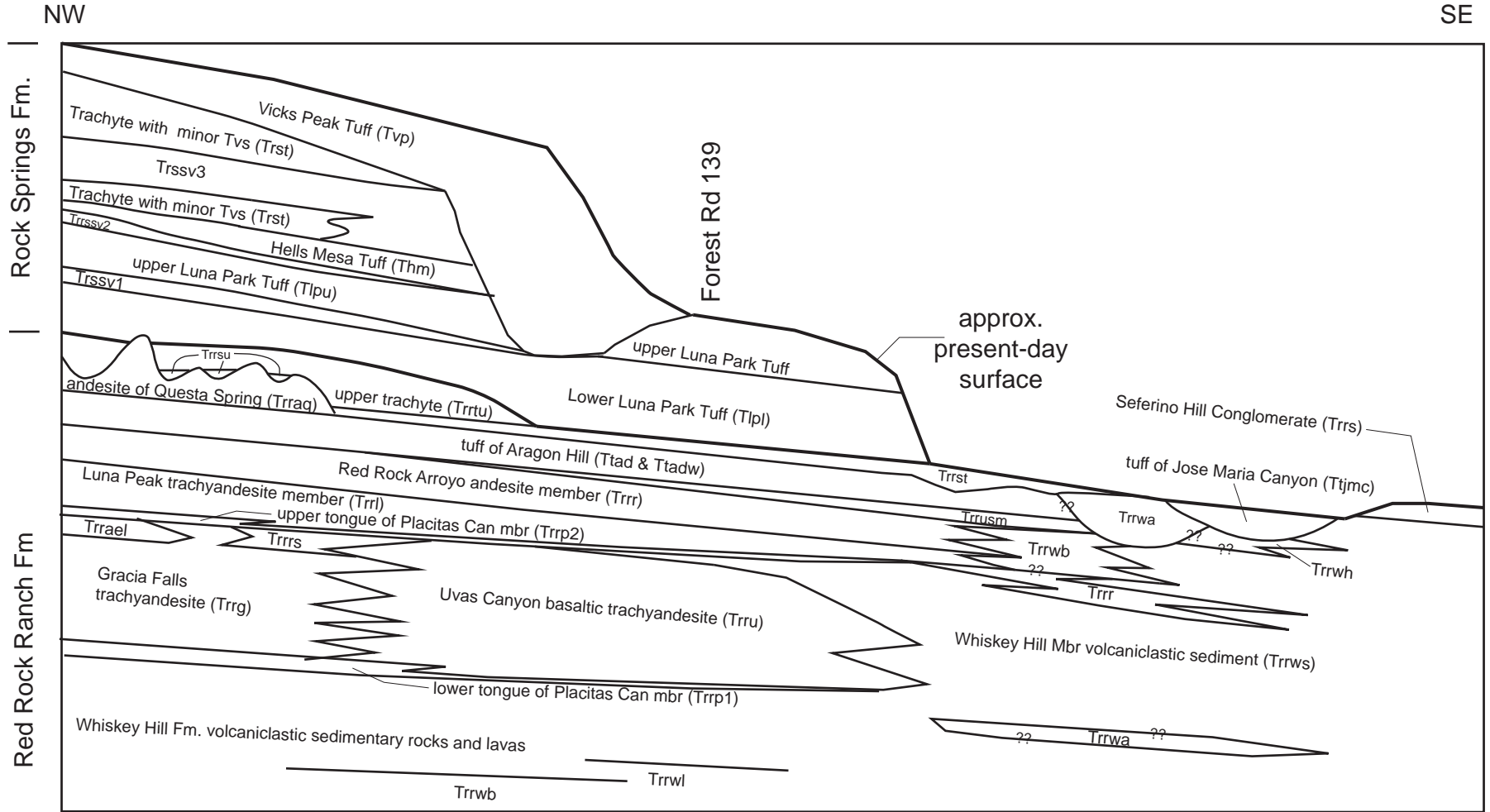


Figure 07



Figure 07



Figure 08

A



B



Figure 08

C



D



Figure 08

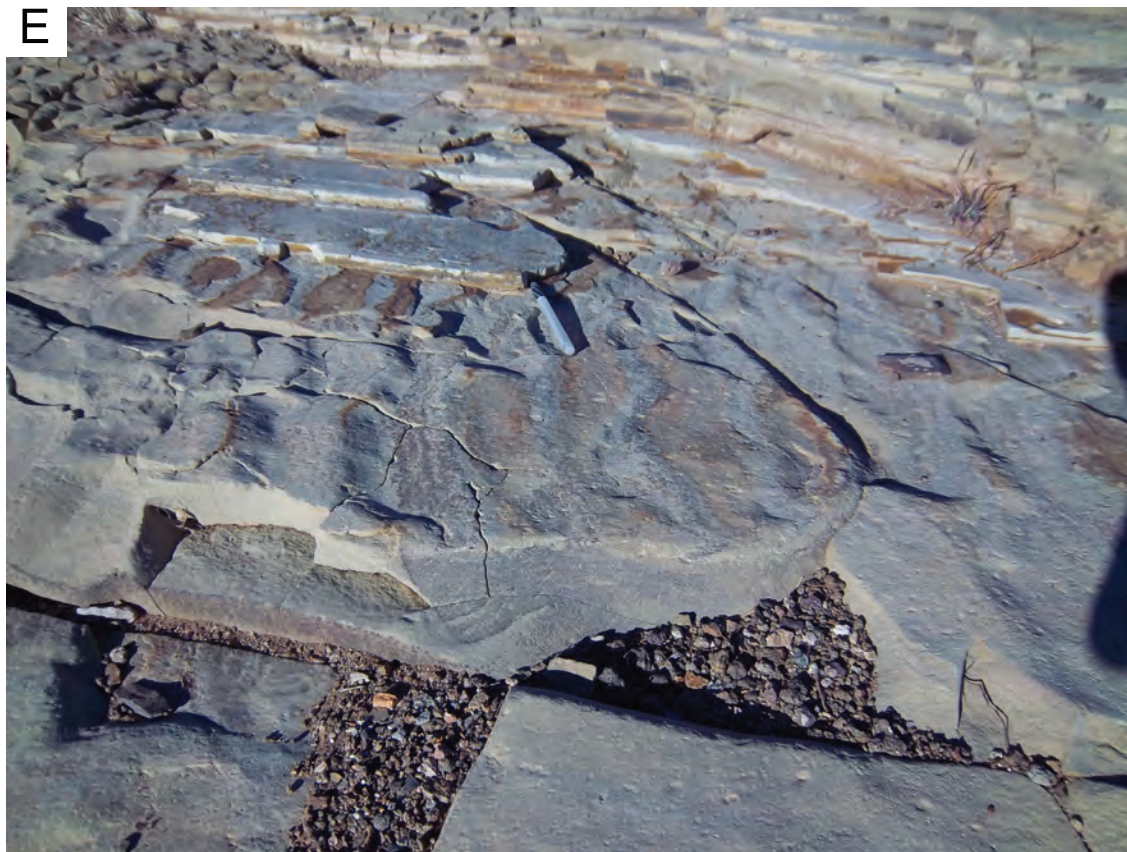


Figure 09

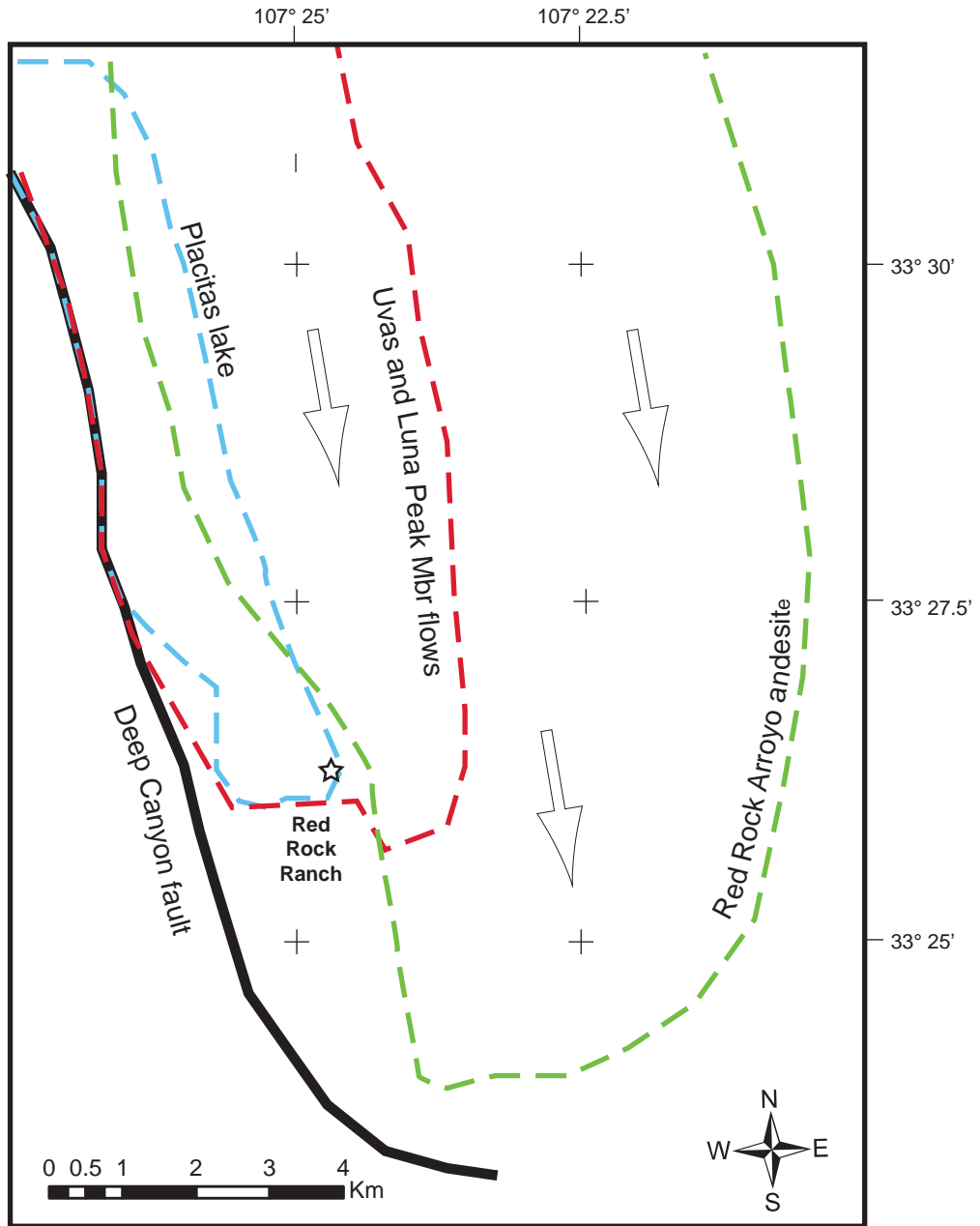


Figure 10

A



B



Figure 11

TAS (Le Bas et al. 1986)

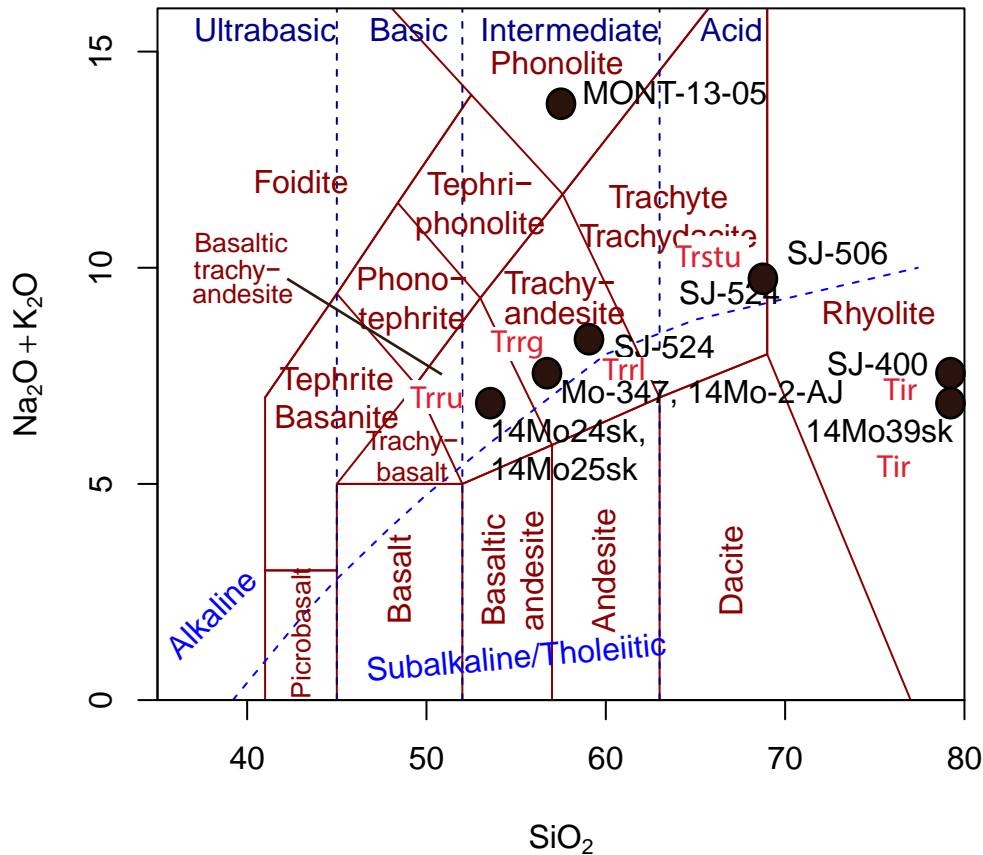


Figure 12

A



B



Figure 13

A



B



Figure 14

A



B

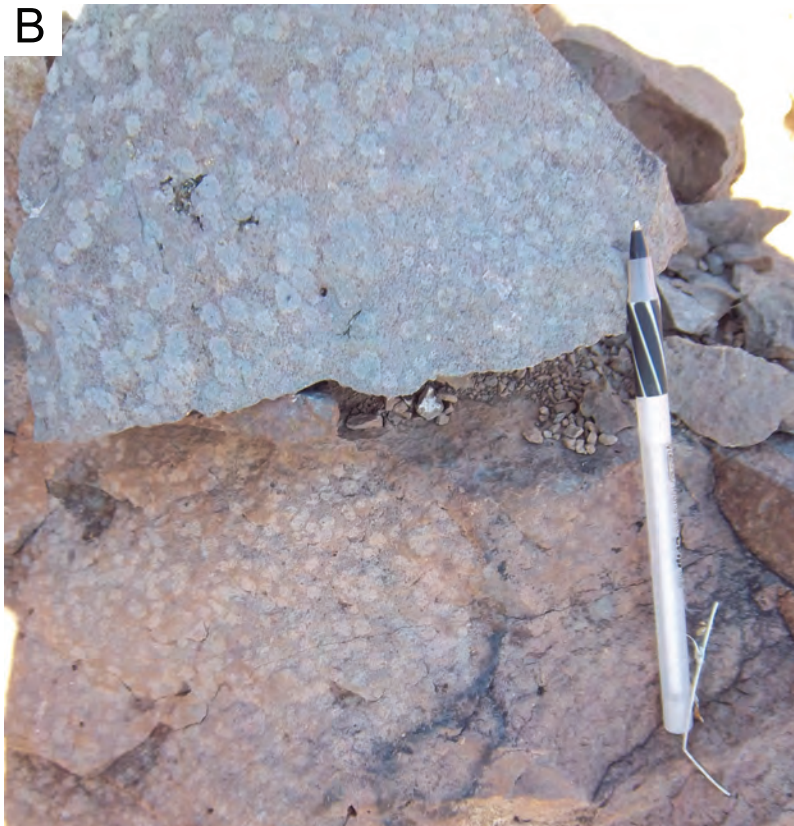


Figure 15



Figure 16



Figure 17

A



B



Figure 17

C



D



Figure 18



Figure 19

A



B



Figure 20

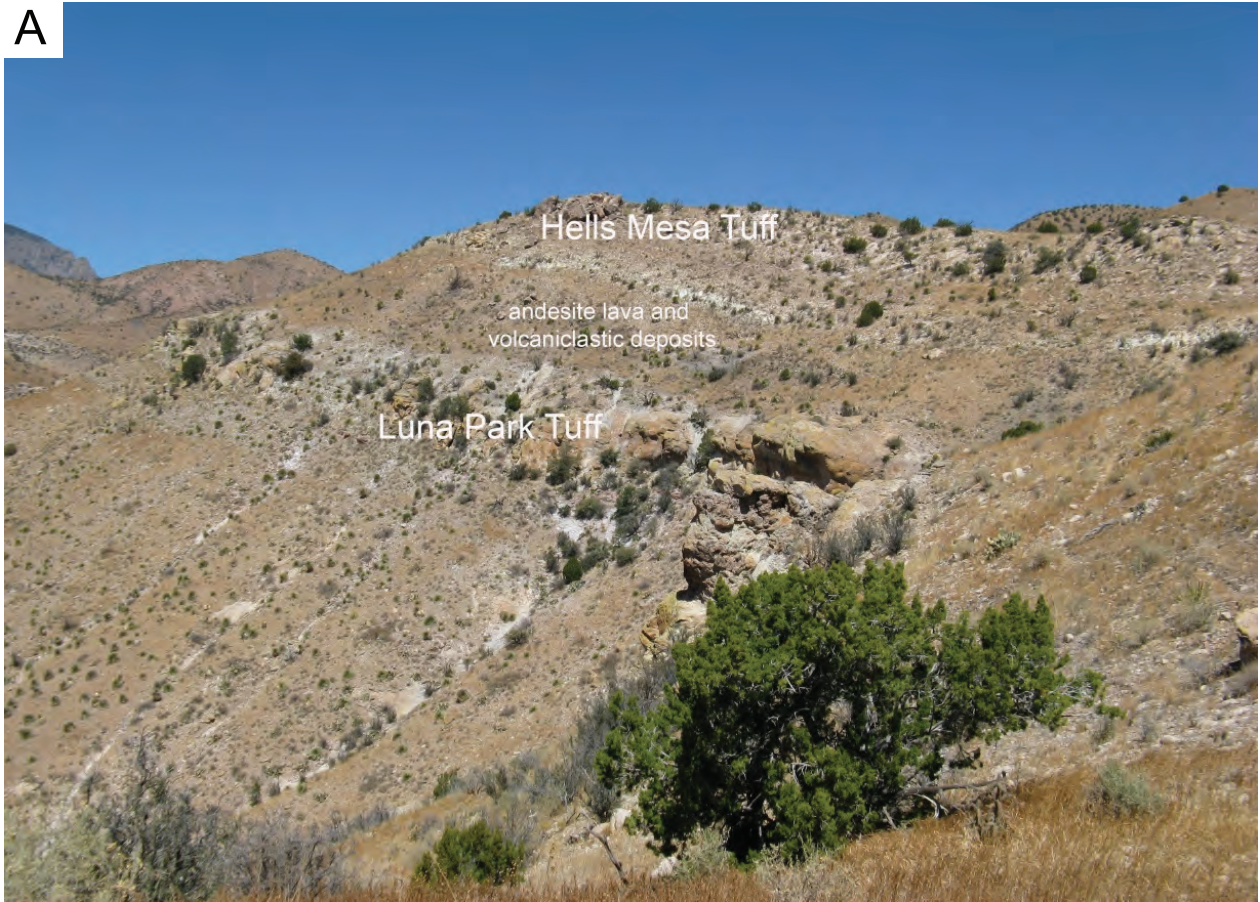


Figure 21



Figure 22

A



B

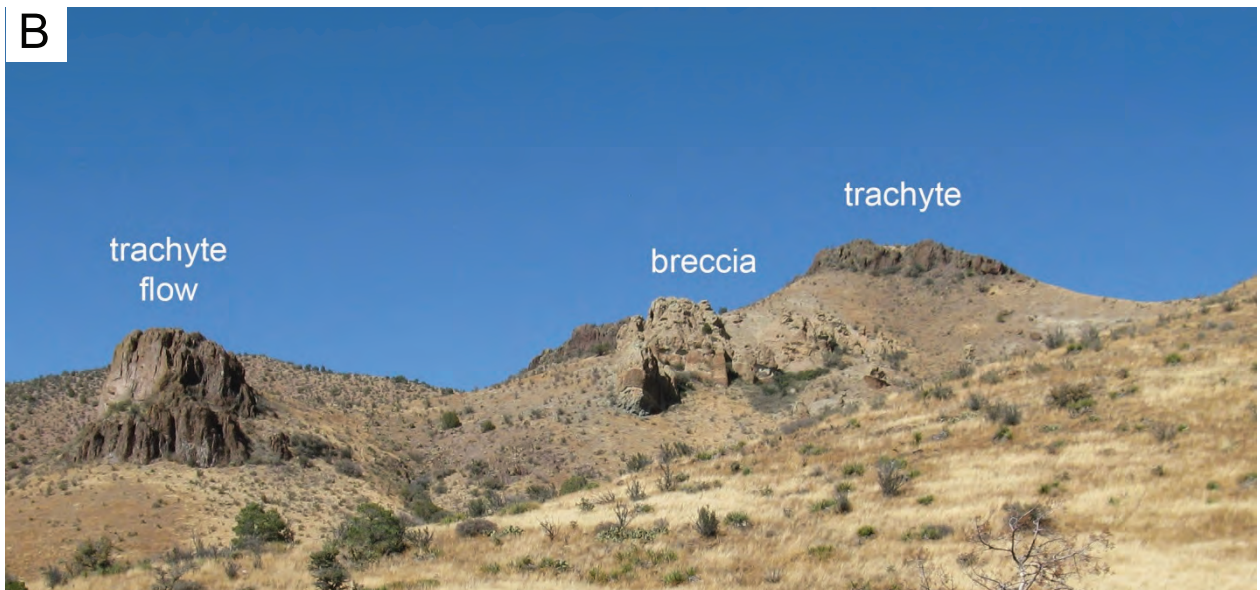


Figure 23

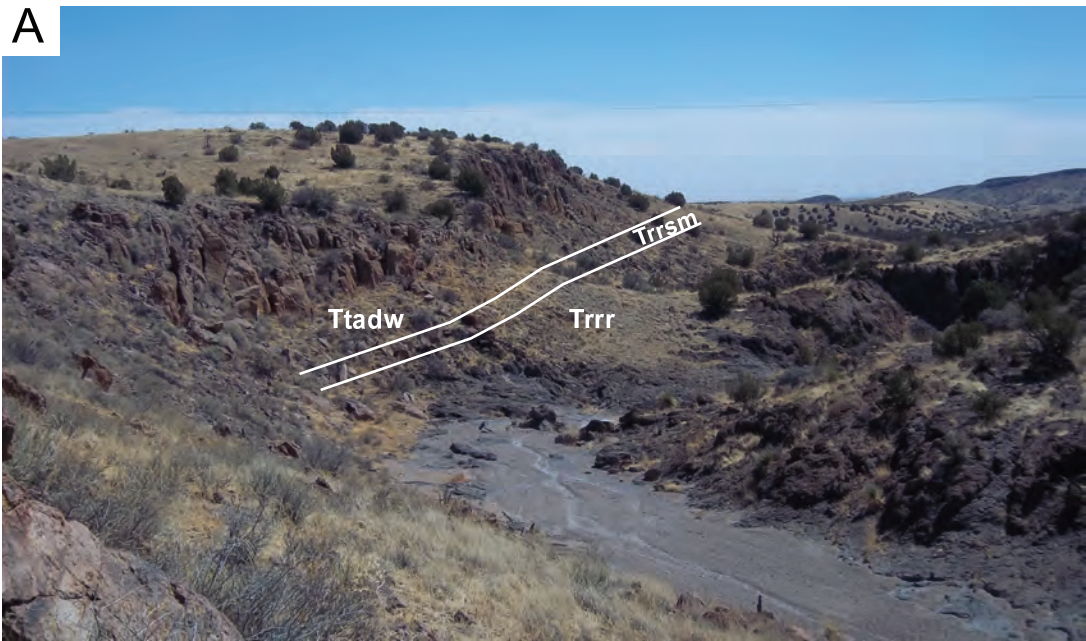


Figure 23

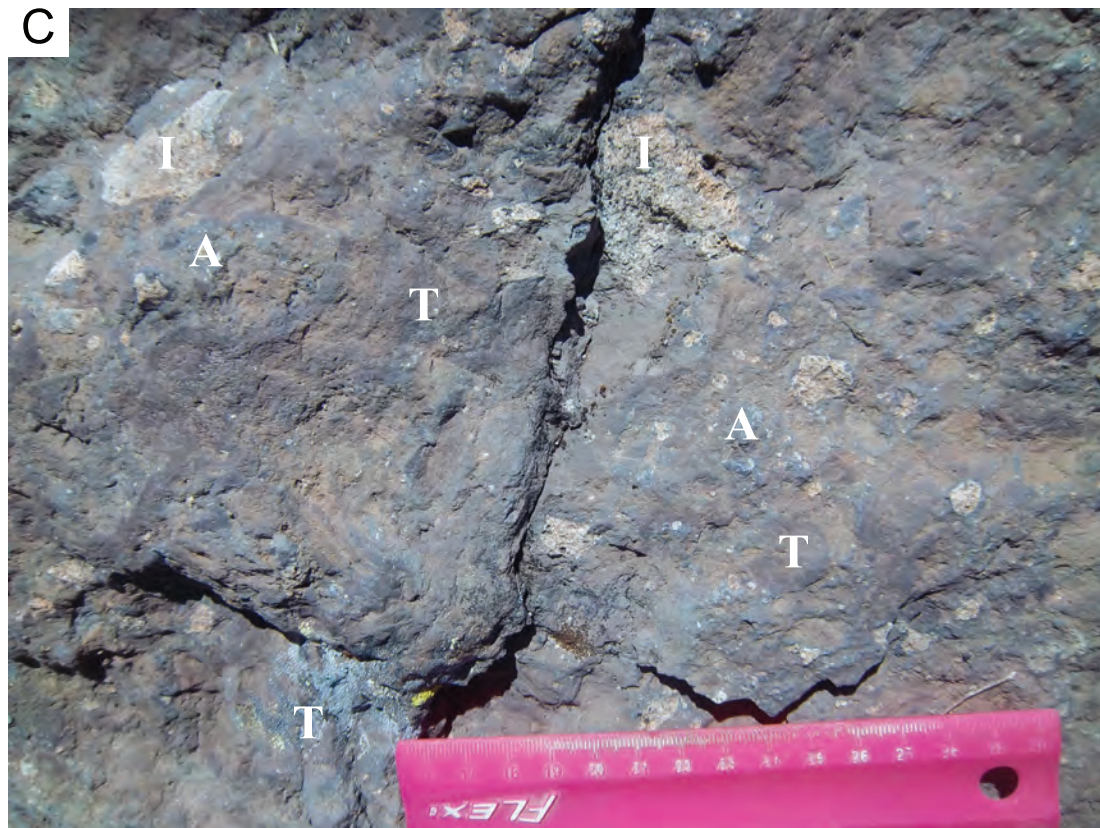


Figure 23

E



F



Figure 23



Figure 24

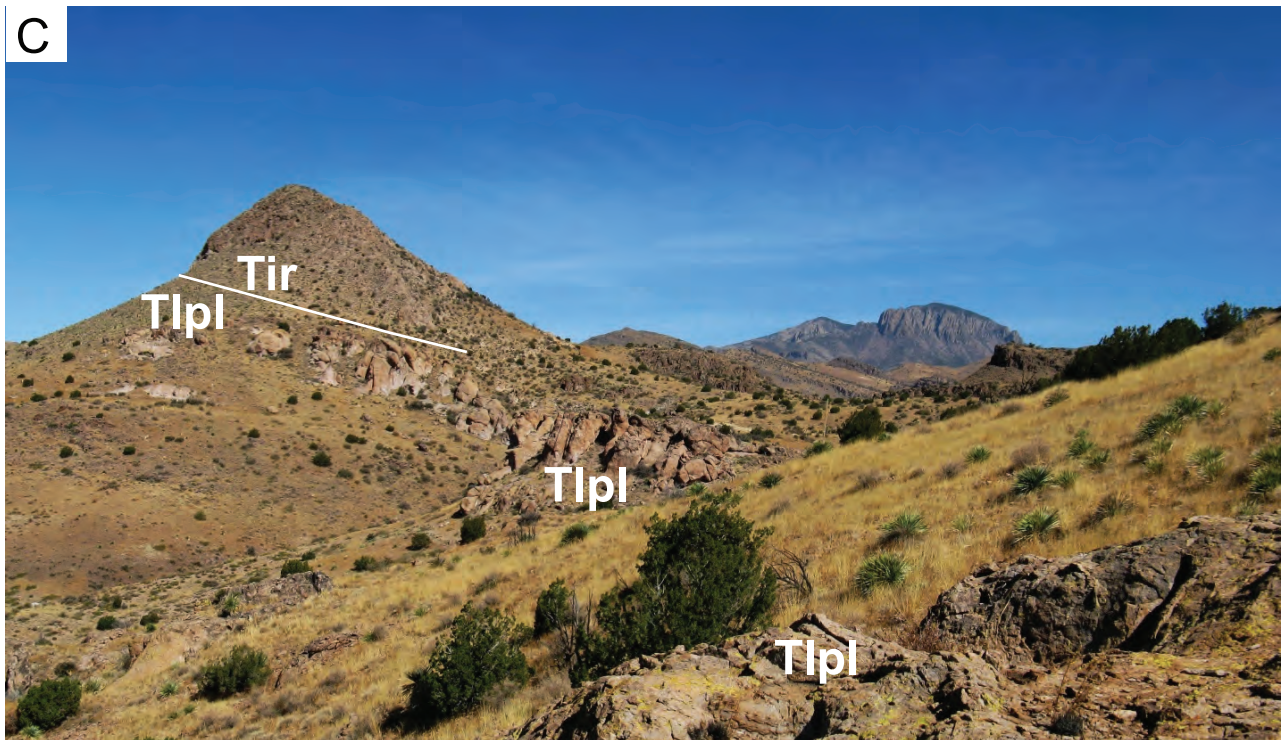


Figure 25

A



B



Figure 26

A



B



Figure 27

A



B



Figure 28

A



B



Figure 28

C



D



Figure 29

A



B



Figure 30



Figure 31

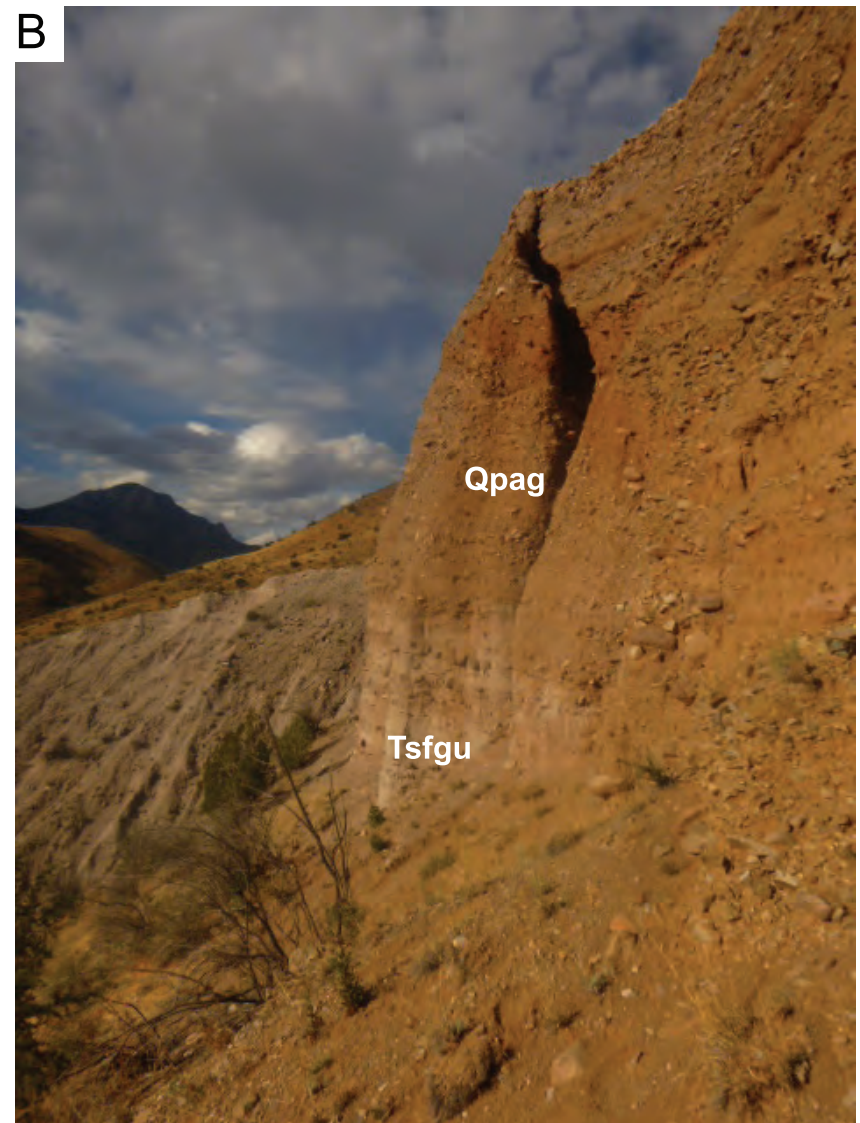
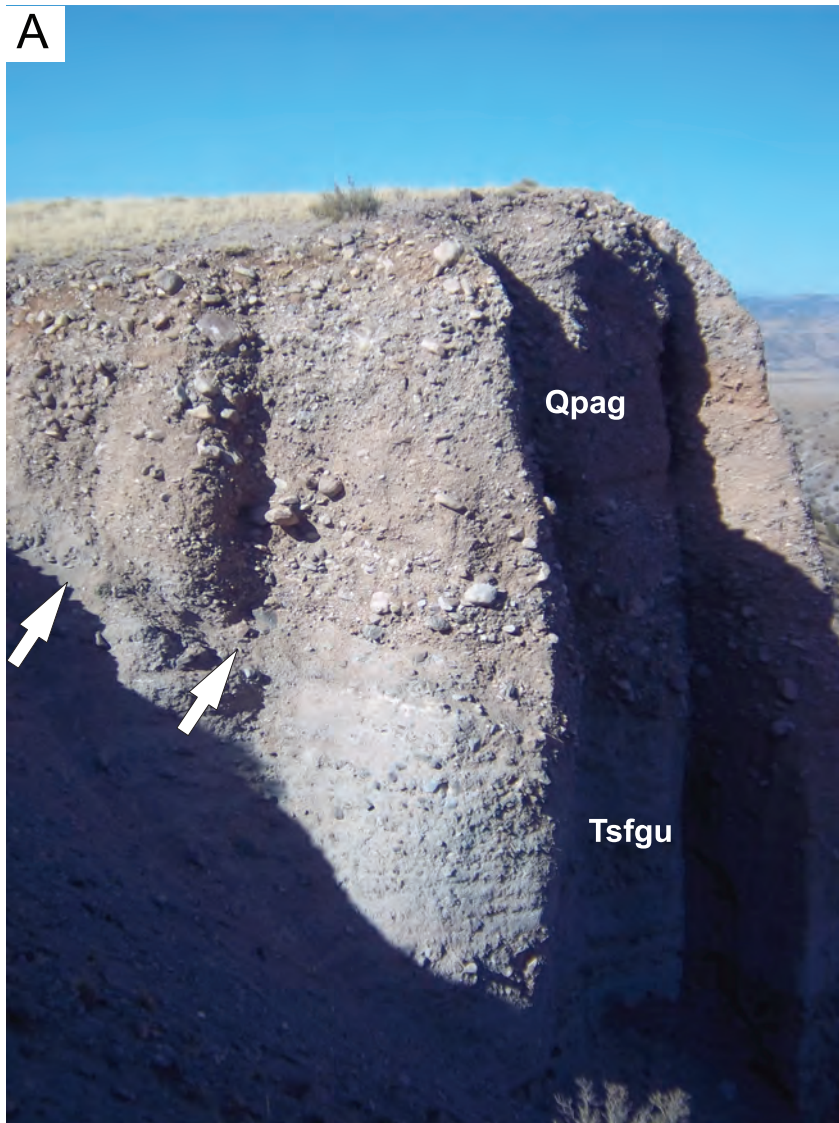


Figure 32

A



B



Figure 33

C



D

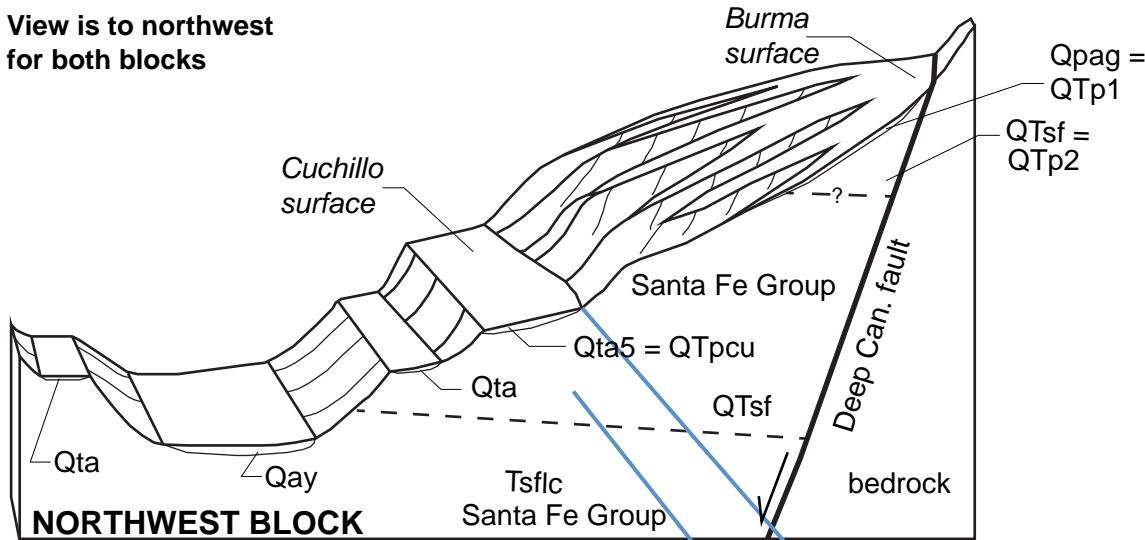


Figure 33

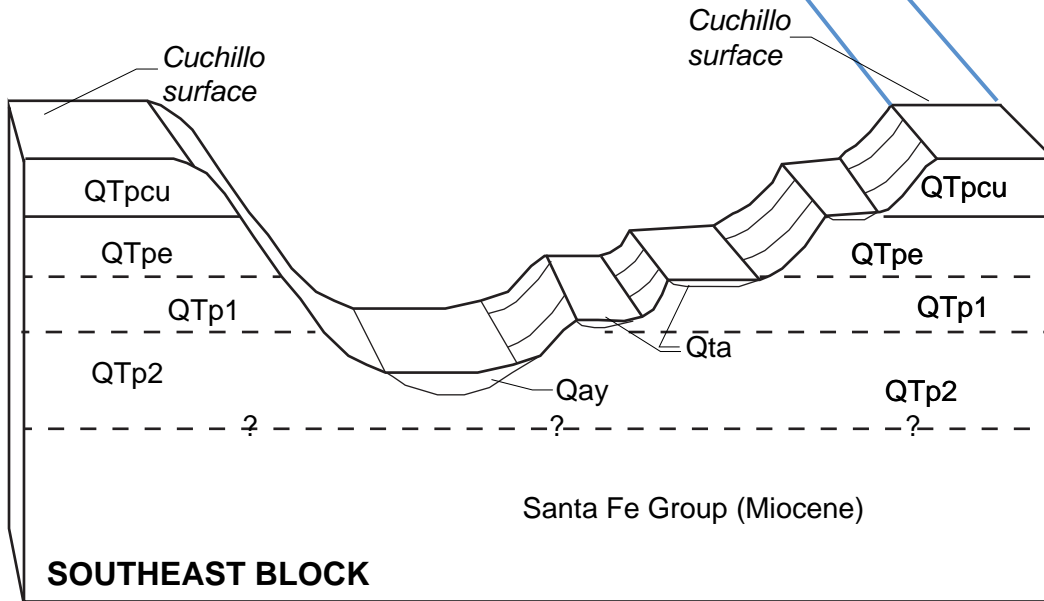


Figure 34

View is to northwest
for both blocks



NORTHWEST BLOCK



SOUTHEAST BLOCK

Preliminary interpretations:

- 1) Uppermost QTsf to NW aggrading contemporaneously with QTp2 in SE?
- 2) After minor erosion, Qpag aggrades in NW concomitantly with QTp1 in SE.
- 3) Formation of Burma surface
- 3) Early Pleistocene-age, major erosion in NW, resulting detritus is deposited in SE as QTpe
- 4) Aggradation of Qta5 and QTpcu between 0.8-1.0 Ma
- 5) Cessation of aggradation. Cuchillo surface forms at 0.78-0.80 Ma.
- 6) middle-late Pleistocene erosion and episodic terrace formation

KEY for SE block:

Palomas Formation

QTpcu -- upper, coarse unit

QTpe -- usediment deposited during erosion in NW block

QTp1 -- Lower Palomas Fm; sediment deposited during Qpag aggradation

QTp2 -- Lower Palomas Formation

Figure 35



Figure 36

A

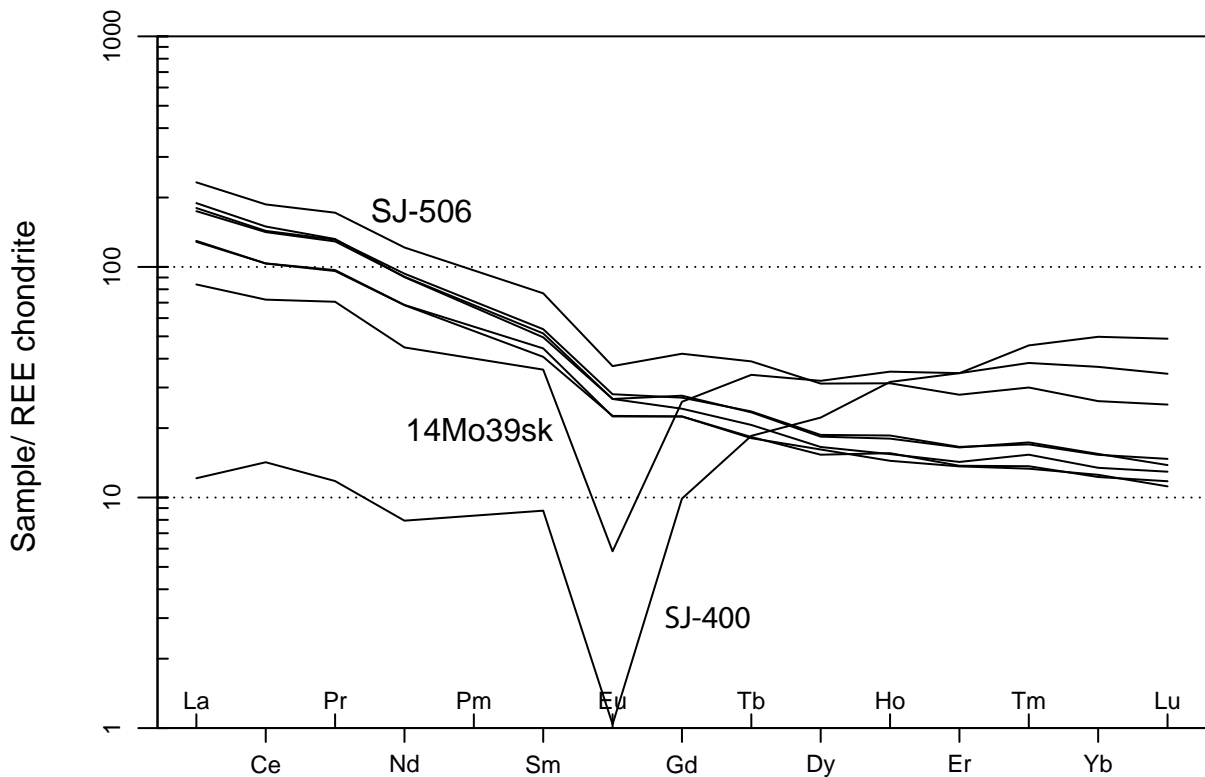


B



Figure 38

Spider plot – REE chondrite (Nakamura 1974)



Appendix 1. Detailed descriptions of lithologic units on the Monticello quadrangle

UNIT DESCRIPTIONS

The units described below were mapped using aerial photography coupled with field checks. Stereogrammetry software recently acquired by the N.M. Bureau of Geology (i.e., Stereo Analyst for ARCGIS 10.0, an ERDAS extension, version 11.0.4) results in relatively accurate placement of geologic contacts. Grain sizes follow the Udden-Wentworth scale for clastic sediments (Udden, 1914; Wentworth, 1922) and are based on field estimates. Pebbles are subdivided as shown in Compton (1985). The term "clast(s)" refers to the grain size fraction greater than 2 mm in diameter. Descriptions of bedding thickness follow Ingram (1954). Colors of sediment are based on visual comparison of dry samples to the Munsell Soil Color Charts (Munsell Color, 1994). Soil horizon designations and descriptive terms follow those of the Soil Survey Staff (1992), Birkeland et al. (1991), and Birkeland (1999). Stages of pedogenic calcium carbonate morphology follow those of Gile et al. (1966) and Birkeland (1999). Description of sedimentary and igneous rocks was based on inspection using a hand lens.

Surface characteristics aid in mapping Holocene and middle-late Pleistocene units. Older deposits generally have older surfaces, so surface processes dependent on age -- such as desert pavement development, clast varnishing, calcium carbonate accumulation, and eradication of original bar-and-swale topography -- can be used to differentiate terrace, alluvial fan, and valley floor deposits. Locally, erosion may create a young surface on top of an older deposit, so care must be exercised in using surface characteristics to map Quaternary deposits.

Hillslope and landslide units (Quaternary)

Qct Colluvium and talus (middle to upper Pleistocene and Holocene) – Poorly sorted, angular to subangular, clayey-silty sand and gravel mantling middle-lower hillslopes. <8 m thick.

Qs Slopewash deposits (upper Pleistocene to Holocene) – Sand and pebbly sand forming thin mantles on older Quaternary gravel or bedrock underlying footslopes and toeslopes. Deposit is unconsolidated and massive. Matrix is very pale brown (10YR 7/3), moderately to well sorted, subangular to subrounded, silty, very fine- to medium-grained sand. Clasts include sparse pebbles ($\leq 15\%$) that are poorly to moderately sorted and angular to subrounded. Maximum thickness 4 m (13.1 ft).

Qs/Qao Slopewash deposits overlying older alluvium (upper Pleistocene to Holocene) -- Slopewash deposits, as described above (Qs), overlying unit Qao (described below).

Qs/Qao1 Slopewash deposits overlying the younger allostratigraphic unit of the older alluvium (upper Pleistocene to Holocene) -- Slopewash deposits, as described above (Qs), overlying unit Qao1 (described below).

Qs/Qao2 Slopewash deposits overlying the middle allostratigraphic unit of the older alluvium (upper Pleistocene to Holocene) -- Slopewash deposits, as described above (Qs), overlying unit Qao2 (described below).

Qs/Qao3 Slopewash deposits overlying the older allostratigraphic unit of the older alluvium (upper Pleistocene to Holocene) -- Slopewash deposits, as described above (Qs), overlying unit Qao1 (described below).

Qs/Trrwb Slopewash deposits overlying biotite-bearing dacite of the Whiskey Hill Member of the Red Rock Ranch Formation (upper Pleistocene to Holocene) -- Slopewash deposits, as described above (Qs), overlying unit Trrwb (described below).

Qsc Slopewash and colluvium deposits, undivided (middle Pleistocene to Holocene) -- Undifferentiated slopewash and colluvium, mapped at the footslope of the hill labeled 6256 in the southeastern quadrangle. Here, colluvium grades laterally into slopewash deposits as the slope decreases. 1-4(?) m thick.

Qls Landslide deposits (middle to upper Pleistocene) -- Poorly exposed landslide deposits that flank the hill labeled 6256 in the southeastern quadrangle. The deposit there consists of clay to sand mixed with gravel of the Luna Park Tuff. Large blocks of Luna Park Tuff within the landslide deposits are differentiated (see below). Here, shear planes likely developed in the underlying, relatively fine-grained unit of Trrst. Also mapped on the northeast side of Serefino Hill and in upper Cedro Canyon. In the latter, ~ 5 m of weakly consolidated sandy gravel, belonging to unit QTsf, appears to have slid downhill along a basal shear zone.

Qls-lp -- Fractured block of undivided Luna Park Tuff that was translated downslope in a landslide.

Qls-lpl -- Fractured block of Lower Luna Park Tuff that was translated downslope in a landslide.

Qls-lpu -- Fractured block of Upper Luna Park Tuff that was translated downslope in a landslide.

Qlsi Individual lobe of a landslide deposits (middle to upper Pleistocene) -- Landslide deposit as described above (unit Qls) that is inset into older landslide deposits, indicating a younger age.

Valley bottom units (Quaternary)

Unless otherwise noted, gravel is composed of rhyolite and minor felsic tuffs (both mainly crystal-poor) along with 5-15% andesite. The latter is typically dark gray and

contains plagioclase ± pyroxene phenocrysts. Clasts are subrounded (minor subangular). Sand is subrounded to subangular and a volcanic litharenite.

daf Dam-related artificial fill (modern) -- Valley bottom sand and gravel that has been moved by humans to form dams for impounding water.

Qam Modern alluvium (0 to ~50 years old) – Sand and gravel in active channels or underlying very low surfaces astride active channels. Unit inferred to receive runoff from high-precipitation, monsoonal storms that likely have multi-year to decadal recurrence intervals. Bar and swale topography and channel forms are sharp on gravelly surfaces, with 30-100 cm of typical surface relief. Sandy surfaces are relatively flat and smooth. Vegetation is sparse on both sandy and gravelly surfaces. Sediment is commonly in very thin to thin, tabular to lenticular beds; sand is typically horizontal-planar laminated to cross-laminated. Gravel is poorly sorted and consists of pebbles through boulders (mostly pebbles). Clasts are subrounded to angular (mostly subangular) and poorly sorted. Sand is grayish brown to brown (10YR 5/2-3), fine- to very coarse-grained (mostly medium- to very coarse-grained), subrounded to subangular and poorly to moderately sorted. Loose and no soil development. Thickness is unknown but likely 1-3 m.

Qamh Modern and historical alluvium, undivided (0 to ~800 years old) – Modern alluvium (**Qam**) and subordinate historical alluvium (**Qah**). See detailed descriptions of those individual units.

Qah Historical alluvium (50 to ~800 years old) – Interbedded sand and gravel in valley bottoms. Sediment is typically well-bedded, although locally it may be bioturbated and massive. Gravelly sediment is generally in very thin to medium, tabular to lenticular beds; reverse grading locally observed. Sandy beds are commonly internally horizontal-planar laminated to low-angle cross-laminated. Gravel consists of pebble, 25-40% cobbles, and 10-20% boulders, and clast- to matrix-supported. Clasts are subrounded to subangular and moderately to poorly sorted. Gravel composition is dependent on the local source area. Sand is brown (7.5YR 5/2; 10YR 4-5/3), very fine- to very coarse-grained, subrounded to subangular, and well to poorly sorted. Surface is vegetated, gravelly, and exhibits muted bar and swale topography and channel forms; generally 10-40 cm of surface relief. Sparsely to moderately vegetated and exhibits no obvious soil development. Tread is generally less than 2 m above modern grade. Loose. Base not observed in thickest deposits; possibly up to 3-4 m maximum thickness.

Qaha Historical alluvium Alamosa Creek (50 to ~800 years old) -- Mostly clayey-silty, very fine- to fine-grained sand, with subordinate gravelly interbeds. Finger-grained sediment is brown to pale brown (10YR 5-6/3) and contains 25% scattered, coarser sand and pebbles; it is typically massive, with local horizontal-laminations or ripple-marks. Gravelly beds are in very thin to thin, tabular to lenticular beds. Gravel consist of pebbles with 15-20% cobbles and 1% boulders;

these are typically subrounded to subangular, clast-supported, imbricated, and poorly to moderately sorted. Sand associated with the gravel beds is fine- to very coarse-grained, grayish brown to light brownish gray (10YR 5-6/2), subrounded to subangular, poorly sorted, and contains abundant volcanic grains. Weakly to moderately consolidated and non-cemented. Base is not observed; deposit is possibly up to 4 m thick.

Qaham Historical alluvium Alamosa Creek (50 to ~800 years old) --
Historical alluvium of Alamosa Creek (**Qaha**) and subordinate modern alluvium (**Qam**), which are described in detail above.

Qahm Historical alluvium and modern alluvium, undivided (0 to ~800 years old) -- Historical alluvium (**Qah**) and subordinate modern alluvium (**Qam**), which are described in detail above.

Qahy Historical alluvium and younger alluvium, undivided (~50 to 8,000 years old) -- Historical alluvium (**Qah**) and subordinate younger alluvium (**Qay**). See detailed descriptions of those individual units.

Qar Subequal modern and historic alluvium (modern to ~800 years old) --
Subequal modern (**Qam**) and historical alluvium (**Qah**), which are described in detail above.

Qary Recent alluvium (historical + modern) and younger alluvium, undivided (0 to 8,000 years old) -- Recent alluvium (**Qah** and **Qam** -- grouped together as a "recent" deposit) and subordinate younger alluvium (**Qay**). See detailed descriptions of these individual units.

Qay Younger alluvium, undivided (middle to upper Holocene) -- Sand -- with subordinate clay, silt, and gravel, occupying the bottoms of modern valleys and underlying low-level terraces alongside modern arroyos. Fining-upward trends locally observed; unit is overall browner than **Qao**, and less well-bedded and finer-grained than **Qah**. Gravelly sediment is in very thin to medium, lenticular to tabular beds. Clasts are dominated by pebbles and cobbles; boulders are minor. Gravel is typically clast-supported and poorly sorted. Sand is brown (10YR 4-5/3) -- with lesser grayish brown or light brownish gray (10YR 5-6/2) -- but may redden down-section, very fine- to very coarse-grained, subrounded to subangular, and poorly sorted. Sand and pebbly sand intervals are commonly massive, contain notable silt and clay, and may be overprinted by cumulic soils; these contain subordinate, very thin to medium, lenticular interbeds of pebbly sediment or feature minor, scattered coarser sand and pebbles. Except where eroded, the top of this unit typically exhibits a weak soil marked by calcium carbonate accumulation (stage I to II carbonate morphology). Surface clasts are non- to weakly varnished and generally the surface is smooth, although locally subtle bar- and swale- topography may be evident. Surface exhibits a weak clast armor and is slightly higher than the surface associated with **Qah**. Loose to

weakly consolidated. Estimated thickness of 1-5 m (base is typically not exposed).

Qaym Younger alluvium and modern alluvium, undivided (0 to 800 years old) – Younger alluvium and subordinate active alluvium, the latter typically occupying an incised channel. See descriptions for **Qay** and **Qam** above.

Qayh Younger alluvium and historic alluvium, undivided (50 to 8000 years old) – Younger alluvium and subordinate historic alluvium. See descriptions for **Qay** and **Qah** above.

Qayr Younger alluvium and recent (historical + modern +active) alluvium, undivided (800 to 8000 years old) – Historic and modern alluvium (**Qah** and **Qam** -- grouped together as a “recent” deposit) and subordinate modern alluvium (**Qam**) deposited on alluvial fans in Monticello Canyon. See detailed descriptions of these individual units. Up to ~10 m thick.

Terrace deposits and older alluvium

Unless otherwise noted, gravel is composed of rhyolite and minor felsic tuffs (mainly crystal-poor) along with 5-10% andesite. The latter is typically dark gray and contains plagioclase ± pyroxene phenocrysts. Clasts are typically subrounded to subangular. Sand is subrounded to subangular and a volcanic litharenite.

Terrace deposits associated with Alamosa Creek

Qta1 Lower Alamosa terrace deposit (upper-middle to upper Pleistocene) -- A remarkably coarse terrace deposit. It is coarser and browner than unit **QTp**, which it commonly overlies. Thick alluvial fans prograde across it and houses are commonly found on its flat surface. Consisting of sandy gravel, its bedding is poor and characterized by thin to thick, tabular to lenticular to low-angle (and very thin) cross-stratified bed geometries. Gravel is well-graded (pebbles through boulders), clast-supported, subrounded to rounded, very poorly sorted, and imbricated (indicating southwest, south, and southeast paleoflow directions). The sand is gray to brown (10YR 6/1 to 5/3), mostly medium- to very coarse-grained, and moderately to poorly sorted. 1-3% clay chips and argillans. Weakly to moderately consolidated and non- to weakly cemented (by clays). Surface is subjected to sheetflooding and erosion, and the development of the preserved soil is variable (stage I to stage III carbonate morphology). Tread stands 8-15 m above modern stream grade. Detailed soil data for the **Qta1** terrace can be found in McCraw and Williams (2012, where it is called Qta5). These workers interpret 35-55 cm-thick illuviated clay horizon(s) overlying 10-53 cm-thick calcic horizon(s) possessing a stage I carbonate morphology (soil pits CA5

and CA6b, note that we correlate include their Qta6b as part of Qta5). 2-6 m thick. Locally, **Qta1** can be subdivided into three subunits:

Qta1a Lower subunit of the lower terrace deposit along Alamosa Creek (upper-middle to upper Pleistocene) – Sandy gravel whose sediment resembles that of units **Qta1b** and **Qta1a**. Not described in detail. 1-2 m thick.

Qta1b Middle subunit of the lower terrace deposit along Alamosa Creek (upper-middle to upper Pleistocene) – Sandy gravel whose sediment resembles that of units **Qta1c** and **Qta1a**. Not described in detail. Tread lies 2-3 m above the tread of **Qta1c**. Thickness not accurately measured but likely 1-2 m thick.

Qta1c Upper subunit of the lower terrace deposit along Alamosa Creek (upper-middle to upper Pleistocene) – A Sandy gravel whose sediment resembles that of units **Qta1b** and **Qta1c**. Not described in detail. Tread lies ~2 m above the tread of **Qta1b**. Thickness not accurately measured but likely 1-2 m thick.

Qtau Undifferentiated Alamosa terrace deposit (Pleistocene) – Sandy gravel terrace deposit that was not correlated. 1-5 m thick. Lies between the **Qta1** and **Qta2** terrace levels.

Qta2 Lower-middle terrace deposit along Alamosa Creek (middle Pleistocene) – A strath to fill terrace of variable thickness. Composed largely of clast-supported, sandy gravel. Gravel contains pebbles with 30-35% cobbles and 5-30% boulders that are subrounded to rounded, poorly sorted, and composed of: 30-40% gray, fine-grained rhyolites; 20% reddish, fine-grained Vicks Peak Tuff; 10-30% leucocratic (yellow to tan), feldspar- and quartz-bearing, porphyritic to equigranular felsic rocks; 5-10% tuffs with distinct flame; and 7-30% feldspar-phyric, tan porphyritic rocks; and 7-20% plagioclase- to pyroxene-phyric andesites;; trace to 1% basalts and miscellaneous clasts. Weakly to moderately consolidated. East of Monticello, exposures show a sandy gravel in very thin to thin, tabular beds (with 15-25% thin to medium, lenticular beds), together with 10-15% horizontal-planar laminated sand. Gravel are subrounded to subangular and moderately to poorly sorted within a bed. Sand is brown to yellowish brown (10YR 5/3-4), fine- to very coarse-grained, subrounded to subangular, and poorly sorted. Strath lies 18-30 m above modern stream grade. Loose. 2-12 m thick, generally thinning upstream. Locally subdivided into three subunits:

Qta2a -- Strath lies 18-20 m above modern stream grade

Qta2b -- Strath lies 1-2 m above the strath of **Qta2a**, but tread lies a few meters above the tread of **Qta2a**.

Qta2c -- A 6-12 m-thick fill terrace mapped west and north of Placitas. Tread slopes towards southwest and is at least 5 m above the tread of **Qta2b**.

Qta3 Upper-middle terrace deposit along Alamosa Creek (middle Pleistocene) – A 12-18 m-thick fill terrace mapped in the west-center part of the quadrangle. Gravel consist of pebbles through boudlers that are rounded to subrounded. Clasts are composed of tan, porphyritic volcanic rocks (where phenocrysts are 1-8 mm long), fine-grained rhyolite and tuffs, plagioclase- and pyroxene-phyric andesite, and porphyritic tuffs. Strath lies 30-38 m above modern stream grade and is inset 10-12 m below the strath associated with unit **Qta4**.

Qta4 Upper terrace deposit along Alamosa Creek (middle Pleistocene) -- A 7-15 m-thick fill terrace mapped in the west center part of the quadrangle. Strath lies about 45-54 m above modern stream grade. Composed of a sandy gravel, with minor pebble sand, in very thin to medium, tabular to lenticular beds. Gravel consists of pebbles with 30% cobbles and 10-15% boulders; it is clast-supported, subrounded, and moderately to poorly sorted within a bed. Gravel composition: 20-30% light gray, fine-grained felsites, 30% plagioclase- and pyroxene-phyric andesite, 20-30% maroon-colored Vicks Peak Tuff, 10-15% tan, porphyritic volcanic rock similar to the andesite of Questa Spring (unit **Trraq**), and 10% reddish brown to light gray porphyritic volcanic rocks. Sand is light brown (7.5YR 6/3), mostly medium- to very coarse-grained, subrounded, poorly to moderately sorted, and dominated by volcanic grains. Unit contains ~10%, 1-2 m-thick intervals of massive, white (5YR 8/1), silty (est. 10% silt), very fine- to fine-grained sand with minor, scattered medium to very coarse sand and pebbles; this sand locally has 5-7% rhizoliths. Weakly to moderately consolidated. 7-15 m thick.

Qta5 Terrace deposit whose tread projects to the Cuchillo surface (uppermost lower Pleistocene) -- A sandy gravel disconformably overlying older Santa Fe Group basin-fill. Strath lies 65-85 m above modern stream grade. Strata are in thin to thick, vague beds that are locally cross-stratified (with foresets up to 1 m thick). Gravel are well-graded pebbles through boulders that are subrounded to rounded. Estimated clast composition of: 60% light gray to gray, fine-grained rhyolite or tuffs; 15% light gray, porphyritic rhyolite; 15% pink to purple, fine-grained rhyolite; 5-10% dark gray, plagioclase- to pyroxene-phyric andesites; ~10% tan, feldspar-phyric clasts that look similar to the andesite of Questa Spring. Sand is reddish brown to light reddish brown (5YR 4-5/4; 6/3), mostly medium- to very coarse-grained, subrounded to rounded, moderately to poorly sorted, and dominated by volcanic grains. 4-8 m thick.

Older alluvium and terraces associated with streams other than Alamosa Creek

Qao Older alluvium, undivided (middle to upper Pleistocene) – Alluvium alongside drainages other than Alamosa Creek whose surfaces are higher than those associated with unit **Qay** and whose bases are buried by modern alluvium or very close to, modern stream grade. Generally consists of interbedded pebbly sand, sandy pebbles, and sand. Occurs in clast- to matrix-supported, very thin to thick, tabular to lenticular beds; locally massive, imbricated, or cross-stratified. Clasts include poorly to moderately sorted, subrounded to angular pebbles, cobbles, and sparse ($\leq 20\%$) boulders. Matrix locally has up to 5% clay-silt and consists of brown to strong brown (7.5YR 4-5/4; 10YR 4-5/3) to reddish brown (5YR 4-5/3), poorly to well sorted, subangular to rounded, silt to very coarse-grained sand with 40% lithic, 30% feldspar, and 30% quartz grains; sand is subrounded to subangular, and poorly sorted. Sand likely to be laminated. Clay may coat sand grains. Matrix-supported debris flow deposits are abundant near steep slopes. Above ~5500 ft elevation, this unit's matrix is notably redder than the matrix of Holocene deposits (e.g., **Qay**). Deposit is unconsolidated. Topsoil contains an illuviated clay horizon(s), up to 60 cm thick, underlain by calcic horizon(s) (stage II carbonate morphology) up to 1 m thick. Moderately to well consolidated. 2.7-4.4 m (8.9-14.4 ft) thick. 2-4 m thick. Locally subdivided where distinguishable fill terraces, whose bases are not observed, are present along a given stream. It is assumed these terraces represent allostratigraphic units, although buttress contacts have not been observed:

Qao1 Younger allostratigraphic unit of older alluvium -- Top is 2-3 m above modern stream grade.

Qao2 Middle allostratigraphic unit of older alluvium -- Upper surface is 1-6 m above the surface of Qao1.

Qao3 Older allostratigraphic unit of older alluvium -- Upper surface is 2-3 m above the top surface of unit Qao2.

Qtt Tributary terrace deposit, undivided (middle to upper Pleistocene) -- Sandy gravel occurring in terrace deposits 1-2.7 m (3.3-8.9 ft) thick with surfaces and straths higher than those associated with Qao (compared to modern stream grade). Clast compositions are typically volcanic, but may include some Paleozoic carbonates in Placitas Canyon and drainages to its east. In a given drainage, this unit is locally subdivided into three terraces whose heights differ in elevation above the modern drainage:

QttH Higher tributary terrace deposit – Sandy pebble-cobble gravel similar to deposits of *Qttl* and *Qttm* terraces but with $\geq 70\%$ of clasts varnished at surface. More poorly exposed than lower (younger) terrace gravels. Tread height varies from 20 m (66 ft) above modern grade in Shipman Canyon to 57 m (187 ft) above modern grade in Garcia Falls Canyon. Maximum thickness 2.6 m (8.5 ft) in Shipman Canyon.

Qttm Middle tributary terrace deposit – Sandy pebble-cobble gravel and subordinate sand lenses in thin to very thick, lenticular beds comprising strath terraces. Gravel is clast-supported and imbricated. Clasts are poorly sorted, dominantly subrounded, and consist of 65% pebbles, 30% cobbles, and 5% boulders. Red clay films are common on clast undersides. Approximately 60-70% of clasts are varnished at the surface. Matrix consists of light brown (7.5YR 6/4), moderately sorted, subangular to subrounded, silty, very fine- to medium-grained sand composed of 60% lithic, 35% feldspar, and 5% quartz grains. Deposit is unconsolidated and exhibits little evidence of carbonate soil development. Weakly silica-cemented in places. Tread height varies from 18 m (59 ft) above modern grade in Shipman Canyon to 40 m (131 ft) above modern grade in Garcia Falls Canyon. 1-1.9 m (3.3-6.2 ft) thick in Shipman Canyon.

Qttl Lower tributary terrace deposit – Sandy pebble-cobble gravel in medium to very thick, broadly lenticular beds comprising strath terraces. Gravel is clast-supported and imbricated. Clasts are poorly sorted, dominantly subrounded, and consist of 50-65% pebbles, 30-45% cobbles, and 0-5% boulders. Clay films are common on pebbles. Approximately 60-70% of clasts are varnished at the surface. Matrix consists of reddish brown (5YR 4/4), moderately well sorted, subangular to subrounded, fine- to medium-grained sand composed of 70% lithic, 25-30% feldspar, and 0-5% quartz grains. Deposit is unconsolidated and exhibits little evidence of carbonate soil development. Tread height varies from 10 m (33 ft) above modern grade in Shipman Canyon to 22 m (72 ft) above modern grade in Garcia Falls Canyon. 2.5-2.7 m (8.2-8.9 ft) thick in Shipman Canyon.

Alluvial fan units

Fan gravel is dominated by the lithologies exposed in the catchments from which fans emanate. Clasts are typically angular to subangular (occasionally subrounded), and may be $\geq 90\%$ volcanic lithologies in the northern and western parts of the quadrangle and $\geq 60\%$ Paleozoic carbonates in the eastern parts of the quadrangles.

Qfam Modern-active alluvium in alluvial fans (0 to ~50 years old) – Unit is similar to that described in **Qam** but is found on alluvial fans. Probably less than 3 m thick.

Qfamh Modern and historic alluvium in alluvial fans, undivided (0 to ~800 years old) – Modern-active alluvium (**Qfam**) and subordinate historical alluvium (**Qfah**) deposited on alluvial fans. See descriptions of **Qfam** and **Qfah**. <3 m thick.

Qfamy Modern alluvium and younger alluvium in alluvial fans, undivided (0 to ~800 years old) – Modern-active alluvium (**Qfam**) and subordinate younger

alluvium (**Qfay**) deposited on alluvial fans. See descriptions of **Qfam** and **Qfah**. Several meters thick.

Qfah **Historical alluvium in alluvial fans (0 to ~50 years old)** – Unit is similar to that described in **Qah** but is found on alluvial fans. <3 m thick.

Qfahm **Historic and modern-active alluvium in alluvial fans flanking Monticello Canyon, undivided (0 to ~800 years old)** – Historic alluvium (**Qfah**) and subordinate modern alluvium (**Qam**) deposited on alluvial fans. See descriptions of **Qfah** and **Qfam** above. <3 m thick.

Qfary **Recent alluvium (historical + modern-active) and younger alluvium in alluvial fans flanking Monticello Canyon, undivided (0 to ~800 years old)** – Historic and modern alluvium (**Qfah** and **Qfam**, grouped together as a “recent” deposit) and subordinate younger alluvium (**Qfay**) deposited on alluvial fans. See descriptions of **Qfah**, **Qfam**, and **Qfay**. Up to ~10 m thick.

Qfay **Younger alluvium in alluvial fans (Holocene)** – Pebbly sand and pebble-cobble-boulder gravel in medium to very thick, tabular to broadly lenticular beds graded to the surface of *Qay*. Deposit is matrix-supported and massive. Gravel may be imbricated in subordinate clast-supported intervals. Clasts are poorly to moderately sorted, and consist of 40-95% pebbles, 5-50% cobbles, and 0-10% boulders. Clasts occasionally exhibit clay films and are typically unvarnished at the surface. Matrix consists of brown to pale brown (10YR 5-6/3), poorly to moderately sorted, subangular to subrounded, clayey silt to very coarse-grained sand composed of 70-80% lithic and 20-30% feldspar grains ($\leq 5\%$ quartz grains). Finer-grained beds may display stage II carbonate morphology with common Bk horizons and carbonate nodules and/or tubules; otherwise, soil development is weaker (e.g., Bk horizons have a stage I carbonate morphology) or negligible where surface is eroded. Bioturbation (fine to coarse roots, burrows) is common. Deposit is unconsolidated. Minimum thickness 1.3 m (4.3 ft).

Qfayh **Younger alluvium and historic alluvium (0 to ~800 years old)** – Younger alluvium (**Qfay**) and subordinate Historic alluvium (**Qah**) deposited on alluvial fans. See descriptions of **Qfay** and **Qfah** above. Up to ~10 m thick.

Qfayr **Younger alluvium and recent (modern + historic) alluvium in alluvial fans (0 to ~8000 years old)** – Younger alluvium (**Qfay**) and subordinate recent alluvium (grouped modern and historical alluvium, **Qam** and **Qah**) deposited on alluvial fans. See descriptions of **Qfay** and **Qfah** above. Up to ~10 m thick.

Qfao **Older alluvium in alluvial fans flanking Monticello Canyon, undivided (upper-middle Pleistocene to lower Holocene)** – Sandy pebble-cobble gravel to gravelly sand occurring in thin to very thick, tabular to lenticular beds graded to the surface of *Qao*. Deposit is mostly matrix-supported with subordinate stringers and lenses of clast-supported granule-pebble or pebble-cobble gravel.

Clasts are poorly to moderately sorted, angular to subangular (less commonly subrounded), and consist of 55-80% pebbles, 20-90% cobbles, and 0-10% boulders. Clay films are common on clasts. Matrix consists of brown (7.5YR 5/3) to light reddish brown (5YR 6/3-4), moderately to well sorted, subangular to subrounded, clayey silt to fine-grained sand dominated by lithic grains ($\leq 4\%$ quartz grains). Deposit may exhibit weak to moderate carbonate cementation, and carbonate rinds up to 1 mm on a plurality of clasts indicate stage II+ carbonate morphology in places. Unconsolidated. Minimum thickness 1.7 m (5.6 ft).

Qfaa1 Alluvial fans graded to the upper-lower terrace tread of Alamosa Creek (upper-middle(?) to upper Pleistocene) – An extensive unit composed of sandy gravel and sand. Fan surface is similar to the surface developed on **Qta1**. Up to 15 m thick.

Qfaa2 Alluvial fans graded to the middle terrace tread of Alamosa Creek (upper-middle(?) to upper Pleistocene) – Sandy gravel comprising alluvial fans that have prograded westward onto the **Qta2** terrace tread. 1-5 m thick.

Qfaa3 Alluvial fans graded to the upper-lower terrace tread of Alamosa Creek (upper-middle(?) to upper Pleistocene) – Sandy gravel comprising alluvial fans that have prograded westward onto the **Qta3** terrace tread. 1-5 m thick.

High-level piedmont deposits

Qpag High-level piedmont deposits near Garcia Falls (upper Pleistocene to Holocene) – Pebble-cobble to cobble gravel in medium to thick, tabular beds. Deposit is unconsolidated and massive to weakly imbricated. Clasts include moderately sorted, subangular cobbles (80-85%) and pebbles (15-20%) with very rare boulders. Clast lithologies include subequal proportions of *Tgfa* and *Tvp*. Matrix consists of brown (10YR 4/3), moderately sorted, subangular, fine- to coarse-grained sand composed of approximately 50% lithic, 30% feldspar, and 20% quartz grains. Deposit may exhibit stage I carbonate morphology in upper 40 cm (16 in). Typically 1-3.5 m (3.3-11.5 ft) thick.

Qpas High-level piedmont deposits south of Serafino Hill (middle to upper Pleistocene) – Pebble-cobble gravel in medium to thick, tabular beds. Deposit is unconsolidated and massive. Clasts include poorly to moderately sorted, subangular to subrounded pebbles (50-60%), cobbles (35-45%), and sparse boulders ($\leq 5\%$). Clast lithologies dominated by *Trrs*. Matrix consists of reddish brown (5YR 4/3), poorly to moderately sorted, angular to subrounded, fine- to coarse-grained sand. Rarely more than 3 m (9.8 ft) thick.

Tertiary Basin-fill

QTsf Santa Fe Group basin-fill (Lower or Middle Miocene through Pliocene, possibly lowest Quaternary) – Sandy gravel in very thin to thin (minor medium), tabular beds. Gravel is clast-supported, commonly imbricated, and consists of pebbles and subordinate cobbles. ~10% pebbly sand. Clasts are subrounded to subangular and moderately to poorly sorted within a bed. No debris flow deposits observed. Gravel are composed of gray to pink, crystal-poor rhyolite, 20-25% pink-red-gray, porphyritic rhyolite (largely feldspar-phyric), and 10-15% dark gray, porphyritic andesite (plagioclase +/- pyroxene phenocrysts). Sand is gray to light reddish brown (5YR 6/1-3) if clayey, light gray to light brown (7.5YR 5/1 to 6/3) if not clayey, fine- to very coarse-grained (mostly medium- to very coarse-grained), subrounded (mostly) to subangular, poorly to moderately sorted, and a volcanic litharenite. Some gravelly intervals exhibit partial clay films on clasts and coarse sand grains; clay chips occupy 1-3% of sand fraction, locally as much as 10-15%. 1-20% of sediment exhibits dm-scale intervals of clay-rich (1-5% clay) pebbly sand; the sand is very fine- to very coarse-grained and the pebbles are very fine to very coarse. The contact between **Tsflc** and the overlying **Santa Fe Group** is conformable and gradational over several 10s of meters of stratigraphic distance.

Moderately to well consolidated and weakly cemented by clay. Sediment was deposited in a proximal piedmont setting.

Tsfgu Upper Gracia falls lithosome in the Santa Fe Group (upper Miocene) -- Pebbly sand/sandstone and subordinate pebble-cobble gravel/conglomerate in thin to thick, tabular beds. Sandy beds make up approximately 85% of unit and are weakly to moderately carbonate-cemented, massive to broadly planar cross-stratified, and reverse graded. Matrix consists of light brownish gray to light gray (10YR 6-7/2), typically well sorted, subangular to subrounded silt to fine-grained sand. Matrix is quartz-poor ($\leq 10\%$) with 30-70% feldspar and 30-70% lithic grains; volcanic litharenite is most common. Gravel/conglomerate beds feature poorly to moderately sorted, subangular to rounded pebbles (80-90%), cobbles (5-20%), and boulders (0-5%) dominated by intermediate volcanic lithologies, including 30-40% clasts of *Tgfa*. Approximately 75-80 m (246-262 ft) thick.

Tsfgl Lower Gracia falls lithosome in the Santa Fe Group (upper Miocene) -- Sandy pebble-cobble and pebble-cobble-boulder gravel/conglomerate in medium to thick, tabular to broadly lenticular beds. Gravel is clast-supported and massive to commonly imbricated. Imbricated clasts yield an average paleocurrent direction toward SSW (197°). Clasts are poorly to moderately sorted, subangular to subrounded, and consist of 55-65% pebbles, 35-40% cobbles, and 5-10% boulders. Clast lithologies include subequal proportions of plagioclase-phyric andesite (typically *Tgfa*), crystal-poor *Tvp*, and aphanitic rhyolite. Matrix consists of grayish brown to light gray (10YR 5-7/2), poorly to moderately sorted, subangular to subrounded, silty, fine- to coarse-grained sand.

Matrix is quartz-poor ($\leq 10\%$) with 30-70% feldspar and 30-70% lithic grains; volcanic litharenite is most common. Unit may be very weakly carbonate-cemented, particularly in pebble-rich beds. Clasts occasionally feature moderately developed carbonate rinds on their undersides. Minimum thickness 25 m (82 ft).

Tsflc Lower, coarse-grained Santa Fe Group (Oligocene to lower Miocene) -- Sandy conglomerate, with minor pebbly sandstone intervals. Bedding is mostly very thin to medium and tabular; 10-20% thin to medium, lenticular beds of coarse to very coarse pebbles and cobbles; 10% very thin, cross-stratified beds. . Clast imbrication is variable and mostly to the south-southeast. Gravel consists of 50-80% pebbles, 20-40% cobbles, and 10-15% boulders. Clasts are subrounded to subangular and moderately to very poorly sorted. Clast- to matrix-supported. Gravel are mainly composed of light gray, crystal-poor rhyolite, 1-20% welded tuff, and 10% crystal-rich rhyolite, and trace-3% dark gray andesite. Other clast types are more variable and include: 1) 2-5% vesicular, dark gray basalt, and 2) 0-20% plagioclase-phyric latite or andesite; 3) 3% megacrystic latite (with plagioclase phenocrysts >5 mm long). Sand is 7.5YR 6/4-6/6, medium- to very coarse-grained (mostly coarse- to very coarse-grained), subrounded, moderately to poorly sorted, and a volcanic litharenite. The contact between **Tsflc** and the overlying **Santa Fe Group** is conformable and gradational over several 10s of meters of stratigraphic distance. Weakly to strongly cemented, becoming more cemented with depth; weakly to well consolidated. 1500 m thick.

Intrusions

Ti Undifferentiated intrusions – Probably felsic in northern part of the quadrangle. In northern Serefino Canyon, this unit is a highly weathered sill with maroon, clay-rich material at the surface.

Tir Rhyolitic intrusions (upper Oligocene) -- Intrusions filling dikes and (less commonly) stocks that are composed of potassium feldspar and lesser quartz phenocrysts. Intrusions in the Aragon Hill area are altered to iron oxides, clay, and traces of alunite, pyrite, and native gold.

Tid Dacitic intrusion (upper Oligocene to early Miocene) -- Dacite dikes. Rock is light gray (fresh) and composed of: 1) plagioclase (0.2-2.0 mm, euhedral to subhedral), 7% hornblende; (0.5-4.0 mm, euhedral), 2-4% biotite (0.2-1.0 mm, eu to subhedral), and $<5\%$ qtz. Surface weathers to produce a strong varnish.

Volcanic bedrock

Tsc Tuff of Shipman Canyon (upper Oligocene) -- Purplish gray weathering brownish tan, massive to thick-bedded, porphyritic-aphanitic, hypocrySTALLINE, fine- to medium-grained ash-flow tuff. Forms cliffs in lower Shipman Canyon. Phenocrysts include 6-8% quartz (up to 3 mm, anhedral), 2% sanidine (up to 2

mm, euhedral), and trace to 1% biotite (up to 1 mm, euhedral). Also contains 2-3% glass shards up to 2.5 mm. Somewhat to densely welded. Pumice fragments display flattening (length:width) ratios between 3:1 and 9:1. Unit consists of many interbedded flows, including light purplish gray air-fall tuff containing lapilli to fine bombs of aphanitic rhyolite and tuff. Spherulitic to vesicular tuff and rhyolite may also be present. Generally unaltered throughout section. Overlies rhyolite of Alamosa Creek, $^{40}\text{Ar}/^{39}\text{Ar}$ -dated at 28.4 Ma (Lynch, 2003; McLemore, 2010), in an angular unconformity ~150 m west of the quadrangle boundary in Shipman Canyon. Approximately 75 m (246 ft) thick.

Trac Rhyolite of Alamosa Creek (upper Oligocene) -- Light gray to gray, weathering to a reddish brown to brown, fine-grained, flow-banded rhyolite that is massive to vesicular to granular. In the latter texture, the granules are typically 1.5-2.0 mm wide. Trace to 2% sanidine phenocrysts 0.5-2.0 mm long and subhedral. Margins (including tops and bases) of flows exhibit thick (tens of meters) breccia zones. This rhyolite may extend into the northern Ramos Hills, but near the quadrangle boundary the bedrock has been mapped as a rhyolitic tuff by Heyl et al. (1983), which they call the "coarse Moonstone porphyritic rhyolite tuff (unit Trct). We were not able to access the Ramos Hills to map the contact between the two units. The rhyolite of Alamosa Canyon is as much as 60 m thick inside the caldera (Lynch, 2003) and 50-220 m thick west of the caldera boundary (McLemore, 2010). Age is 28.4 ± 0.04 Ma by $^{40}\text{Ar}/^{39}\text{Ar}$ (McLemore, 2010).

Tvp Vicks Peak Tuff (upper Oligocene) – Pink to white, crystal-poor welded tuff with less than 1% sanidine, commonly is foliated. Greenish black vitrophyre is common near the base. In places, a 1-3 m-thick, ledge-forming interval of gray to pink, crystal-poor, flow-banded tuff with trace amounts of sanidine, pyroxene, and quartz is present below the vitrophyre. Flattened pumice lapilli and sparse lithic fragments can be found near the base. Spherulitic features are present in certain zones. $^{40}\text{Ar}/^{39}\text{Ar}$ age is 28.39 ± 0.19 Ma (Chapin et al., 2004). The Vicks Peak Tuff is more than 690 m thick inside the caldera boundary (Lynch, 2003; McLemore, 2010) and ranges in thickness from 5-200 m thick west of the caldera boundary (Maldonado, 1974, 1980; McLemore, 2010). Maximum preserved thickness of 105 m. Top not exposed.

Rock Springs Formation (upper Eocene to lower Oligocene) -- Volcaniclastic sediment and trachyte flows interbedded with formation-rank ignimbrites (note that these ignimbrites are not included in this formation).

Trssv3 Interbedded sediment and trachytic volcanic flows, stratigraphically above the Hells Mesa Tuff (lower Oligocene) -- Breccia composed of clast-supported, angular to subrounded clasts of light gray trachytic lava containing hornblende and sanidine phenocrysts in an aphanitic matrix; higher up-section the matrix of the lava clasts is more equigranular and contains 1 to 2 mm-long hornblende and plagioclase. Interbedded with trachytic lavas (unit Trst). About 30 m thick.

Trst Trachytic lava (lower Oligocene) -- Lavas that contain less than 1% phenocrysts of sanidine and pyroxene (<2 mm long) in an aphanitic to trachytic matrix. Above the Hells Mesa Tuff, this unit includes sandy to conglomeratic to ashy intervals. Individual flows are <30 m thick.

Trssv2 Interbedded sediment and andesite volcanic flows, stratigraphically between the Hells Mesa and the Upper Luna Park Tuffs (lower Oligocene) -- Red volcanoclastic deposits interbedded with andesites. Sediments are variably silty to conglomeratic. Lavas include vesicular andesite lava containing 15-20% plagioclase phenocrysts (1-2 mm long) and <1% xenocrystic quartz (3-4 mm long) in a fine-grained crystalline matrix, Other lavas in this interval have no phenocrysts and exhibit a fine-grained crystalline matrix. Total interval is 3 to 15 m thick.

Trssv1 Interbedded sediment and andesite volcanic flows, stratigraphically between the Upper and Lower Luna Park Tuffs (upper Eocene to lower Oligocene) -- In the vicinity of Red Rock Arroyo, the lower 1.5-3 m of this unit consists of a reddish-brown pebble conglomerate in a sandy to silty matrix; clasts are composed of rounded tuff and lava, and pebbles are <1 cm long. Overlying lavas in this interval include brown, foliated, porphyritic andesite(?) containing 3-5% phenocrysts in an aphanitic to crystalline matrix; phenocrysts include plagioclase, clear and equant potassium feldspar (< 5 mm long), and pyroxene (~1 mm long). ~15 m thick.

Thm Hells Mesa Tuff (upper Oligocene) -- White to pink to peach-colored, lithic-poor (<5%), moderately welded tuff with 5-20% phenocrysts of quartz, biotite, sanidine, titanite, and sparse hornblende. $^{40}\text{Ar}/^{39}\text{Ar}$ age is 31.97 ± 0.12 Ma (Chapin et al., 2004). Thickness variable, ranging from 15 to 60 m.

Tlpu Upper unit of Luna Park (upper Eocene) -- Gray to tan to white and contains 5-15% phenocrysts of sanidine, plagioclase, and biotite. Welding is variable but generally most pronounced at the base and less welded near the top. The welded intervals are gray and can have rheomorphic fluidal textures. The top of Upper Luna Park Tuff in the north-central part of the quadrangle has 5-10% lithic fragments (up to 0.5 m long), but most lithics are <15 cm in diameter. In the southeastern quadrangle, the lower part of this unit is distinctly reddish (2.5-7.5YR 6-7/2) and contains 15-30% sanidine (0.2-2.0 mm), trace biotite, trace quartz, and trace hornblende. May be equivalent to the 34.98 ± 0.19 Ma Datil Well Tuff or 34.96 ± 0.04 Ma Bell Top 4 (Chapin et al., 2004). Approximately 75 m thick.

Tlpl Lower unit of Luna Park (upper Eocene) -- Near its base, this unit has 15-25% sanidine as well as subordinate biotite, plagioclase, magnetite, and a trace of quartz; near the top of the unit there is 2-15% lithic fragments. The top of this unit near Luna Park Campground is gray, welded, and contains 3-5% biotite, sanidine, and plagioclase phenocrysts with a trace of quartz; the unit here has

<1% 5mm lithics. The top of the lower Luna Park Tuff on the east side of Red Rock Arroyo has 10-15% lithic fragments. In the southeastern quadrangle, this unit is relatively thin (6-15 m), reddish gray (5YR 5/2) to brown (7.5YR 5/2), has 10-15% fiamme (up to 18 cm long) and 1-25% volcanic lithic fragments (mostly aphanitic, some with local biotite or hornblende phenocrysts), and contains 5-10% sanidine (up to 5 mm long), 1-3% biotite, and 0.5% hornblende; a basal 2-3 m-thick vitrophyre is locally present. Pumice in less welded section is crystal-poor and vapor-phase altered. Overlies Andesite of Questa Spring (**Trraq**), upper trachyte of the Red Rock Ranch Formation (**Trrut**), or the Tuff of Aragon Draw (**Ttad**). Age and correlation is uncertain; could be Bell Top 3 (35.69±0.12 Ma; Chapin et al., 2004) or from the Organ Mountains caldera (35.5-36.2 Ma; Chapin et al., 2004). 10-100 m thick.

Tlp Luna Park Tuff, undivided (upper Eocene) -- Unit includes **Tlpu** and **Tlpl**, described above.

Ttjmc Tuff of Jose Maria Canyon (upper Eocene) -- Light gray weathering gray or tannish orange, poorly outcropping, aphanitic tuff. Correlative to the Jose Maria andesite of Farkas (1969). Underlies two prominent hills east of Seferino Canyon. Contains trace amounts of medium-grained, euhedral sanidine and rare lithic fragments up to 1.2 cm (0.5 in) across. Fiamme and spherulites are 1-4 cm (0.4-1.6 in) wide. Approximately 40 m (131 ft) thick.

Ttad Tuff of Aragon Draw (upper Eocene) -- A coarse-grained, upward-coarsening, inferred ash-fall tuff whose basal 1-12 m is commonly welded (see **Ttadw** description below). Overlying the welded zone is a reddish, massive, breccia-like, hard unit consisting of scattered pebble- to cobble-size clasts (minor boulder-size) in a silt to fine sand matrix. The clasts contain three main lithologic types (listed from most to least common): 1) fine-grained and laminated tuff, typically flattened (up to a few 10s of cm long and a <5 cm tall) parallel to the lower contact and commonly folded; 2) 1-8% white igneous granules to pebbles (containing feldspar and minor hornblende, with very minor biotite and quartz), also locally flattened but not near as much as the tuff clasts; and 3) 1-5% plagioclase-phyric, light gray-gray-reddish gray andesite. Locally, the tuff clasts enclose the gray, plagioclase-phyric clasts. Gravel-size increases up-section, where the tuff clasts are as large as 45x45 cm. The matrix is pale red (507.5R 6-7/2) to light gray (5-7.5YR 7/1) to pinkish gray (7.5YR 7/1), fine-grained (silt to very fine- to fine-grained sand) with up to 30% scattered coarse to very coarse feldspar grains (probably from disintegration of the white igneous clasts; matrix locally contains trace biotite and/or hornblende <2 mm long, where the biotite is locally deformed. Remorphic textures are observed, manifested by the folded or swirly tuff clasts, and are especially prominent in the north-central part of the quadrangle. About 25-30 m thick, not including the lower welded unit.

Ttadw Welded basal part of Tuff of Aragon Draw -- Lower 1-12 m of the aforementioned tuff that is marked by 10-20% flattened pumices (fiamme) 5-

20 mm long and 1-4 mm tall. Pale red to reddish gray (5-10R 6/2, 5YR 5/2), weathering to pale red to light red (2.5YR 6/2-6; 2.5YR 7/2; 10R 7/2). Phenocrysts include trace to 12% (mostly <8%) mafic grains (hornblende and biotite), both 0.2-2 mm long and euhedral to subhedral, and 5-20% sanidine-dominated potassium feldspar (0.5-4.0 mm long and subhedral). Up to 10% granules of the white, feldspar-rich, igneous clast noted in the overlying tuff (unit Ttad) Groundmass is aphanitic. Thickness increases to the south.

Red Rock Formation (upper Eocene)

Trrs Seferino Hill conglomerate – Brownish red, well indurated, clast-to matrix-supported, tabular, massive, poorly sorted, angular to subrounded conglomerate containing clasts up to 1.5 m (4.9 ft). Clast lithologies dominated by Jose Maria tuff and Whiskey Hill hornblende andesite. Matrix features 9-12% volcanic lithic fragments, ≤ 5% quartz, and 3% plagioclase grains. Subordinate beds consist of weakly cross-bedded, coarse-grained sandstone. Unit is deeply altered at Fifty-Fifty Hill and contains many voids partially filled by globular chalcedony. Approximately 35-65 m (114-213 ft) thick.

Trrst Tuffaceous, fine-grained sediment (upper Eocene) -- Tuffaceous, massive sediment in the southeastern part of the quadrangle that lies stratigraphically between the tuff of Aragon Draw (bottom) and the Lower Luna Park Tuff (top). This poorly sorted sediment is white (2.5-7.5YR 8/1; 10YR 8/1) to very pale brown (10YR 8/2) to light brown to pink (7.5YR 6-7/3). It consists of clay, subordinate sand (very fine to very coarse, with quartz and sanidine grains), and 1-15% scattered pebbles (up to 8 mm long) composed of subangular to subrounded, gray, andesite-dacite pebbles. Locally, white pumice is observed (2-10 mm long). To the southeast, 3-4% fresh biotite crystals are observed in the matrix (0.2-1.0 mm long). On the northwest side of the hill labeled 6022, this unit includes massive sandy conglomerate (pebbles and 20% cobbles,) but this may possibly be part of the underlying tuff unit (Ttad). Clay probably includes altered ash. In the southeastern quadrangle, the unit reddens and fines-upsection. There, a tuffaceous sandstone lies in the lower part of the unit that is massive to horizontal-planar laminated to very thinly bedded; the sand is very fine- to very coarse-grained, subrounded to subangular, poorly sorted, and composed of feldspar, 12% quartz, ~12% volcanic lithic grains, and 10% mafic grains. Thickness is poorly constrained, but is at least 15 m, and the unit thins to the northwest.

Trrtu Upper trachyte (upper Eocene) -- Bluish-gray lava that contains < 1% phenocrysts of sanidine (1 to 2 mm long) in an aphanitic to crystalline matrix. This lava is exposed on both sides of Red Rock Arroyo and pinches out toward the east. This lava filled in a rugged paleotopography that developed on top of the Questa Spring andesite. Thickness is variable, ranging from 20-45 m.

Trrsu Upper volcanlastic sediment (upper Eocene) -- Reddish gray to light greenish maroon, volcanlastic sediment consisting of siltstone and sandstone, with minor pebbly sandstone. Laminated to very thin, tabular beds. Unit is preserved between the upper trachyte (**Trrut**) and the Questa Spring andesite(**Trraq**) on the west side of Red Rock Arroyo. At least 5 m thick.

Trraq Andesite of Questa Spring (upper Eocene) -- Brownish to greenish gray lava, highly porphyritic andesite. Phenocrysts include 30-50% plagioclase with lesser amounts of pyroxene and magnetite. The plagioclase crystals are conspicuously large (< 1 cm and generally 5 to 8 mm long). Unit overlies the Tuff of Aragon Draw in upper Uvas Canyon. Pinches out toward the south near Las Uvas Spring. Thickness ranges from 30-90 m.

Trrsm Middle sediment tongue (upper Eocene) -- Fine-grained sand (loess) and sandy pebbles that lie stratigraphically between the Red Rock Arroyo andesite(**Trrr**) and the tuff of Aragon Draw (**Ttad**). To the south, the sediment is light brown to pink (7.5YR 6-7/4), slightly silty-clayey (est. 5-10% fines) and tuffaceous (15-20%), and consists of very fine- to fine-grained, arkosic(?) sand. Likely eolian or eolian sand reworked by sheetflooding. To the north, this unit is 10 m of sandy pebbles to pebbly sand. Clasts are monolithic and composed of light gray, vesicular, flow-brecciated andesite that is plagioclase-phyric; gravel are angular to subangular, poorly sorted, and consist of very fine to very coarse pebbles with 10-15% cobbles, and 1% boulders. Matrix is a pinkish gray (7.5YR 6/2), silty very fine- to very coarse-grained sand composed of same rock as the gravels; sand is subrounded to subangular and poorly sorted. Massive to weakly consolidated. 1-10 m thick.

Trrr Red Rock Arroyo andesite (upper Eocene) -- Gray (typically weathering to light brown to reddish brown), vesicular, ledge-forming, plagioclase-phyric lavas with minor pyroxene phenocrysts. Fresh color of gray (N5-6/; 5-7.5YR 5/1) to reddish gray (5R-2.5YR 6/1), weathering to various reddish shades: brown (7.5YR 5/2), light brown (7.5YR 6/3), dark reddish gray (5YR 4/2), pink (5-7.5YR 7/3), pinkish gray (5YR 6/2), strong brown (7.5YR 5/6), or light reddish brown (2.5-5YR 6/3-4) to reddish brown (2.5YR 5/4). Phenocrysts include: 7-25% plagioclase (0.2-11 mm long, subhedral, lesser euhedral) and 0.5-5% pyroxene (0.1-2.0 mm and subhedral, locally altered to reddish minerals). Hornblende is locally seen (trace to 3%, 1-15 mm), especially north of Red Rock Ranch. 3-40% vesicles 0.5-10 mm long (some to 30 mm). Locally observed large amygdules (7-60 mm wide) filled with quartz or calcite. Outcrops are relatively resistant and make prominent ledges; within the ledge, however, spheroidal weathering is common. Basal contact may disconformably overlie the Luna Peak trachyandesite because it is sharp and exhibits up to 2 m of relief (with local vertical buttresses). 50-110 m thick, being thickest near Forest Road 139 and thinning to the north and south.

Trrl Luna Peak trachyandesite (upper Eocene) – Gray to light gray, plagioclase-megacrystic trachyandesite flows, where >10% of the plagioclase phenocrysts are ≥10 mm. Very porphyritic and vesicular. Commonly weathers to produce corestone topography. Color is light gray to gray (2.5-5Y 6/1; N/6 - N/7; 2.5-5Y 7/1-2) and weathers to brown or light brown (7.5YR 5/2-6/3-4); weathering also produces a dark varnish. Phenocrysts include: 40-70% plagioclase that are commonly aligned (0.5-28 mm long, euhedral to subhedral) and 0.5-7% pyroxene (0.5-9 mm long, eu to subhedral and locally altered to a reddish brown mineral). Groundmass is ≤0.2 mm and composed of plagioclase with minor mafic grains. Locally exhibits propylitic alteration. 3-35% vesicles 0.5-20 mm long (some to 7 cm long), some of which are filled with calcite or an amorphous black substance; to the south, geodes with calcite or quartz crystals. 120 m thick in the north-central part of the quadrangle, thinning to the south-southeast until it pinches out near Jose Maria well (in Jose Maria Canyon).

Trrp2 Placitas member (upper Eocene) -- Interbedded shale and limestone, with sandstone beds becoming more common to the north. The main body lies stratigraphically between the top of the Uvas basaltic trachyandesite and the base of the Luna Peak trachyandesite; however, 1-5 m-thick interbeds of this unit are present in the overlying Luna Peak trachyandesite. Shale is light to dark gray, finely laminated and friable, and contains up to 25% organic-rich, very dark grayish brown shale (2.5Y 3/2). To the south is 0.5-1%, gray, very fine- to fine-grained, lithic-rich sandstone beds containing fine to very coarse grains of angular feldspar. Also found locally to the south are 0-5%, biotite-bearing, altered ash interbeds (up to 4 cm thick). Limestone is in very thin to thick, tabular beds; it is light gray to gray, largely micritic, and interbedded with limy gray shale; locally, trace hornblende grains are seen in the limestone. To the north, the unit consists of a 10-15 cm-thick limestone overlain and underlain by fine- to coarse-grained, volcanoclastic sandstone -- transitioning to a gray to light brownish gray (10YR 6/1-2) sandstone at the northern quadrangle border (horizontal planar-laminated to wavy lamianted to massive, very fine- to fine-grained with minor medium to coarse grains of subangular to angular feldspar. 1-50 m thick, thinning to the north. Not mapped where it is less than 3 m thick.

Trrael Andesite east of Luna Peak (upper Eocene) -- Relatively fine-grained, gray, and porphyritic andesite, located on the west slopes of Luna Peak, that lies stratigraphically between the Garcia Falls trachyandesite (bottom) and Luna Peak andesite (top). Correlates to Hermann's (1986) upper andesite member of the Red Rock Ranch Formation. Fresh color of gray (N6\), weathering to light gray to light brownish gray (10YR-2.5Y 6-7/2); varnishes to a light brown or reddish yellow (7.5YR 6/4-6). Phenocryst assemblage includes: 25-40% plagioclase (0.2-10 mm, subhedral to euhedral) and 1-10% pyroxene (1-6 mm, subhedral). Plagioclase are locally aligned and locally some are 10-18 mm long. 1-15% vesicles up to 10 mm long). Lower

part forms relatively smooth slopes but upper 10 m is a cliff-former. Included in the upper ~30 m of the unit is a tongue of Garcia Falls trachyandesite. Approximately 100-120 m thick.

Trrrs Rhyolite southeast of Stanley Springs (upper Eocene) -- Light bluish-light greenish gray, porphyritic, relatively fine-grained lava that forms cliffs on the hill immediately southeast of Stanley Spring. Rock typically is well foliated (wavy to irregular), which causes it to erode into platy colluvium. Probably rests on top of the Garcia Falls andesite and may occupy the same stratigraphic position as unit **Trrael**. Fresh colors range from light greenish gray (10G to 5BG 7/1) to bluish gray (10B to 5 PB 6/), weathering to light gray (5Y 7/1; 10YR 7/2) to pale brown (10YR 6/3). Phenocrysts include: 10-15% hornblende (0.1-4.0 mm long and euhedral), 8-10% potassium feldspar + lesser plagioclase (0.2-5.0 mm and subhedral), and 1-3% quartz (0.5-2.0 mm, anhedral to subhedral). Aphanitic groundmass. Locally exhibits porphyritic alteration. 100-110 m thick.

Trrg Gracia Falls trachyandesite (upper Eocene) -- Greenish gray to gray, porphyritic, fine- to coarse-grained trachyandesite. In a southward direction, unit extends slightly over the Uvas member, but in general the two interfinger with one another. Fresh colors are gray to light gray (N5-7/), weathering to brown to light brownish gray (10YR 5/3/-6-7/2) or light brownish gray to light yellowish brown to light gray (2.5Y 6/2-3 or 7/1; 10YR 6/4). Phenocrysts include 15-80% plagioclase (0.1 to 12.0 mm, eu to subhedral) that are locally aligned, 5-10% pyroxene (0.1-5.0 mm, subhedral), and trace to 1% hornblende (up to 1.25 mm). Pyroxene may be surrounded by reddish reaction rims of magnetite or limonite. About 5-15% vesicles (0.5-15 mm long), locally as much as 50% vesicles. Commonly altered to chlorite-epidote±albite assemblage, especially near the Deep Canyon Fault. At least 400 m thick.

Trru Uvas Canyon basaltic trachyandesite (upper Eocene) -- Dark gray, porphyritic, relatively coarse-grained basaltic trachyandesite. Commonly bounded above and below by the Placitas member. Fresh color ranges from gray to light olive gray to greenish gray to light greenish gray to dark gray (2.5-5Y 6/1; 5Y 6/2; 10Y 6-7/1), varnishes readily to a strong brown to light brown to brown (7.5YR 5/3-6; 6/4). Phenocryst assemblage includes: 30-70% plagioclase (0.2-10 mm long, subhedral to euhedral), 3-10% pyroxene (1-10 mm long, subhedral); trace to 5% megacrysts of plagioclase and pyroxene (10-18 mm long); trace olivine(?). Aphanitic groundmass. Not notably vesicular. Chlorite locally is an alteration product and phenocrysts may be altered to goethite or limonite. Weathers to spheroidal outcrops and is crumbly; forms gentle slopes and commonly underlies valley bottoms. 300-480 m thick.

Trrp1 Placitas member (upper Eocene) -- Shale interbedded with minor sandstone. In the east, strata consist of light gray to very dark gray, thinly

laminated with occasional ripple laminae, fissile and carbonaceous, silty shale. Locally interbedded within the shale are very thin to thin, tabular to lenticular beds of (very) pale brown (10YR to 2.5Y 7/3-4) very fine- to medium-grained sandstone and silty sandstone; the sand is subangular, well to moderately sorted, and a tuffaceous volcanic litharenite. Fossil flora commonly found along bedding planes of both shale and sandstone include impressions and casts of needles and cone scales of *Pinus*. Meyer (2012) identified the additional conifers *Picea* and *Abies*. Farkas (1969) identified leaf impressions of the elms *Fagopsis* and *Mahonia*; however, Meyer (2012) argued that *Fagopsis* samples were actually *Zelkova* or *Cedrelospermum* based on their concave morphology.

To the west, strata consist of light greenish gray (5GY 6/2-7/1), very fine- to medium-grained sand interbedded with siltstone-shale, with 5% coarse-very coarse sandstone and pebbly sandstone (pebbles are <6 mm long) in thin to medium beds, that grades upward into a fining-upward interval of yellow sand. As a whole, this interval becomes finer-grained northward (i.e., fines up-section), transitioning to strata dominated by horizontal-laminated, light to dark gray shale. Lower strata are massive or in vague, thin to thick, tabular beds; sand is subangular, well to moderately sorted, and composed of feldspar grains with minor biotite and other mafics -- no volcanic lithic grains except for feldspar-phyric volcanic pebbles; trace claystone laminae. Upper sandstone ranges from pale yellow to light olive gray (5Y 7/3; 5Y 6-8/2) and is in very thin to thin, tabular beds. The sand is very fine- to medium-grained, and interbedded with minor light gray to dark gray shale; sand is well-sorted and composed of feldspar and quartz(?), ~3% mafic grains, with no obvious volcanic detritus. Assymetric ripple marks and toolmarks are relatively common and indicate a northerly paleoflow direction. Locally beds are bioturbated. Lower contact appears to be in a buttress relation with underlying hornblende-phyric lavas. Upper contact is not exposed. Entire unit is 15-75 m thick and thickens to the northwest.

Trrup Uvas Canyon basaltic trachyandesite lavas interbedded with the Placitas Canyon Member (upper Eocene) --

Uvas Basaltic Andesites, as described above, that are interbedded with sediment correlative to the Placitas Member. Locally mapped at the top of the main Uvas Canyon basaltic andesite body, where it underlies a 15 m-thick tongue of Whiskey Hill volcanoclastic sediments and andesite flows. 20-25 m thick.

Whiskey Hill member (upper Eocene)

Trrws Volcanoclastic sedimentary rocks interbedded with dacite and andesite flows – Light bluish gray or purplish gray (weathering orange-tan or maroon-brown), volcanoclastic pebble-cobble gravel and fine-grained sandstone interbedded with dacite and fine- to medium-grained

andesite. Exposed along Cañada de la Cruz and valley bottoms to its east, as well as south and west of Red Rock Ranch. Moderately to well indurated volcanoclastic gravel consists of flow breccias and conglomerates with poorly sorted, angular to subrounded dacite and plagioclase-phyric andesite clasts up to 44.5 cm (17.5 in) across. Andesitic flows are porphyritic, containing up to 38% plagioclase phenocrysts (up to 3.5 mm, occasionally occurring as laths), trace to 14% biotite (up to 1.5 mm), trace to 8% hornblende (up to 2.75 mm, occasionally exhibiting contact twinning), and trace to 7% pyroxene (up to 3 mm). Some andesite flows are equigranular and/or propylitized to chlorite-albite±epidote assemblages. The dacites are porphyritic and have the following phenocrysts: 30-40% plagioclase and sanidine phenocrysts, trace to 15% biotite, trace to 8% hornblende, and trace to 7% pyroxene. Unit underlies abrupt contacts with Red Rock Arroyo andesite or Uvas Canyon pyroxene trachyandesite in the Red Rock Ranch area. This unit spans the entire member, which is 270-330 m (900-1080 ft) thick when volcanic units below are included.

Trrwsj Jasperized volcanoclastic and sedimentary rocks –
Strata correlative to unit Trrws (described above) that have been replaced and cemented by jasper. Mapped on hill west of Red Rock shooting range.

Trrwa Plagioclase-phyric andesites of Whiskey Hill member --
Porphyritic andesite containing 10-30% aligned plagioclase phenocrysts (1-10 mm long and euhedral), 1-5% pyroxene +/- hornblende phenocrysts (1-3 mm long and euhedral). Gray to dark gray (2.5Y 4-5/1), weathering to brown to yellowish brown to grayish greenish brown. Weathered surfaces show distinct plagioclase casts that are commonly stained black.

Trrwhe Equigranular hornblende-phyric dacite (upper Eocene) –
Equigranular hornblende dacite lava – 7-15% mafics hornblende phenocrysts are 3-5 mm. 2 of these

Trrwhn Dacite with needle-like hornblende phenocrysts --
Porphyritic dacite lava with 10% needle-like hornblende phenocrysts; other phenocrysts include plagioclase laths and pyroxene. Locally plagioclase-phyric.

Trrwx Crystal-rich dacite -- Crystal-rich dacite lava with phenocrysts that include gray feldspar (1-1.5 mm long), hornblende (up to 7 mm), and pyroxene.

Trrwr Rhyolite lava in eastern quadrangle -- Laminated, reddish gray to pale red (2.5YR 5-6/1, 6/2, 10R 5/3), aphanitic rock interpreted as a rhyolite. Fine flow-banding in the form of 1 cm-tall ridges. The foliation is locally folded or crenulated.

Trrwbu Upper biotite-bearing dacite– Thin (2 m-thick), porphyritic dacite lava with phenocrysts of plagioclase, pyroxene, hornblende, and a trace of biotite. 3% xenoliths.

Trrwp Pyroxene-bearing dacite -- Pyroxene-bearing, porphyritic dacite with 15% phenocrysts of plagioclase, potassium feldspar, hornblende, and pyroxene.

Trrwh Hornblende-bearing dacite -- Hornblende-bearing, porphyritic dacite with 4-30% phenocrysts that include plagioclase (up to 3 mm long), hornblende (up to 10 mm long, mostly 2-10 mm), and pyroxene (<1 mm long). Locally trace biotite; locally has an equigranular matrix.

Trrwt Tuff (upper Eocene) --Dacitic tuff, pink to white, where lithics are more common near the top. Contains phenocrysts of hornblende, pyroxene, and biotite. 1 m thick.

Trrwk Potassium-bearing dacites (upper Eocene) -- Crystal-rich lava that contains phenocrysts of potassium feldspar (< 1 cm long).

Trrwb Biotite-bearing dacite (upper Eocene) – Dacite with biotite and hornblende phenocrysts. At the Red Rock shooting range, this unit is light gray (N6,7/ , fresh and weathered), but becomes whiter and more altered to the west, and includes the following phenocrysts: 5% biotite (0.5-2.0 mm long), 2% hornblende (1-4 mm long), and 12% plagioclase and sanidine (1-6 mm long and commonly altered); all phenocrysts are euhedral.

Trrwl Lowest dacite lava -- Porphyritic dacite that includes the following phenocrysts: hornblende, pyroxene, and plagioclase. Its relation to other lavas is not exposed. Underlies the hill whose top is labeled 5923 on the map. At least 60 m thick.

Paleozoic bedrock

Paleozoic rocks in the Monticello quadrangle consist of carbonates and clastic sedimentary rocks of the Pennsylvanian Magdalena Group. Depositional environments for the Bar B, Nakaye, and Red House formations have been interpreted as restricted marine/intertidal or supratidal, open-marine below wave base, and restricted/shallow-marine shelf, respectively (Seager and Mack, 2003). Ages for these formations are primarily based on microfossil biostratigraphies constructed for correlative rocks found in the Fra Cristobal and Caballo mountain ranges to the east and southeast. These ages are given in Lucas et al. (2012a) and Lucas et al. (2012b).

Pennsylvanian Magdalena Group

¶bj, ¶nj, ¶rj Jasperoids replacing sedimentary strata of the Bar B, Nakaye, and Red House formations (Pennsylvanian?) – Brownish maroon to dark or pinkish gray weathering orange-tan, commonly massive, pervasively silicified carbonate, sandstone, and conglomerate. Drusy quartz and globular chalcedony commonly fill voids. Rarely retains sedimentary structures or fossils, but occasionally features secondary nodular texture. Where discernible, bedding is thick to very thick; a single outcrop displays weak trough cross-bedding in relict sandstone of *r. Commonly brecciated. Forms rubbly slopes and ledges. Found throughout local Pennsylvanian section, particularly in *b. Jasperoids typically occur along faults and less commonly along bedding. Individual outcrops are 2-4 m (7-13 ft) thick.

¶b Bar B Formation (upper Desmoinesian-Missourian) – Dark gray to dark brownish gray, thin- to medium-bedded limestone and conglomerate. Limestone beds consist of massive, fossiliferous, chert-poor wackestone and packstone. Fossils include bryozoans (*Fenestella*), echinoderm fragments (especially crinoid columnals), fusulinids, and vertical burrows (*Skolithos?*). Marine conglomerate occurs in the upper 10 m (33 ft) of the section and consists of subangular to subrounded granules and pebbles of limestone, dolostone, and chert. Its matrix features crinoid columnals, shell fragments, and sponges cemented by reddish calcite. Covered intervals below the conglomerate are underlain by poorly exposed gray shale. Approximately 75 m (250 ft) thick.

¶n Nakaye Formation (upper Atokan to middle Desmoinesian) – Light tannish to dark maroon-gray, ledge- to cliff-forming, blocky weathering, thin- to thick-bedded limestone. Limestone commonly consists of wavy bedded, fossiliferous, and cherty packstone and wackestone; grainstone and micrite are subordinate. Fossils include brachiopods, bryozoans (*Fenestella*), and echinoderm fragments. Sponges replaced by chert are found in the upper part, though beds near the top of the section are typically fossil-poor. Chert occurs as crusts, lenses, and nodules up to 15 cm (6 in) across. A single, ~2 m (7 ft) thick chert bed lies 35 m (115 ft) above the base of the section. Rare covered intervals are probably underlain by poorly exposed, grayish yellow shale. Approximately 330 m (1080 ft) thick.

¶r Red House Formation (upper Morrowan to Atokan) – Interbedded maroon to pinkish white sandstone and conglomerate, dark gray shale, and light gray- to yellowish tan-weathering limestone. Quartzose sandstone beds are typically laterally discontinuous, well sorted, subangular to subrounded, and fine- to medium-grained. Quartz pebble conglomerate in the lower section grades upward into breccia that may be locally jasperized. Shale beds are poorly exposed, except for calcareous, fissile, slightly silty shale containing subrounded limestone clasts near the base of the section. Limestone beds are commonly

composed of thin- to thick-bedded, fossiliferous packstone containing brachiopods (including Order *Spiriferida*), crinoid columnals, and fusulinids, with the latter found in the upper 30 m (98 ft) of section. Chert is rare and occurs as nodules up to 30 cm (12 in) across in limestone beds. Intruded by 11 m (36 ft) thick andesitic sill southwest of La Petra. Approximately 555 m (1820 ft) thick.

Dikes

Tia Intermediate composition dikes - gray dikes that variably have a fine-grained, equigranular matrix with no obvious phenocrysts or are slightly porphyritic (<<1% plagioclase and pyroxene < 2 mm across) with an aphanitic matrix.

Subsurface units

Tvu **Oligocene volcanic strata, undivided (lower Oligocene)** – Includes andesite-latite of Montoya Butte and perhaps associated basal mudflow breccia (Maldonado, 2012). Maximum thickness ~900 m (2953 ft) according to Jahns (1955).

Ku **Cretaceous strata, undivided (upper Cretaceous)** – Includes the McRae Formation, Dakota Sandstone, and Mancos Shale. Maximum thickness of ~200 m (656 ft) extrapolated from the Gartland 1 Brister exploratory well (Cikoski and Koning, 2013).

Pu **Permian strata, undivided (lower to upper Permian)** – Includes the San Andres, Yeso, Abo, and Bursum formations. Mostly siliciclastic beds interbedded with limestone and gypsum in places. Maximum thickness of ~525 m (1723 ft) extrapolated from the Gartland 1 Brister exploratory well (Cikoski and Koning, 2013).

Pz **Lower Paleozoic strata, undivided (Cambrian through Ordovician)** – Includes the Bliss Sandstone, El Paso Group, and Montoya Formation. The Bliss Sandstone is overlain by a thick sequence of limestone and dolostone. Silurian and Devonian strata are absent in the northern Mud Springs Mountains (Maxwell and Oakman, 1990), and are likely not present in cross-section A-A'. Maximum thickness of ~230 m (755 ft) extrapolated from the West Elephant Butte Federal No. 1 well (Cikoski and Koning, 2013).

XYu **Proterozoic strata, undivided (Meso- to Neoproterozoic)** – Reddish gray quartzite, dark gray to brown quartz schist, quartz-biotite schist, foliated amphibolite, and reddish, porphyritic granitic gneiss. Complexly interlayered and contorted (Maxwell and Oakman, 1990).

APPENDIX 2. Chemical analyses of unmineralized igneous rocks in the Monticello quadrangle.

SAMPLE	Sample descri	rock type	symbol	Latitude	Longitude	SiO2
SJ-400	mineralized rl	rhyolite		16 33.462862	-107.444796	77.2
SJ-506	upper andesit	trachyte		16 33.4807007	-107.3882179	67.5
SJ-524	Red Rock and	trachyandesite		16 33.4583001	-107.3948963	57.3
Mo-347-131106-djk		trachyandesite		16		54.3
14Mo-2-AJ		trachyandesite		16		53.7
14Mo39sk		rhyolite		16		78.7
14Mo24sk		basaltic trachyandesite		16		52.6
14Mo25sk		basaltic trachyandesite		16		52.2
MONT-13-05	latite	phonolite		16 33.4934262	-107.4608497	50.25
ARAGON2	rhyolite Tr	rhyolite		16 33.472652	-107.38451	84.66

TiO2	Al2O3	Fe2O3T	Fe2O3	FeO	MnO	MgO	CaO	Na2O
0.15	10.35	1.88				0.01 <0.01		0.05 3.2
0.61	15.8	3.2				0.02 0.28		1.46 4.77
1.03	18.75	5.62				0.12 0.89		5.84 4.39
1.1	16.3	7.97				0.13 3.4		5.75 3.61
1.09	16.15	7.86				0.14 3.39		6.01 3.58
0.19	11.9	0.75				0.03 0.1		0.27 1.75
1.32	17.2	8.2				0.11 4.01		7.3 3.74
1.3	16.9	8.12				0.12 4.26		7.19 3.73
0.932	15.26			4.81 5.29	2.19	2.82	0.139	3.38
0.11	9.72			0.66 0.00	0.06	0.14	0.1	0.02

K2O	P2O5	SrO	BaO	Cr2O3	LOI 1000	Total	S	C	
3.97	<0.01		0.01	0.01	0.01	1.07	100.55	1.02	0.01
4.77	0.15		0.03	0.16	<0.01	0.38	99.21	0.01	0.01
3.59	0.51		0.1	0.11	<0.01	0.9	99.28	<0.01	0.16
3.74	0.44		0.1	0.12	<0.01	3.03	100.1	<0.01	0.38
3.69	0.44		0.1	0.13	<0.01	3.33	99.71	<0.01	0.44
4.97	0.04	<0.01		0.02	<0.01	0.87	99.61	<0.01	0.01
2.89	0.62		0.1	0.09	0.01	0.83	99.15	0.01	0.03
2.72	0.6		0.09	0.09	0.01	1.11	98.56	0.01	0.05
8.64	3.83					0.349	97.882	2.22	
2.64	0.01					1.89	100.010		

Au	Ba	Ce	Cr	Cs	Dy	Er	Eu	Ga	
	0.01	62.7	12.3	10	1.59	7.62	7.79	0.08	19.6
		1605	161.5 <10		2.01	10.7	6.28	2.86	24.3
		1010	129.5	20	1.15	5.68	3.21	2.06	23.1
		1150	89.6	30	2.32	5.54	3.07	1.73	21.5
		1160	89.5	30	2.45	5.26	3.09	1.74	21.6
		151.5	62.4	10	3.37	11	7.79	0.45	20.7
		787	122.5	50	2.31	6.3	3.71	2.06	22.1
		824	124	50	1.2	6.41	3.73	2.16	22.7
		31		9.30	17	41		52	715
		54		6.0					18

Gd	Hf	Ho	La	Lu	Nb	Nd	Pr	Rb	
	2.73	20.8	2.22	4	1.66	65.4	5	1.32	242
	11.6	13.2	2.19	76.8	0.86	29.7	76.5	19.25	124.5
	6.7	10.6	1.08	62.4	0.44	34.1	56.9	14.8	124.5
	6.2	6.6	1.01	42.8	0.38	15.4	43.1	10.85	107.5
	6.2	6.3	1.09	42.4	0.4	15.2	43	10.75	106.5
	7.18	6.5	2.46	27.7	1.17	35.4	28.2	7.91	288
	7.63	9.3	1.26	57.6	0.47	26.1	57.1	14.45	96.9
	7.48	9.2	1.3	59.4	0.5	27	58.9	14.7	97.3
	101					71			70.5
						39.0			183

Sm	Sn	Sr	Ta	Tb	Th	Tm	U	V	
	1.78	3	93.8	4.9	0.87	39	1.37	16.1 <5	
	15.6	3	299	1.5	1.83	13.75	0.9	2.79	18
	10.05	4	909	1.8	0.97	22.5	0.46	4.45	106
	9	3	828	0.9	0.85	10.4	0.4	1.39	146
	8.27	4	830	0.8	0.86	10.1	0.41	1.36	142
	7.28	4	36	2.5	1.6	27.7	1.15	5.61	5
	10.45	2	813	1.4	1.1	16.7	0.52	3.79	196
	10.9	2	822	1.3	1.11	16.65	0.51	3.78	200
			13			22		27	
			19			26		7	

W	Y	Yb	Zr	Ag	Be	Cd	Co	Cu
	1	69.8	10.95	568	0.6	<0.5		1 <1
	1	59.1	5.76	546	<0.5	<0.5		2 1
	2	30.7	2.96	463	<0.5	<0.5		10 103
<1		29.1	2.76	257	<0.5	<0.5		22 64
	1	29	2.7	258	<0.5		0.5	21 64
	4	71.2	8.11	167	<0.5	<0.5		1 2
	1	35	3.4	386	<0.5	<0.5		26 102
	1	34.7	3.37	388	<0.5	<0.5		26 102
		617		101		9		286
		36		120				

Li	Mo	Ni	Pb	Sc	Zn	As	Bi	Hg
	10	12 <1		112	4	59	27.7	0.67 0.008
	10	1	1	21	7	122	0.5	0.04 0.014
	20	1	10	21	8	55	1.8	0.1 <0.005
	10 <1		29	12	15	70	1.6	0.01 <0.005
	10 <1		27	10	14	79	1.6	0.02 0.008
	20	1 <1		10	3	27	1.5	0.13 0.008
	20	1	36	14	18	94	0.5	0.03 <0.005
	20 <1		34	14	18	92	0.6	0.02 <0.005
	2		0.00	13.6	2381.19	21		108
				49		16		

Sb	Se	Te	Tl
0.39	3.4	10.4	0.13
0.08	0.6	0.01	0.03
0.15	0.7 <0.01	<0.02	
0.1	0.7	0.01 <0.02	
0.12	0.7 <0.01	<0.02	
0.12	1.3 <0.01		0.09
0.07	0.8 <0.01		0.04
0.06	0.7 <0.01	<0.02	

APPENDIX 1. Mines and prospects in the San Mateo Mountains district, Socorro and Sierra Counties, New Mex

Mine id	County	District id	Mine name	Township	Range	Section
NMSI1765	Sierra	DIS194	Aragon Hill	10S	5W	6
NMSI1761	Sierra	DIS194	Aragon Hill	10S	5W	6
NMSI1763	Sierra	DIS194	Aragon Hill	10S	5W	6
NMSI1764	Sierra	DIS194	Aragon Hill	10S	5W	6
NMSI1762	Sierra	DIS194	Aragon Hill	10S	5W	6
NMSI1767	Sierra	DIS194	Aragon Hill	10S	5W	6
NMSI0268	Sierra	DIS194	Aragon Hill	10S	5W	5, 6
NMSI0267	Sierra	DIS194	Aragon placer	10S	5W	6
NMSO0017	Socorro	DIS194	Douglas	9S	6W	35
NMSI0269	Sierra	DIS194	Douglas	10S	6W	2
NMSO0568	Socorro	DIS194	Douglas	9S	6W	35
NMSO0574	Socorro	DIS194	Douglas	9S	6W	35
NMSO0569	Socorro	DIS194	Douglas	9S	6W	35
NMSO0570	Socorro	DIS194	Douglas	9S	6W	35
NMSO0571	Socorro	DIS194	Douglas	9S	6W	35
NMSO0572	Socorro	DIS194	Douglas	9S	6W	35
NMSO0573	Socorro	DIS194	Douglas	9S	6W	35
NMSO0567	Socorro	DIS194	Douglas	9S	6W	35
NMSI1770	Sierra	DIS194	East Aragon Hill	10S	5W	4
NMSI0270	Sierra	DIS194	Fifty-fifty	11S	5W	6
NMSI0271	Sierra	DIS194	Lookout	10S	5W	5
NMSO0125	Socorro	DIS194	Luna	9S	6W	35
NMSI0272	Sierra	DIS194	Monticello tin placers	10, 11S	6, 7W	
NMSI0279	Sierra	DIS194	Stanley	10S	6W	3
NMSI1757	Sierra	DIS194	Stanley	10S	6W	3
NMSI0273	Sierra	DIS194	Terry	10S	6W	26
NMSI1769	Sierra	DIS194	unknown	10S	5W	31
NMSI1768	Sierra	DIS194	unknown	10S	5W	5
NMSI1760	Sierra	DIS194	unknown	10S	5W	5
NMSI1758	Sierra	DIS194	unknown	10S	6W	11
NMSI1759	Sierra	DIS194	unknown	10S	6W	11
NMSO0153	Socorro	DIS194	unknown	9S	6W	36
NMSI1766	Sierra	DIS194	unknown	10S	5W	8
NMSI0274	Sierra	DIS194	unknown	10S	6W	1

ico.

Subsection	Latitude (degrees)	Longitude (degrees)	UTM easting	UTM northing	UTM zone	ordinate sys	Production
	33.473336	-107.3853045	278342	3706116	13	NAD27	yes
	33.4732692	-107.3854963	278324	3706109	13	NAD27	yes
	33.472549	-107.3863695	278241	3706031	13	NAD27	no
	33.4736382	-107.3860013	278278	3706151	13	NAD27	no
	33.4720881	-107.3859588	278278	3705979	13	NAD27	no
	33.4691838	-107.3874069	278136	3705660	13	NAD27	no
NW NE	33.4728162	-107.3842036	278443	3706056	13	NAD27	yes
NE	33.471887	-107.388541	278036	3705962	13	NAD27	yes
SE	33.4815073	-107.422386	274916	3707102	13	NAD27	no
NE	33.476865	-107.422317	274907	3706587	13	NAD27	no
	33.4868298	107.417622	275373	3707682	13	NAD27	no
	33.4809079	-107.4151979	275583	3707020	13	NAD27	no
	33.4863938	-107.4177821	275357	3707634	13	NAD27	no
	33.4833978	-107.4202166	275123	3707307	13	NAD27	no
	33.4825538	-107.4214197	275009	3707216	13	NAD27	no
	33.4812673	-107.4226536	274891	3707076	13	NAD27	no
	33.4810404	107.421808	274969	3707049	13	NAD27	no
	33.4809896	-107.4220971	274942	3707044	13	NAD27	no
	33.4742907	-107.3654415	280191	3706180	13	NAD27	no
NE	33.3861046	-107.3877334	277894	3696447	13	NAD27	no
NW	33.471464	-107.378426	278976	3705893	13	NAD27	no
SE	33.4807596	-107.4210945	275035	3707016	13	NAD27	no
	33.292992	-107.3869319	277732	3686119	13	NAD27	no
SE	33.4628619	-107.444796	272785	3705083	13	NAD27	unknown
	33.4629289	-107.4459705	272676	3705093	13	NAD27	no
	33.412404	-107.426505	274354	3699447	13	NAD27	yes
	33.4682255	-107.4015894	276625	3697351	13	NAD27	no
	33.4682255	-107.3809795	278731	3705540	13	NAD27	no
	33.4755949	-107.3813103	278719	3706358	13	NAD27	no
	33.44814	-107.435047	273653	3703429	13	NAD27	no
	33.4492175	-107.4352815	273634	3703549	13	NAD27	no
SW	33.481042	-107.416306	275480	3707037	13	NAD27	no
	33.4577104	-107.382456	278567	3704377	13	NAD27	no
SE	33.466047	-107.406304	276368	3705352	13	NAD27	no

commodity category	commodities produced	minerals present	year of initial production	year of last production	Comments on production	Development	depth of workings		
metals	Au					adit, caved			
metals	Au					caved			
metals		Au				cut into			
metals		Au				covered			
metals		Au				shaft	15 ft		
metals		Au, Ag				pit	2 ft		
metals	Au	F, Cu, Sn				unknown production	adits,		
metals	Au					minor placer production	pits, cuts		
metals		Au					trenches	10 ft	
metals		Au, Ag					pits, shaft	10 ft	
metals		Au, Ag					decline	10 ft	
metals		Au, Ag					pit	5 ft	
metals		Au, Ag					pit	5 ft	
metals		Au, Ag					pit	4 ft	
metals		Au, Ag					2 pits	10 ft	
metals		Au, Ag					2 pits	3 ft	
metals		Au, Ag					pit	3 ft	
metals		Au, Ag					pit	4 ft	
metals		Au, Ag					drill roads		
metals		Au, U					trench	6, 45 ft	
metals		Au, U					unknown production	pits	50 ft
metals		U, Cu, Au						pits	
metals		Sn						placer	
metals		Au					unknown production	drilling	100 ft
metals		Au, Ag						pit	5 ft
uranium	U	F			1955	1960	uranium production table	trenches, pits, shaft	80 ft
metals		Ag						adit	
metals		Au, Ag						pit	3 ft
metals		Au, Ag						pit	4 ft
metals		Au, Ag						pit	4 ft
metals		Au, Ag				pit	2 ft		
metals		Au, Ag, Cu				pits	5 ft		
metals		Cu, Ag				pit	10 ft		
metals		Cu, Ag				pit			

Length of work	Disturbed area	Operating status	Mining method	Surface land status	Federal land status	Ownership	Primary company	Access	Mining history
		inactive	underground	federal	federal			hike	
		inactive	underground	federal	federal			hike	
		inactive		federal	federal			hike	
		inactive	underground	federal	federal			hike	
		inactive	underground	federal	federal			hike	
3 ft		inactive	surface	federal	federal			hike	
		inactive	underground	federal	federal	Service	D.M.	hike	
		inactive	surface	federal	federal	Service	Swainstain	4WD	
50 ft		inactive	surface	federal	federal	Service		4WD	
		inactive	surface	federal	federal	Service		4WD	
		inactive	underground	federal	federal			hike	
8 ft		inactive	surface	federal	federal			4WD	
5 ft		inactive	surface	federal	federal			4WD	
4 ft		inactive	surface	federal	federal			4WD	
		inactive	surface	federal	federal			4WD	
3 ft		inactive	surface	federal	federal			4WD	
5 ft		inactive	surface	federal	federal			4WD	
5 ft		inactive	surface	federal	federal			hike	
		inactive	none	federal	federal			4WD	
		inactive	underground	federal	federal		Woody	4WD	1980 by
		inactive	underground	federal	federal			4WD	
		inactive	surface					4WD	
		inactive	surface					hike	
	0.2	inactive	underground	federal	federal	Service		2WD	
		inactive	surface	federal	federal			4WD	
		inactive	underground	federal	federal	Bureau of Land	Ministry	4WD	discovered 1948
15 ft		inactive	underground	federal	federal			hike	
		inactive	surface	federal	federal			hike	
		inactive	surface	federal	federal			hike	
		inactive	surface	federal	federal			4WD	
		inactive	surface	federal	federal			hike	
15 ft	0.1	inactive	surface	federal	federal	Service		2WD	
5 ft		inactive	surface	federal	federal			hike	
		inactive	surface	federal	federal	Bureau of Land		4WD	

Mineral resource	Host formation	Age of host rock	Age of mineralization	Rock type	Geology	Primary Mineralogy	Secondary mineral	Size	Alteration
none		Tertiary	Tertiary	rhyolite	fractures				ion,
none		Tertiary	Tertiary	rhyolite	fractures				ion,
none		Tertiary	Tertiary	rhyolite	fractures				ion,
none		Tertiary	Tertiary	rhyolite	fractures				ion,
none		Tertiary	Tertiary	rhyolite	fractures				ion,
none		Tertiary	Tertiary	intrusion					clay
none		Tertiary	Tertiary	rhyolite	fractures,	hematite,			ion,
		Quaternary	Quaternary	gravels	mineral				
none		Tertiary		andesite	N140E	pyrite, quartz,			n
		Tertiary		rhyolite	N40E	quartz,		to 20 ft	n, acid
		Tertiary	Tertiary	dike	N115	trace pyrite			
none		Tertiary	Tertiary	andesite	fault N345	pyrite, Fe			
none		Tertiary	Tertiary	dike		trace pyrite			ion, acid
none		Tertiary	Tertiary	dike		trace pyrite			silicification
none		Tertiary	Tertiary	dike	quartz vein in rhyolite.	pyrite,			n
none		Tertiary	Tertiary	dike	N40	trace pyrite			
none		Tertiary	Tertiary	dike		trace pyrite			
none		Tertiary	Tertiary	dike	N90	trace pyrite			acid sulfate
none	Vicks Peak	Tertiary	Tertiary	rhyolite					ion,
none		Tertiary		breccia	along fault	gold,		wide, 450	n,
none	Formation	Tertiary		Vicks Peak		quartz			n
none		Tertiary		dikes	altered	pyrite			alteration
		Quaternary	Quaternary	alluvium		in cons			
buildings		Tertiary		rhyolite	N35E	gold, pyrite		wide, 750	n
buildings		Tertiary	Tertiary	andesite					
none		Tertiary, Silurian		limestone, quartz	breccia	granophane, fluorite,		wide, 375	n
none	Conglomer	Tertiary		ate	calcite-	quartz (no			chloride
none		Tertiary	Tertiary	ate	along fault				
none		Tertiary	Tuff	rhyolite					acid sulfate
none		Tertiary	Tertiary	dike					
none		Tertiary	Tertiary	dike					
none		Tertiary		andesite	zone	calcite,			n
none		Tertiary	Tertiary	latite		trace pyrite			chloride
		Tertiary		rhyolite		calcite			silification

type of deposit	USGS quadrangle	Elevation	method of obtaining	Land use	is hazardous	is potential acid	Hydrology	receiving stream
epithermal	Monticello			grazing		pyrite		
epithermal	Monticello			grazing		pyrite		
epithermal	Monticello			grazing		pyrite		
epithermal	Monticello			grazing		pyrite		
epithermal	Monticello			grazing		pyrite		
epithermal	Monticello	6400	est	grazing	none	pyrite		Draw
placer gold	Monticello	6160	est	grazing	none	none		Draw
epithermal	Monticello	6400	est	recreation	none	none	none	Arroyo
epithermal	Monticello	6460	est	grazing	none	none		Canyon
epithermal	Monticello			grazing	none	none		
epithermal	Monticello			grazing	none	none		
epithermal	Monticello			grazing	none	none		
epithermal	Monticello			grazing	none	none		
epithermal	Monticello			grazing	none	none		
epithermal	Monticello			grazing	none	none		
epithermal	Sierra Fijardo			grazing		none		
epithermal	Monticello	5370	est	grazing		none		
epithermal	Monticello	6300	est	grazing		none		
epithermal	Monticello	6440	est					
placer tin	Priest Tank			grazing		none		Ramos
epithermal	Monticello	6270	est	grazing		none		Draw
epithermal	Monticello			grazing	none	none		
epithermal	Monticello	5710	est	grazing	and	none	none	
epithermal	Monticello			grazing	none	none		
epithermal	Monticello			grazing	none	none		
epithermal	Monticello			grazing	none	none		
epithermal	Monticello			grazing	none	none		
epithermal	Monticello			grazing	none	none		
epithermal	Monticello	6400	est	grazing	none	none	none	Arroyo
epithermal	Monticello			grazing		pyrite		
epithermal	Monticello	6300	est	grazing		none		Arroyo

Reclamation	mitigation status	ative environ	Comments	References	ata reliability	Inspected by	Date inspected	e of last modifica
					field	VTM	1/23/2014	4/25/2014
		none			field	VTM	1/23/2014	4/25/2014
					field	VTM	1/23/2014	4/25/2014
					field	VTM	1/23/2014	4/25/2014
		none			field	VTM	1/23/2014	4/25/2014
					field	VTM	4/24/2014	4/25/2014
		none	746: 15-	and Heyl	field	JVM	1/23/2014	4/25/2014
					field	JVM	12/28/1995	5/28/2002
		none		(1992)	field	VTM	8/7/1996	6/12/2002
				(1992)	literature	VTM	8/7/1996	5/28/2002
		none		(1992)	field	VTM	11/29/2011	12/27/2013
		none		(1992)	field	VTM	11/30/2013	12/27/2013
		none		(1992)	field	VTM	11/29/2011	12/27/2013
		none		(1992)	field	VTM	11/29/2011	12/27/2013
		none		(1992)	field	VTM	11/29/2011	12/27/2013
		none		(1992)	field	VTM	11/29/2011	12/27/2013
		none		(1992)	field	VTM	11/29/2011	12/27/2013
		none		(1992)	field	VTM	11/29/2011	12/27/2013
		none		(1992)	field	VTM	11/29/2011	12/27/2013
		none		(1992)	field	VTM	11/29/2011	12/27/2013
		none	oz/ton Au,	(1982),	field	JVM	2/2/2014	4/25/2014
open shafts	fencing	none	y bkgrd 90	RRA-1157	field	VTM	12/26/2013	12/27/2013
				(1982, No.	field	VTM	11/29/2011	12/27/2013
				R file data,	literature			1/1/1998
open shafts		none	744: less	al. (1995),	field	VTM	11/20/2013	12/27/2013
		none		(1992)	field	VTM	11/22/2013	12/27/2013
		none	743:29-95	(1983),	field	JVM	2/2/2014	4/25/2014
		none			field	VTM	2/9/2014	4/25/2014
					field	VTM	4/24/2014	4/25/2014
					field	VTM	12/26/2013	12/27/2013
			y bkgrd 70		field	VTM	11/22/2013	12/27/2013
			y bkgrd 70		field	VTM	11/22/2013	12/27/2013
	needed			(1992)	field	VTM	8/7/1996	5/28/2002
					field	VTM	1/27/2014	4/25/2014
				(1992)	literature			5/28/2002

APPENDIX 4. Geochemistry of mineralized whole-rock samples in the San Mateo Mountains district. Analyses a

Field id	Mine id	location	Sample_descripti	Latitude	Longitude	reference
Gold 10	NMSO0570	Douglas claims	grab of outcrop	33.4833978	-107.4202166	VTM
Gold 11	NMSO0570	Douglas claims	grab of outcrop	33.4833978	-107.4202166	VTM
Gold 12	NMSO0570	Douglas claims	5 ft chip of pit wa	33.4833978	-107.4202166	VTM
Gold 14	NMSO0567	Douglas claims	grab of dump	33.4825538	-107.4214197	VTM
Gold 15	NMSO0567	Douglas claims	grab of dump	33.4809896	-107.4220971	VTM
Gold 16	NMSO0574	Douglas claims	select dump	33.4809079	-107.4151979	VTM
35 (Terry1)	NMSI0273	Terry	2 ft chip	33.412404	-107.426505	VTM
36 (Terry2)	NMSI0273	Terry	select dump	33.412404	-107.426505	VTM
37 (fiftyfifty1)	NMSI0270	Fifty-fifty	5 ft chip	33.386223	-107.387768	VTM
38 (fiftyfifty1)	NMSI0270	Fifty-fifty	5 ft chip	33.386223	-107.387768	VTM
67 (Gold)	NMSI0279	Stanley	select dump	33.4628619	-107.444796	VTM
68 (Aragon1)	NMSI1765	Aragon	1 ft chip	33.472652	-107.38451	VTM
ARAGON2	NMSI1764	Aragon	grab of rhyolite o	33.472652	-107.38451	VTM
741	NMSI0273	Terry	3 ft chip	33.412404	-107.426505	Korzeb et al
742	NMSI0273	Terry	1.5 ft chip	33.412404	-107.426505	Korzeb et al
743	NMSI0273	Terry	select	33.412404	-107.426505	Korzeb et al
744	NMSI0279	Stanley	grab	33.4628619	-107.444796	Korzeb et al
745	NMSI1762	Aragon Hill	select	33.472652	-107.38451	Korzeb et al
746	NMSI1767	Aragon Hill	select	33.472652	-107.38451	Korzeb et al

re by instrumental neutron activation and induced coupled plasma spectroscopy. Analyses are in parts p

Ag	Al%	As	Auppb	Ba	Be	Br	Ca%	Co
<0.4	0.52	18	4	<50	2	<0.5	0.04	1
1.1	4.69	46	<2	420	5	<0.5	0.07	1
0.6	5.43	23	<2	300	4	<0.5	0.06	2
0.6	5.24	5	<2	370	5	<0.5	0.2	2
0.4	5.47	<0.5	<2	200	4	<0.5	0.5	1
0.6	8.1	<0.5	15	870	<2	<0.5	4.57	25
1.6	0.56	42	61	95	<2	<0.5	11.47	2
3.4	1.72	80	58	100	<2	<0.5	9.11	2
1.6	5.04	22	347	810	2	0.8	0.27	9
49	2.8	36	3150	440	2	1.4	1.26	6
<0.4	4.94	14	21	160	2	<0.5	0.03	<1
26	4.65	3.9	42800	210	<2	<0.5	0.04	<1
<0.5	6.75	2	700	<50	4	<0.5	0.07	19
0.5	1.2	72	29	200		1	>10	4
1	0.68	35	35	430		<0.5	>10	2
4.6	0.73	112	95	1700		4	>10	2
5	0.56	6	9	18		<0.5	0.14	2
<5	0.99	7	15	310		<0.5	0.51	27
<5	1.19	<0.5	523	660		<0.5	1.25	5

per million (ppm), except for gold, which is in parts per billion (ppb) and major elements, which are in pe

Cr	Cs	Cu	Fe%	Hf	Hg	K%	Mg%	Mn
120	1	7	1.41	51	<1	0.14	0.01	77
69	2	6	1	60	<1	1.82	0.03	293
28	3	6	2.25	52	<1	2.61	0.07	340
47	1	6	2.05	47	<1	2.22	0.04	141
27	3	4	0.71	6	<1	3.67	0.11	86
68	1	567	5.75	4	<1	1.24	1.33	797
320	<1	19	1.25	1	0.64	0.06	0.02	6
260	2	86	2.11	<1	0.46	0.13	0.04	5
150	3	17	2.12	2	<0.18	3.55	0.35	107
180	2	24	2.15	2	0.17	0.56	0.18	33
68	<1	4	1.48	25	0.3	3.39	0.08	1084
150	3	19	0.49	6	0.28	4.7	0.05	126
	7	<1	0.3	6	<1	2.79	0.08	458
160	<1	72	1.31	<1		0.08	0.01	152
200	1	29	1.14	<1		0.16	0.02	145
220	<1	54	1.73	<1		0.15	0.01	246
85	2	16	1.85	21		0.26	0.13	394
80	8	23	1.88	6		0.34	0.06	3519
56	6	17	2.05	8		0.28	0.28	4697

Percent (%). Location is in NAD27.

Mo	Na%	Ni	P%	Pb	Rb	Sb	Sc	Sn
6	0.04	7	0.004	95	23	0.7	6.5	
5	1.05	4	0.008	66	260	1	9.2	
52	0.28	4	0.012	131	280	1.2	8.5	
3	2.83	6	0.006	117	330	0.7	8.3	
3	1.47	5	0.003	23	340	0.4	3.3	
2	2.98	40	0.136	18	54	0.3	19	
17	0.01	11	0.003	391	<15	5.4	4.8	
24	0.02	8	0.019	1291	<15	8.1	7.8	
<2	0.04	22	0.067	38	180	8.1	5.9	
2	0.02	12	0.012	41	30	16	5.3	
27	0.6	4	0.002	985	250	2	5.4	
58	<0.01	4	0.003	42	340	3.3	3.2	33
6	0.06	1	0.004	50	210	3.9	3.8	
11	0.13	7		969	<15	6.6	3.6	<20
30	0.21	5		468	<15	4.7	4.5	<20
51	0.22	4		2792	<15	27.7	4	<20
28	1.3	4		663	300	2	5.9	<20
5	0.62	15		157	430	1.7	3.3	<20
11	1.3	6		242	240	3.2	7.4	<20

Sr	Ta	Te	Th	Ti%	U	V	W	Y
5	10		130	0.1	38.0	10	<1	84
39	12		150	0.1	51.0	4	<1	138
46	11		130	0.13	38.0	12	<1	98
25	10		130	0.11	41.0	18	<1	122
37	3.4		45	0.06	6.8	3	2	40
624	<0.5		6	0.57	2.2	48	<1	26
103	<0.5		1.3	0.03	870.0	72	9	151
130	<0.5		1.5	0.09	640.0	197	12	222
107	<0.5		2.8	0.2	12.0	136	6	12
132	<0.5		2.9	0.1	25.0	112	11	29
49	3.4		42	0.08	14.0	7	2	42
33	1.7		26	0.07	6.7	10	<1	22
22	3.1		31	0.06	7.6	4	160	26
55	<0.5	<10	<0.5		128.0	129	14	70
65	<0.5	<10	<0.5		1230.0	106	4	89
88	<0.5	<10	2.9		1430.0	230	9	101
12	6	55	52.6		20.0	11	<1	19
30	3	<10	28		12.0	17	<1	40
83	3	<10	22		6.6	23	6	32

Zn	La	Ce	Nd	Sm	Eu	Tb	Yb
28	9	28	5	1.3	0.2	1.4	29.2
60	15	40	6	2.1	0.2	1.8	34.5
50	80	130	25	5.6	0.8	1.7	29.2
141	54	100	15	4.4	0.8	2.2	29.3
43	45	65	14	2.4	0.2	0.7	7.7
110	37	59	26	5.6	1.7	0.8	2.8
55	42	78	67	7.5	1.9	1.9	7.9
120	36	71	49	6.5	2.3	3.6	17
200	17	33	14	2.7	0.9	<0.5	1
100	14	32	13	3.1	1.1	0.8	2.3
520	8.7	25	<5	1.6	<0.2	1.1	13
24	15	27	<5	1.4	<0.2	<0.5	6.6
17	20	46	11	2.3	0.3	0.6	6.4
52	9	20	<5	6.6	2	2	15
91	12	<10	<5	<0.1	4	2	19
270	15	<10	<5	<0.1	<0.2	2	18
400	15	<10	<5	3.3	<0.2	2	16
87	40	87	<5	6	<0.2	1	9
280	55	89	<5	12	2	2	9

Lu
5.22
6.26
5.18
5.35
1.41
0.54
<0.05
2.03
0.18
0.28
1.98
0.92
1.12
<0.05
<0.05
2.3
1
<0.05
0.7